BNL 50611



# PROCEEDINGS OF THE 1976 ISABELLE WORKSHOPS

## May - August 1976

ACCELERATOR DEPARTMENT

BROOKHAVEN NATIONAL LABORATORY

ASSOCIATED UNIVERSITIES, INC.

UNDER CONTRACT NO. EY-76-C-02-0016 WITH THE

UNITED STATES ENERGY RESEARCH AND DEVELOPMENT ADMINISTRATION

## DISCLAIMER

BNL 50611

(Particle Accelerators and
High-Voltage Machines - TID 4500)

# PROCEEDINGS

# OF THE

# 1976 ISABELLE WORKSHOPS

May - August 1976



BROOKHAVEN NATIONAL LABORATORY
ASSOCIATED UNIVERSITIES, INC.
UPTON, NEW YORK

093 6000

PRINTED IN THE UNITED STATES OF AMERICA
Available from
National Technical Information Service
U.S. Department of Commerce
5285 Port Royal Road
Springfield, VA 22161

Price: Printed Copy $ 8.00 ; Microfiche $3.00

## PREFACE

The summer of 1976 saw a number of visiting physicists at Brookhaven. Many came to participate in the seven ISABELLE-sponsored workshops that were held from May through August. Each workshop dealt with a specific subject concerning the design of storage rings. :hnical matters ranging from the confinement of high intensity ams of protons and antiprotons to the design of experimental apparatus were addressed. This booklet includes the summary papers for the workshops as well as a number of contributed papers.

We are indebted to John Herrera and Alan Thorndike for editing all the material while maintaining their good humor. The typing of the Proceedings has been done by Paula Hughes and Judy Ferrero in their usual competent manner.

I particularly want to thank the organizers of the Workshops. With their help and enthusiasm we all enjoyed a stimulating set of meetings. The individuals are:

| | |
|---|---|
| A. Thorndike | Workshop on Experimental Halls |
| D. Brown | Workshop on Cryogenics |
| M. Sakitt | Workshop on Lepton Detectors |
| H. White | Workshop on Hadron Spectrometers |
| R. Chasman | Workshop on Longitudinal Instabilities |
| J. Sandweiss and M. Month | Workshop on Experimental Insertions |
| E. Courant | Workshop on Phase-Space Cooling |

James R. Sanford
December, 1976

THIS PAGE

WAS INTENTIONALLY

LEFT BLANK

## VISITING PARTICIPANTS

A. Abashian, NSF
D. Ayres, ANL
P.J. Channel, LBL
A.W. Chao, SLAC
C.Y. Chien, Johns Hopkins
Y. Cho, ANL
D. Cline, Wisconsin
W. Colyer, LASL
E. Crosbie, LBL
A. Fainberg, Syracuse
T. Ferbel, Rochester
W.B. Fowler, FNAL
W. Frisken, York University
A. Garren, LBL
B. Gibbard, Cornell
R.L. Gluckstern, Maryland
M. Good, SUNY
H. Hereward, England
R. Huson, FNAL
R. Imlay, Rutgers
S. Iwata, Nagoya
S. Jacobs, Brandeis
D. Japikse, Creare, Inc.
D. Johnson, FNAL
T. Khoe, ANL
V. Kistiakowsky, MIT
B. Knapp, Columbia
R. Kraemer, Carnegie-Mellon
M. Kreisler, Massachusetts
P. Kunz, SLAC
R. Lanou, Brown
L.J. Laslett, LBL
W.Y. Lee, Columbia
D. Leith, SLAC
P. Limon, FNAL
S. Lindenbaum, NSF
T. Ludlam, Yale
R. Majka, Yale
K. McDonald, Chicago
B. McIntyre, Harvard
E. Messerschmid, Freiburg
D. Möhl, CERN
D. Nygren, LBL
J. Peoples, FNAL
L. Pondrom, Wisconsin
C.H. Rode, FNAL
C. Rubbia, Harvard
J. Russell, Massachusetts
F.J. Sacherer, CERN
J. Sandweiss, Yale
M. Schwartz, SLAC
A. Seiden, Santa Cruz
W. Selove, Pennsylvania
D.B. Smith, Santa Cruz
R.P. Smith, ANL
T.R. Strobridge, NBS
L. Sulak, Harvard
J. Thompson, Daresbury
J. Thompson, Pittsburgh
T.E. Toohig, FNAL
P.V. Vander Arend, Cryogenic Consultants, Inc.
E. von Goeler, Northeastern
A. Walenta, Heidelberg
D.H. White, Cornell
H. Wiedemann, SLAC
W.J. Willis, CERN
P. Wilson, SLAC
R. Wilson, Harvard
M.S. Witherell, Princeton
R.L. Young, Creare, Inc.
B. Zotter, CERN

TABLE OF CONTENTS

# EXPERIMENTAL HALLS WORKSHOP SUMMARY*

Alan Thorndike
Brookhaven National Laboratory

## I. INTRODUCTION

On May 26 and 27 approximately 50 people met for an informal workshop on plans for experimental halls for ISABELLE. A schedule the workshop, which was followed with minor modifications, is luded as Appendix I. The morning of the 26th was spent in presenting plans as they exist in the May 1976 version of the ISABELLE proposal. The remainder of the 26th and the first part of the 27th were spent in discussions of four general topics by separate working groups:

1. Pros and cons of open areas as compared with enclosed halls.
2. Experimental hall needs of ep, $\bar{p}p$, and other options.
3. Hall for the lepton detector.
4. Hall for the hadron spectrometer.

Many participants spent some time with more than one group, so the workshop developed in a fluid and informal way.

The latter part of the afternoon of the 27th was devoted to an overall summary. Pier Oddone explained the planning for experimental halls at PEP, Mike Kreisler summarized the discussions on the hall for the lepton detector, Satoshi Ozaki those on the hadron spectrometer, Dave Ayres those on open areas, and Lee Pondrom those on options.

The general organization of the workshop was the responsibility of Alan Thorndike, and the following notes have been prepared by him, based largely on the final afternoon session, with thanks to those who esented summaries at it.

---

*. Agoritsas, J. Alspector, D. Ayres, H. Brown, A. Carroll, R. Chasman, C.Y. Chien, Y. Cho, S.U. Chung, E.D. Courant, R. Drucker, A. Etkin, A. Fainberg, T. Ferbel, H. Foelsche, K. Foley, W. Frisken, H. Gordon, H. Hahn, J. Humphrey, S. Jacobs, M. Kreisler, T. Kycia, R. Lanou, Y.Y. Lee, S. Lindenbaum, D. Lowenstein, H. McChesney, K. McDonald, P. Mohn, M. Month, S. Ozaki, L. Pondrom, A. Prodell, N. Samios, J. Sandweiss, J. Sanford, J. Skelly, J. Spiro, A. Stevens, L. Sulak, W. Walker, C. Wang, E. Willen, R. Wilson, M. Witherell, F. Yamin.

## II. PROS AND CONS OF OPEN AREAS

The main reason for interest in having open areas with movable concrete block shielding at some insertions is the flexibility to make substantial changes in arrangements there after ISABELLE has been in operation for some time. This could be used to take care of needs that one could not anticipate before the machine had been in use. In addition, such areas would be likely to be available initially for small experiments (of the "nook and cranny" variety), which would be valuable. Open areas probably could be completed in a shorter time than an enclosed building, and this could be valuable in permitting use at an early time for access to the tunnel and other purposes involved in assembling and installing magnets and other components of ISABELLE.

The cost of open areas would be lower than that of enclosed buildings by perhaps 50 percent so long as the concrete block shielding could be obtained from the AGS inventory at no charge. If all shielding had to be purchased new, the open area approach would be considerably more expensive than for enclosed buildings. A minimal shield around the beam pipe would require about 5000 tons of shielding, while an enclosure big enough to accommodate a modest experiment would need 10 000 tons or more. The present AGS inventory is 84 000 tons. It seemed reasonable to assume that when ISABELLE is running there would be some reduction in scope of the AGS research program and that some fraction of the shielding could be used at ISABELLE. Such a condition would make open areas attractive from a cost standpoint. At the present time, however, all AGS shielding is in use and no surplus is envisioned. One would be reluctant to reduce the AGS research program just to provide shielding for ISABELLE areas, even though ISABELLE research will have a very high priority when the machine begins operation. Clearly plans for ISABELLE must fit into an overall plan for high-energy physics at Brookhaven (and elsewhere). One possibility is given in the report of the scenario group of the Insertion Workshops.[1] At the workshop it was assumed that up to 30 000 tons of shielding might be available.

---

1. A.M. Thorndike, these Proc.

To be useful for doing experiments the space in an open area must be protected against rain and snow and there must be some way to get equipment in and out and to move it around. In these respects it will be less efficient than the enclosed buildings with permanent crane coverage that are included in the present design.

Taking these pros and cons into account, the working group was in general agreement that very serious consideration should be given providing two open areas instead of the Little Hadron and Little ton halls. Several other suggestions were made:

1. Provide road access to both sides of areas if possible.

2. Make dimensions about 40 m by 60 m, with beam height at least 3 m, and 4 m if practical.

3. East and Southeast insertions seem to be the best locations for open areas.

4. Provide a wider tunnel for 20 - 30 m adjacent to the open areas if the cost is not excessive.

5. Shielding block enclosures should be designed for several experiments from the 1975 summer study with real shielding block dimensions to check feasibility.

6. Probably some blocks for the roof about 15 m long should be made.

Two arrangements were discussed. In the first the concrete block enclosure would be large enough to house a small crane, perhaps rolling on wheels like the Travellift, to handle pieces of experimental equipment. In the second the concrete block enclosure would be of minimum size, and an external crane would remove the shielding when access was required. This would probably be in a simple building, like EEBA, but much smaller in size. There was no agreement as which arrangement was preferable.

## III. NEEDS OF $\bar{p}p$, ep AND OTHER OPTIONS

### A. $\bar{p}p$ Option:

The experimental equipment for $\bar{p}p$ interactions would be the same as that for pp, or much like it, in many cases. The $\bar{p}p$ option has bending magnets to reduce the crossing angle to 3 mrad which reduce the free space at the intersections to about ± 13 m instead of ± 20 m. The lepton detector would fit between, but some arrangements would have to be modified, or the larger crossing angle and lower luminosity accepted. In the case of the hadron spectrometer described in the 1975 Summer Study those magnets interfere with the "E-magnet" location. In general, however, experimental halls suitable for pp are also suitable for $\bar{p}p$.

### B. ep Option:

In experiments involving ep interactions the aim will generally be to extend the range in $Q^2$ and s to higher values than have previously been possible. This means an ability to observe electrons at large angles, and over a large range of angles and momenta. Secondary nucleons will tend to be at angles close to the incident proton beam. This would seem to imply a hall with wide central part and beam arms, resembling that for the hadron spectrometer. In the 2-day workshop, however, detailed designs with dimensions were not prepared.

To make it easy to switch electron ring operation on and off, it is envisaged that the electrons would cross the protons at some intersections but not at all of them. The electrons might pass straight through the insertion above or below the proton crossing (about 90 cm away), but this would interfere with most experiments that might be installed and would usually not be possible. The electron ring can have a "bulge" which allows it to pass far enough outside the pp crossing to go around the experimental equipment installed there. This horizontal distance could be as much as 6 meters. The present experimental hall designs do not provide space for this bulge, which would begin to depart from the proton beam lines about 75 m away from the

crossing point. They should be designed so that a bulge can be added when and where it is necessary to do so. Deciding which intersections should have "bulges" is a complex topic which was discussed at some length, but without a firm conclusion.

Perhaps it will be possible to use one proton ring for electrons, somehow, in the end. That would be the simplest solution with respect to experimental halls. Various ideas for doing so were discussed, but was not clear whether they would really work, or would produce an quate electron energy. It seemed good to pursue any such possibilities, though that subject is clearly outside the scope of the workshop.

## IV. LEPTON DETECTOR HALL

### A. Conclusions on Building:

The enclosed building with poured concrete walls is satisfactory, and a construction schedule with main magnet pieces installed before completion of walls and roof would probably work best.[2] A 40-ton crane would be adequate, permitting calorimeter modules of 30 - 40 tons, with hook at least 20 ft above the beam line. The dimensions of the building should be increased to a length of 150 ft and width of 80 ft to provide adequate working space and room for detectors along the beam line. Heat and humidity control similar to EEBA would be adequate. Ventilation and other provision for combustible gases are required.

### B. Further Comments on Design:

Various electron detector and hadron calorimeter modules have to be inserted into the main magnet and removed from it, probably sliding on rails. Scaffolding and walkways will be needed for people to work rom,and space is needed for future "end caps" to detect particles nitted near the beam directions. The dimensions above provide room for these components in addition to the basic magnet structure.

---

2. These conclusions were modified to some degree in the Lepton Detector Workshop held subsequently. See M. Sakitt, these Proc.

Consideration should be given to placing a counting room right at the side of the magnet with sufficient shielding provided that it can be occupied when the proton beams are circulating. The main experimental living space would be in trailers or temporary buildings erected on the external pad as envisaged in the present experimental hall plans.

## V. HADRON SPECTROMETER HALL

The enclosed building with poured concrete walls is satisfactory, but there would be an advantage to having heavy concrete shielding between the hall and fast electronics room to make cables as short as possible. If this wall could be movable blocks or at least easy to penetrate for beam lines or modifications it would be valuable. The distance from floor to beam line in the beam arms should be adequate for the "D" and "E" magnets and detectors that go in them, which may require an increase from present plans. There may be advantages to having beam lines off-center in the hall, and location at a different insertion (now at the West insertion) may be preferable.

While the fast electronics room (for trigger circuitry) can be about 16 ft $\times$ 40 ft, a larger control room for data acquisition electronics and computers will also be needed, about 40 ft $\times$ 50 ft in size. It should be close to the hall since several thousand cables are anticipated, probably set into the sand shielding with a retaining wall.

Magnets are planned to be superconducting. Power supplies are small, but there will need to be space for compressors and gas-handling equipment to provide refrigeration. Experimental magnets would be off during injection and acceleration, and then turned on at a controlled rate so as not to disturb the circulating beams. Some additional service building space may be needed for those magnet-support functions.

It would be desirable to schedule the construction of the hadron spectrometer so that major magnet components could be put in place

before construction of ISABELLE is completed. Present spectrometer designs may not be final, however. During the two days there was an active discussion of the merits of different types of central spectrometers. The summary of the Hadron Spectrometer Workshop, held in July provides further information on hadron spectrometer needs.[3]

3. D.H. White, these Proc.

## APPENDIX I

## ISABELLE EXPERIMENTAL HALLS WORKSHOP

May 26 - 27, 1976

This workshop will provide an opportunity for discussion of topics such as: a) improved experimental flexibility through inclusion of open areas, b) the experimental area needs of experiments using ep, $\bar{p}p$, and other options, and c) the needs of large multipurpose detectors in terms of space, support facilities, installation schedules, etc. The workshop is open to all those interested in attending. There will be a general HEDG meeting on the 28th.

Space for participants will be available in the "Blue Building" (923) east of the AGS office building. The tentative schedule for the workshop is the following:

Wednesday, May 26

| | | |
|---|---|---|
| 9:00 | ISABELLE Status | Sanford |
| 9:15 | Site Plan and Halls in Proposal and Open Area Alternative | Mohn |
| 9:45 | Shielding Constraints | Thorndike |
| 10:00 | Coffee | |
| 10:15 | ep, $\bar{p}p$, and Other Options | Chasman |
| 10:45 | Lepton Detector | Michael |
| 11:00 | Hadron Spectrometer | Foley |
| 11:15 | General Discussion: | |
| | a) Pros and cons of open areas | |
| | b) Needs of ep, $\bar{p}p$, and other options | |
| | c) Needs of large detectors | |
| | d) Any other topics | |
| 12:30 | Lunch | |
| 1:30 | Formation of working groups, and group discussions | |
| 3:30 | Walk around ISABELLE location | |
| 6:00 | Dinner | |
| 7:30 | Working group activity | |

Thursday, May 27

8:30 Continued Working group activity

Informal visits to magnet R&D area

4:00 General session to identify:

a) Any conclusions reached

b) Specific questions for further study

6:00 Cocktails and Dinner - Berkner Hall

day, May 28

HEDG Meeting

# SUMMARY OF ISABELLE CRYOGENIC SYSTEMS WORKSHOP*

D.P. Brown
Brookhaven National Laboratory

## Introduction

Twenty-four people participated in the ISABELLE Cryogenic System Workshop which was held on June 2 and 3, 1976.

The magnet cooling system for ISABELLE, as described in the new proposal, utilizes supercritical helium as the refrigerant instead of pool-boiling helium as in earlier proposals. This new and more cost-effective system was described in detail with discussion of the design parameters for the refrigerator itself, turbomachinery required and the refrigerant distribution system. The testing and prototype development program for ISABELLE cryogenic system components was also reviewed. A small cryogenic turbocompressor/expander system is now on order for testing with an ISABELLE half-cell (2 dipoles and 1 quadrupole).

The main output of the workshop is a checklist of points which should be reviewed as the ISABELLE design proceeds.

The first morning was spent in a detailed description of the magnet cooling system which is summarized in the new (May 1976) ISABELLE proposal.[1] A summary of this material follows:

## Estimated Heat Loads

The magnets (see Fig. 1) to be used in ISABELLE are of the "warm bore" and "cold iron" type. The magnet vessel, which contains

*J.A. Bamberger, W. Colyer, A. Etkin, W.B. Fowler, R.J. Gibbs, H. Hahn J.W. Humphrey, D. Japikse, J.E. Jensen, R.I. Louttit, I.J. Polk, A.G. Prodell, C.H. Rode, W.B. Sampson, A.P. Schlafke, W.J. Schneider, R.P. Shutt, R.P. Smith, J. Sondericker, T.R. Strobridge, P.C. Vander Arend, A.P. Werner, L.R. Young.

1. ISABELLE A Proposal for Construction of a Proton-Proton Storage Accelerator Facility, BNL 50519 (May 1976).

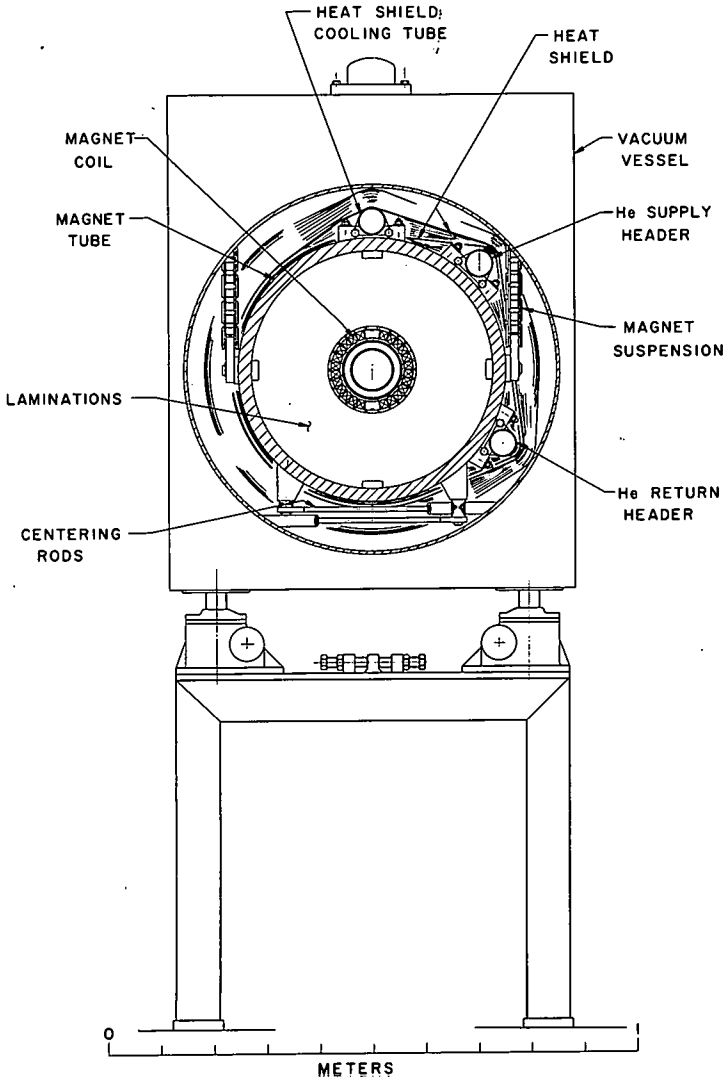


Fig. 1. Dipole dewar cross section.

the iron core as well as the superconducting coil, surrounds the beam pipe which is at room temperature. In the vacuum annulus radially outward from the magnet vessel is located a heat shield. This shield encloses the outside of the magnet vessel and three tubes. One tube carries the helium refrigerant which cools the heat shield. The other two tubes are refrigerant supply and return headers which are continuous completely around the ring. A multilayer insulation system is used inside and outside of the heat shield and between the warm beam tube and the inside wall of the magnet vessel.

Each dipole magnet (with a nominal length of 4.15 m) contributes 12.70 W to the heat load. Each quadrupole magnet (with a nominal length of 1.5 m) contributes 6.54 W. These losses do not include magnet power lead losses which have been considered separately.

Where there are long gaps (primarily at the experimental halls where the beams intersect) in the magnet lattice, it is necessary to transport the refrigerant in transfer lines. A supply header and a return header are carried through these regions in a common vacuum enclosure. A heat shield surrounding the supply header is attached to the return header in order to minimize the loss to the refrigerant supply. About 1440 m of such line is required.

The main magnet current leads are rated at 4000 A and one pair is required in each octant of each ring, i.e., the magnets of each octant are powered in series. The main refrigeration load from magnet current leads comes, not from these leads, but from the "protective leads" which are installed with one lead at each dipole. These leads do not normally carry any current but are only used to shunt current around a magnet which has quenched during the short period of time required to bring the main magnet current to zero. Thus, they "protect" the quenched magnet from overheating due to resistive heating. These "protective" leads contribute almost half of the total lead loss.

The estimated heat loads are listed in Table I. The loads are divided into two groups, primary and secondary. Those in the primary column are heat losses which cause a temperature rise in the helium refrigerant as it passes through the magnets. The heat loads in the secondary column are those which cause the temperature of the refrigerant to rise after it has passed through the magnets, i.e. it is the heat shield and support heat intercept cooling load. The lead flow is, of course, the helium flow required for the gas-cooled magnet current leads.

Design Heat Load and Temperatures

Protons are accelerated in ISABELLE from their injection energy of 30 GeV to the design operating energy of 200 GeV. This acceleration cycle occurs only infrequently, perhaps once per day. During the acceleration cycle additional losses are imposed on the system due to magnetization losses, eddy currents, etc. and beam radiation heating due to particles which are "lost" or escape from the beam during the acceleration cycle.

These losses have been estimated to be less than 2 W per meter of magnet length during the 100 second acceleration cycle. R.P. Shutt[2] has calculated the effect of this heat load on the magnet coil temperature. The conclusion that can be drawn from these calculations is that the temperature of the magnets before the acceleration cycle should be at least 0.2 K below the magnet design temperature of 4.5 K. For this reason, the steady state design temperature for the refrigeration system is chosen at 4.3 K.

On the basis of our past experience, and that of others, it is clear that the refrigerator capacity installed must be substantially greater than the load if the system is to perform reliably. We have chosen to multiply our estimated heat load by a factor of 1.5 in order to arrive at the heat load which is used to size the refrigerator.

2. R.P. Shutt, ISA Technical Note No. 8 (1976).

TABLE I. ISABELLE Estimated Steady-State Heat Load

| | Primary Load (W) | | Secondary Load (W) | | Total Load (W) | | Lead Flow g/s | |
|---|---|---|---|---|---|---|---|---|
| 4.15 m Dipole | | | | | | | | |
| Supports | 0.05 | | 4.95 | | 5.00 | | | |
| Vacuum Tank/Inner Vessel | 0.16 | | 4.22 | | 4.38 | | | |
| Beam Tube/Inner Vessel | 2.06 | | | | 2.06 | | | |
| Connecting Piping | 0.90 | | 0.55 | | 1.45 | | | |
| Total/Magnet | 3.17 | | 9.72 | | 12.89 | | | |
| Total/528 Magnets | | 1674 | | 5132 | | 6806 | | |
| 1.5 m Quad | | | | | | | | |
| Supports | 0.03 | | 2.97 | | 3.00 | | | |
| Vacuum Tank/Inner Vessel | 0.11 | | 1.63 | | 1.74 | | | |
| Beam Tube/Inner Vessel | 1.05 | | | | 1.05 | | | |
| Connecting Piping | 0.95 | | 0.58 | | 1.53 | | | |
| Total/Magnet | 2.14 | | 5.18 | | 7.32 | | | |
| Total/368 Magnets | | 788 | | 1906 | | 2694 | | |
| 3.0 m Quad | | | | | | | | |
| Supports | 0.04 | | 3.96 | | 4.00 | | | |
| Vacuum Tank/Inner Vessel | 0.21 | | 3.14 | | 3.35 | | | |
| Beam Tube/Inner Vessel | 2.10 | | | | 2.10 | | | |
| Connecting Piping | 0.95 | | 0.58 | | 1.53 | | | |
| Total/Magnet | 3.30 | | 7.68 | | 10.98 | | | |
| Total/64 Magnets | | 211 | | 492 | | 703 | | |
| Magnet Power Leads | | | | | | | | |
| Main Current | 153.6 | | | | 153.6 | | 7.68 | |
| Quad Main Correction | 92.8 | | | | 92.8 | | 4.64 | |
| Other Correction | 163.2 | | | | 163.2 | | 8.16 | |
| Protective | 614.4 | | | | 614.4 | | 18.40 | |
| Insertion Quads | 153.6 | | 153.6 | | 307.2 | | 15.36 | |
| Total/All Power Leads | | 1177 | | 154 | | 1331 | | 54.2 |
| Transfer Lines | | 5 | | 573 | | 578 | | |
| ISABELLE Total | | 3855 | | 8257 | | 12112 | | 54.2 |

Table II summarizes the design heat loads and temperatures used in the refrigerator design.

TABLE II. Design Heat Loads and Temperatures

| | |
|---|---|
| Primary Load | 5200 W |
| Secondary Load | 12000 W |
| Lead Flow | 81 g/sec |
| Maximum Magnet Temperature | 4.5 K |
| Maximum Steady-State Magnet Temperature | 4.3 K |

Refrigerator Design

Only a single refrigerator is proposed for ISABELLE. Sufficient distances can be covered, using the distribution system envisaged and without undue pressure drop or other penalties, so that all the refrigeration can be supplied from a single point. More than one smaller refrigerator could have been used at this point, but a single unit was chosen primarily on the basis of reliability and cost considerations.

The magnets in ISABELLE are designed to be cooled with refrigerant at an elevated pressure, 15 atm, at the inlet. Because this type of system is nonisothermal, it is desirable to enter the magnets to be cooled at a low temperature. This reduces the mass flow rate required to remove a given amount of heat below a fixed temperature level and/or allows more magnets to be cooled in series before the maximum desired temperature is reached. We have studied several systems which could be used to produce the desired low temperature.

The system chosen for use with ISABELLE utilizes a turbocompressor to lower the pressure of the subcooler heat exchanger bath. This system is shown schematically in Fig. 2 and a T-S diagram of the cycle is shown in Fig. 3. A turbocompressor/expander operating at this temperature and pressure range has not, to date, been reported in the literature. BNL, therefore, obtained the services of a turbomachinery consultant, Creare, Inc., to perform a feasibility study of

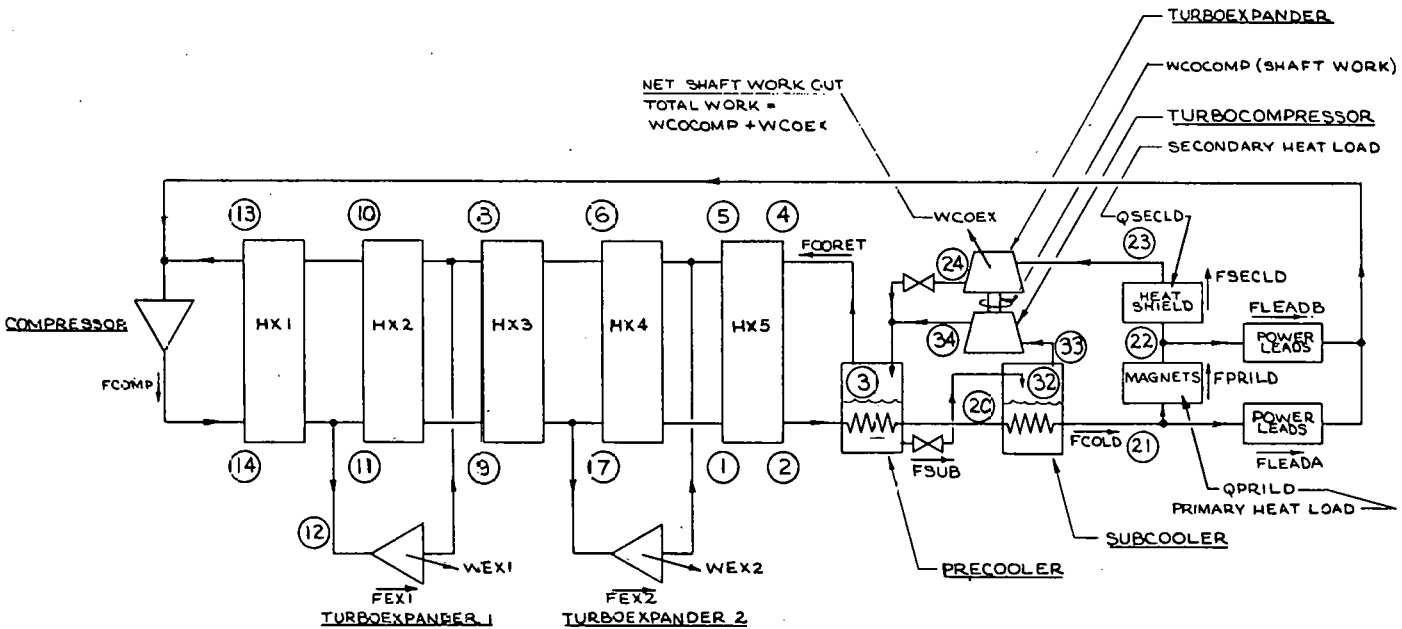


Fig. 2. ISABELLE Refrigerator Flow Schematic.

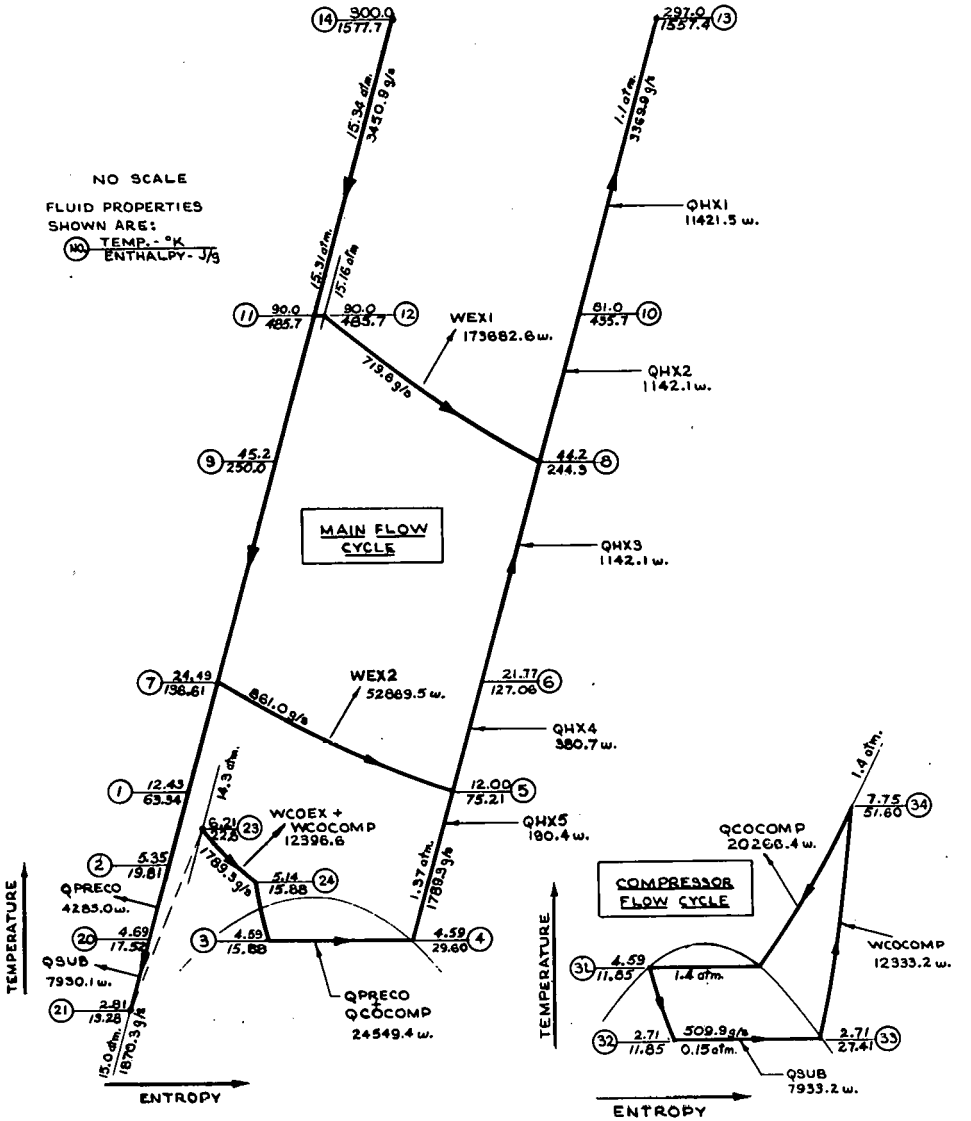


Fig. 3. Helium Refrigerator T-S Diagram.

the requirements for this system. They reported favorably and BNL is now proceeding toward a final design and subsequent procurement of a prototype subcooler system of this type.

Other than the subcooler, the refrigerator required for ISABELLE will be of conventional design. Liquid nitrogen will not be used for precooling. The use of liquid nitrogen during cooldown was studied and it was concluded that it was not required as a reasonable cool-down time (12-14 days) could be obtained without its use.

Refrigeration Distribution and Control

A simplified flow schematic for the refrigeration distribution system for one of the two ISABELLE rings is shown in Fig. 4. A supply header and a return header run completely around the ring. The flow for series cooling of the magnets in each octant is routed from the supply header, through the magnets to be cooled, returns through the heat shield cooling tube around those same magnets and then flows through the return header to the refrigerator. Not shown on this schematic is the fact that the 8 quadrupole magnets in the insertion section are not in series with the rest of the magnets in the octant. This was done to avoid the additional transfer lines required to arrange for them to be in series with the other 52 magnets in their octant. Also not shown is a warm return line to the compressors. This return is for the power lead cooling flow which is taken from the main refrigerant stream as required.

The system is being designed to accept a flow rate of 117 g/sec for each octant. With this flow rate, the expected pressure drop in the supply header (for the octant furthest from the refrigerator) is 0.2 atm. The pressure drop through the magnets is calculated at 0.3 atm. The expected pressure drop in the return header is 0.2 atm. This pressure drop is recognized as one of the inefficiencies in the system and every effort, consistent with good design of the overall magnet/refrigerator system, to reduce it will be made. The pressure drop, as now calculated, is felt to be acceptable and is regarded as

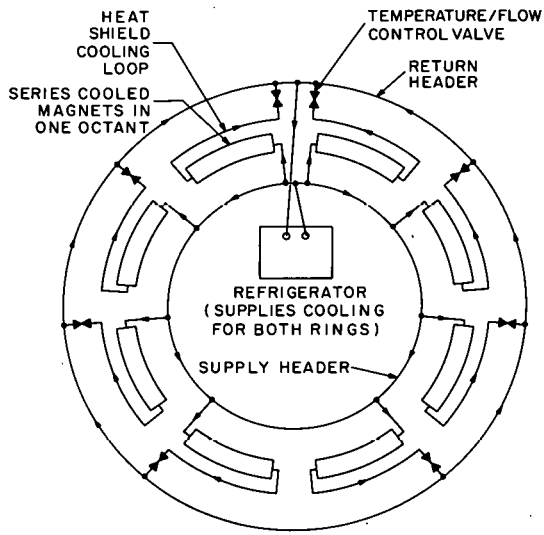


Fig. 4. Simplified schematic of refrigerant distribution system for one ring of ISABELLE.

an upper limit. For a zero pressure drop distribution system the flow requirements would be reduced by 8.3%.

The superconducting magnet coils have fiberglass-epoxy bands inside and outside of them. The bands are 2.5 cm wide and are spaced 2.5 cm apart. These bands are slotted so that the refrigerant can flow along the length of the coil. There are also slots in the outside of iron core to carry the superconducting bus bars which connect the magnets in series as well as instrumentation wiring. The flow through these slots can be adjusted by restricting the flow passage as desired. Some of the flow (perhaps as much as 50%) will be allowed to go through these passages. This permits a lower overall pressure drop. Because the flows recombine to pass from one magnet to the next, the increased temperature rise in a given coil is not a problem until the last magnet (assuming less than 50% is bypassed through the iron core slots). A slight increase in flow rate would bring this last magnet below the required maximum temperature. The reduced pressure drop should more than compensate for the increased flow. The increased flow area and heat exchange area presented by the iron core bypass also permits faster cooldown times.

Because so many magnets are in series, only a relatively few distribution controls are required. The 16 main octant control loops and the loops required for the insertion section quadrupoles will be in parallel. The temperature at the outlet of each loop will be measured and used as the control point for a modulating valve. A control system will monitor the supply header pressure and increase flow to each loop in proportion to its heat load until the entire capacity of the refrigerator is utilized. This would uniformly drive the temperature of all the ISABELLE magnets to the lowest temperature attainable under the given load conditions. The gas returning to the refrigerator as well as the magnets may be below design temperature. A heater will be installed in the return line so that the temperature of the gas entering the turboexpander in series with the load can be raised to its optimum operating temperature when that temperature is too low.

Redundant Components

As a single refrigerator is to be used for ISABELLE, it is very important that it be as reliable as possible. Toward this end, the following components (at least) will be completely redundant (see Fig. 2):

Heat Exchangers 1 and 2 (HX1 and HX2),
Turboexpander 1,
Turboexpander 2.

Turbomachinery

Following this description of the ISABELLE refrigeration system, Larry Young of Creare, Inc. gave a summary of the design work his firm had done for turbomachinery which could meet the requirements for the subcooler in the cycle.

Most of the interest of the group focused on the small prototype expander/compressor unit which BNL now has on order. The small size (the expander wheel is 0.200 inch diameter and the compressor is 0.320 inch diameter) of this equipment presents miniaturization problems which Creare feels can be overcome. Specific problems were discussed: (1) Tolerance stack-up, (2) leakage of warm bearings gas into the cryogenic stream, (3) mechanical integrity of the wheel which has blade thicknesses of 0.004 to 0.006 inches, (4) contamination of process stream, and (5) expense. This unit is designed to match the capability (200 W) of the refrigerator currently used for testing in the ISABELLE Division. One suggestion was to design the unit for one of the larger BNL refrigerators (700 W or 1100 W).

The group toured the cryogenic facilities of the ISABELLE Division and visited the Superconducting Transmission Line screw comessor test facility and their refrigerator installation.

A list of points which should be checked as the ISABELLE design proceeds was generated. Many of the points have been subject to some study already and complete or partial answers on these points are already forthcoming.

Suggested Areas of Engineering Study

I. Steady-State Operation
   A. Refrigeration Cycle Design
   B. Refrigeration Distribution System
      1. Cost
      2. Efficiency
   C. Turbomachinery
      1. Design requirements
      2. Availability of gas bearings in large sizes
   D. Compressor Type Selection Considerations
      1. Reliability
      2. Efficiency
      3. Cost
      4. Availability in required size range
   E. Gas Purification and Impurity Analysis Equipment
   F. Establish Maximum Helium Loss Rate/Usage Allowable
      1. Component design requirements

II. Nonsteady-State Operation
   A. Cryogenic System Purge Procedure
   B. Cooldown
      1. Liquid helium storage desirability
      2. Cooldown rate thermal stress limitations
      3. Warmup/cooldown of single octant for repairs
   C. Quench Behavior and Propagation Patterns
   D. Warmup Method
   E. Failure Mode Analysis
      1. Protective diodes - on-line diagnostics?
   F. Gas Recovery System Operation

III. Magnet/Cryogenic System Interface
   A. Review of Suitability of Materials Used at Cryogenic Temperatures
   B. Possible Cooldown Weight Reduction by "Holes" in Laminations

C. Multilayer Cryogenic Insulation System Evaluation

1. Establish apparent thermal conductivity as installed
2. Pumpdown times
3. Cost effectiveness.

# LEPTON DETECTOR WORKSHOP SUMMARY

R. Imlay
Rutgers University
S. Iwata
Nagoya University
S. Jacobs
Brandeis University
R. Kraemer
Carnegie-Mellon University
M. Kreisler
University of Massachusetts, Amherst
K. McDonald
University of Chicago
P. McIntyre
Harvard University
J. Thompson
University of Pittsburgh
A. Walenta
University of Heidelberg
and
I.H. Chiang, M. Sakitt, A. Thorndike, C. Wang, L.L. Wang
Brookhaven National Laboratory

## 1. INTRODUCTION

The study group met from June 7 to 11, 1976, with the dual purpose of reviewing the earlier Lepton Detector report[1] in order to resolve some of the remaining design problems and of considering possible alternatives. Since the role of this group was primarily that of providing a critique of the earlier work, the reader is referred to that earlier paper[1] for the general motivation and design of the detector, and we will here only describe problems that were studied at this

1. R. Burnstein, W.C. Carithers, M. Duong-van, R. Imlay, M. Kreisler, U. Nauenberg, C. Rubbia, L. Sulak, G. Snow, H.H. Williams, E. Paschos, M. Sakitt, C.L. Wang, and L.L. Wang, Proc. 1975 ISABELLE Summer Study, Brookhaven, BNL 20550, p. 9.

session. The general configuration of the detector is shown in Fig. 1.

During the first day of the study we discussed the old design, which led us to focusing our efforts on the cost estimates and on a more careful look at the inner detector modules. In the original paper there was a fair amount of uncertainty in some of the cost estimates, and we felt an effort should be made to pinpoint where it seems firm and where a rough guess was made. With regard to ier modules we wanted to examine the rate problem for the closest elements more carefully and to discuss the question whether one should use argon or lead-liquid scintillator calorimeters. As is usually the case, in discussion of these major topics many smaller problems were considered and some of them are also discussed below.

We planned to spend the last day or two on new designs which involved major modifications to the lepton detector. The major motivations for alternative designs were twofold. One was that the original detector looked quite expensive, and a study of the tradeoff of money versus physics had not really been done yet. The second point was that, since the physics region to be explored was totally new ground, one would like to leave as many options open as possible and build a detector that was as flexible as possible. While at times these two points were in conflict, the real question that was asked was whether it would be possible to build a cheaper, more modular structure which could be reassembled in different configurations. Three main alternatives were discussed. The first is a scaled-down version (Section III A) of the original design, which was strongly favored by this study. It appears that one can save an appreciable amount of money with a small decrease in the initial physics scope. The more modular signs (Sections III B, III C) seem quite attractive but not enough ime was spent to demonstrate feasibility. They are more in the spirit of a conjecture than a design.

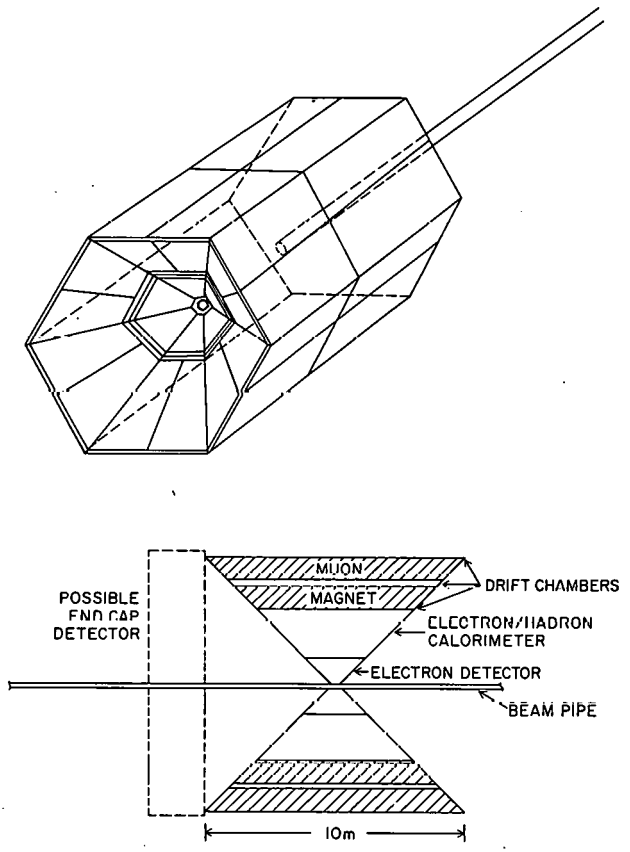


Fig. 1. A schematic drawing of the ISA Summer Study 1975 Design for a Lepton Detector.

## II. COMMENTS ON THE 1975 PLAN

### A. Data Collection and Counting Rates in the Liquid Argon Calorimeters

A fundamental limit on the liquid argon calorimeter data collection is the electron mobility ($\sim$ 5 mm/$\mu$sec at 1 kV/mm). If steel electrodes are rounded, the breakdown voltage is $\geq$ 10 kV for - ? mm gap. Working chambers have been used at 2 kV/2 mm gap with drift time of 180 nsec/mm or $\sim$ 0.4 $\mu$sec time to collect all charge across the gap. The resolving time of the associated circuitry is $\sim$ 0.6 $\mu$sec, well matched to the collection time.

Based on the acceptance of the calorimeter and scaling from ISR energies and luminosities, we estimated $\sim$ 3 particles/event and $\sim$ 1 event/25 nsec, or an average rate of 1 particle in the detector array/8 nsec (at $10^{33}$ luminosity). Whether this is a problem for the liquid argon calorimeter depends on the size of the individual elements.

There are six units, each about 1 meter wide by 2 meters long, so the area is about $6 \times 1\ m \times 2\ m \sim 12\ m^2$.

Originally 5 cm x 5 cm Pb collection plates were proposed. In this case:

$$\text{Average counting rate in 1 collection plate} = \frac{\text{Area of 1 collection plate}}{\text{Area of electron detector}} \times \text{counting rate in total detector (all sextants)}$$

$$= \frac{25 \times 10^{-4}\ m^2}{12\ m^2} \times \frac{3 \text{ particles/event}}{25 \text{ nsec/sec}}$$

$$= 0.25 \times 10^5 \text{ particles/sec.}$$

Thus the accidental rate in one plate, using a time window of 0.6 $\mu$sec, is 1.5%. However, for complexity and cost reasons (see next section), a configuration of 5 cm by 1 m strips was proposed as an alternative.

The average counting rate in these strips would be $0.5 \times 10^6$ particles/sec leading to an accidental rate of $\sim$ 30%.

These accidental rates are quite high. By adding $CH_4$ to the argon one can reduce, by roughly 1/4, the collection time in the calorimeter. Then, if one speeds up the associated electronics, which seems feasible, the accidental rate can be significantly reduced. Since one is interested only in high $P_\perp$ particles, one should note that most of the rates are from very low momentum particles and can be excluded by raising the electron calorimeter threshold and introducing a $P_\perp$ cut-off on the electrons accepted in the trigger. For example, one expects only $\sim$ 2000 $\pi$'s with momentum > 5 GeV, even at $10^{33}$ luminosity in the entire detector, compared with a $10^8$ estimated total counting rate. Thus one may wish to raise the electron calorimeter threshold but to protect the calorimeter circuitry against "pile-up" (a number of small pulses faking a large one) by monitoring the pulse shape.

B. Electron Calorimeter: Spatial Resolution vs Cost

Originally collection plates of 5 cm x 5 cm were proposed for the electron calorimeter. However, collection plates of 5 cm x 5 cm throughout the electron calorimeter volume would imply

$$\frac{\#\text{ channels}}{\text{sampling plane}} = \frac{\text{Area of total detector presented to particles}}{\text{Area of plate}}$$

$$= \frac{12\ \text{m}^2}{25 \times 10^{-4}\ \text{m}^2} = 5\ \text{K channels/sampling plane}$$

If one includes 20-100 sampling planes as was done in the CERN device, the 5 cm x 5 cm plates quickly give an intolerably large number of channels, both in terms of cost and in terms of the number of words read into a computer record.

Thus a decision was made to consider a system of 5 cm crossed strips rather than 5 cm squares, (60 channels/sextant/sampling plane, or 360 channels/sampling plane) and to gang several sampling planes together so that one would only require electronics readouts for

~ 5 groups of sampling planes. Using such a configuration would reduce the number of channels to ~ 1800 and the cost for electronics to 1800 channels x $250/channel or ~ $450 K.

The number of channels may be reduced still further by careful study of the design of the CERN experiment. In that experiment, a rejection of 200:1 with 85% electron efficiency for 4 GeV electrons was achieved by looking only at the first 6 interaction lengths eparately at the first three and the second three interaction ngths) and, in fact, the entire calorimeter in the CERN experiment (comparable to our proposed electron calorimeter) had only 112 channels. High anticipated counting rates may dictate a higher number of channels in our case, but this point should be reviewed with reference to the CERN design.

C. Other Questions Raised but Not Settled, with Respect to Calorimeters

1. Magnetization of calorimeter plates: This has been suggested either advertently, to get more bending for the muon detector, or inadvertently, as a by-product of placing a magnet in the inner electron-hadron detector space. The question here is: how will the operation of the calorimeter be affected? Have calorimeters actually been operated in magnetic fields?

2. How will the stability and performance of the liquid argon compare in an experimental running situation with the known radiation damage problems of Pb-glass or with a possible $BaF_2$ - Decalin solution?

3. The original design allocated 30 cm in the radial direction for the electron calorimeter. One needs 30 cm for the lead and rgon in order to get the necessary 20 radiation lengths. In the ERN design 20 cm was used for insulation which would lead to a total length of 50 cm. Some compression might be accomplished by more careful study but clearly a little more room is necessary.

D. An Alternative Steel-Liquid Scintillator Hadron Calorimeter

A steel scintillator hadron calorimeter was discussed as a possible alternate to the liquid argon calorimeter previously proposed. The calorimeter is assumed to be 1.4 m thick and to start 1.3 m from the beam line. It has 64 steel plates 1.5 cm thick separated by 0.66 cm gaps filled with liquid scintillator. It weighs 500 to 600 tons (the same as the argon calorimeter). The calorimeter is made up of 336 optical units parallel to the beam line with a phototube at each end of an optical unit. Each phototube observes an area of approximately 32 cm by 17 cm (8 gaps). The lengths of the optical units (from 2.75 m to 5.25 m) are chosen to cover the angular region $\pm 45^{\circ}$. The units are assumed to be constructed in a fashion similar to existing calorimeters. The only significant difference is that some of the proposed units are very long (5.25 m). It is felt to be better to use these long units rather than introduce phototubes and substantial dead space in the center of the detector.

The position of the energy deposited in an optical unit can be located to a few centimeters using the ratio of the pulse height on the phototubes at the two ends. The sum of the pulse heights at the two ends will give a measurement of the energy deposited after a correction for the position of the energy deposit. For the longest units (5.25 m) it would probably be necessary to make changes to obtain a more uniform response of the summed pulse height to the position of the energy deposited.

Approximate costs are (a) steel (500 tons) \$300 K, (b) scintillator (50 tons) \$100 K, (c) containers, Teflon, assembly \$250 K, (d) 700 phototubes and bases \$70 K.

E. Cost Estimate for 1975 Plan

The largest single element in the detector cost is the muon detector magnet, which has a weight of 5000 tons and a copper coil of 20 tons. We used \$0.30 per pound for cost of magnet iron (with a

minimum of machining) and $3.00 per pound for the copper coil. This leads to $3000 K for iron and $120 K for coil. An estimate of $100 K was made for the cost of installation, assembly, welding, etc., leading to a total cost of $3220 K.

In addition, the magnet needs to have dc power and cooling water for a maximum level of 4 MW. If all costs of providing this are included the cost might be as great as $1000 K, but some fraction of it is needed is included in the general facilities planned for ABELLE. The incremental cost of the lepton detector may be considerably less, but the $1000 K sum is included to be conservative.

The cost of the transition radiation unit was taken to be $215 K as estimated in the summer study.

The cost of hadron and electron calorimeters were estimated on the basis of $1.25 per pound to include machining plates, supports, providing vacuum systems, etc., for a unit consisting primarily of steel plates, made with moderate precision. The total weight of the hadron calorimeter was taken to be 550 tons and the electron calorimeter 35 tons. The corresponding costs (exclusive of electronics) are then $1400 K and $87 K. In addition, a refrigerator would be needed for liquid argon calorimeters. Its cost was estimated (very roughly) at $40 K. To move these heavy calorimeter units in and out of the magnet structure will require a well-engineered mounting and support system, which has not been designed. To give some rough estimate of its cost, 10% of the calorimeter cost was used, an additional $150 K.

Electronics for this large calorimeter system add a substantial cost. As described previously, approximately 2600 analog channels were envisaged in order to provide adequate space resolution, 1800 for the electron calorimeter, 800 for the hadron. Estimated cost per channel of $250 led to a total electronics cost of $650 K.

Drift chamber costs were taken at $30 per wire for construction and $50 per wire for electronics, based on current experience with large drift chambers. About 50 chambers would be required, each 4 m x 4 m in size with 160 wires, for a total of 8000 wires. This leads to a drift chamber construction cost of $240 K and an electronics cost of $400 K.

A data-acquisition computer will certainly be needed. It might be possible to use a central facility, but since data rates may be quite high it was thought wise to provide $200 K for data handling dedicated to the lepton detector.

Cost Summary 1975 Design
($ in thousands)

| | | |
|---|---|---|
| Magnet | 3 220 | |
| Magnet power supply and cooling system | 1 000 | (max) |
| Transition radiation unit | 215 | |
| Hadron calorimeter units | 1 400 | |
| Electron calorimeter units | 87 | |
| Refrigerator for calorimeters | 40 | |
| Calorimeter supports | 150 | |
| Calorimeter electronics | 650 | |
| Drift chamber construction | 240 | |
| Drift chamber electronics | 400 | |
| Data handling computer | 200 | |
| TOTAL | 7 600 | |

These estimates are quite rough, but the intention was to put in all major items and to put in amounts that ought to be adequate. No large additional contingency should be needed. The incremental cost for the magnet power supply and cooling, estimated at $1000 K, due to the lepton detector may be much lower, if these needs are met by general ISABELLE facilities. The overall estimate might be rounded off to $8 000 000. This does not include any cost escalation to some future time at which it might be built. It does not include the experimental hall and supporting space to house electronics, which are assumed to be provided as ISABELLE facilities.

F. Construction Schedule for 1975 Summer Study Design

The schedule outlined below is aimed at having a useful lepton detector in June 1983, the time scheduled for ISABELLE turn-on in the May 1976 ISABELLE proposal.

| Fiscal Years | Activities |
|---|---|
| 1977-78 | Prepare proposal for funding with general design and costs. |
| 1979 | Design magnet in detail. |
| 1980-81 | Finish detector design.<br>Procure main components of magnet.<br>Build first detector elements. |
| 1982 | Install magnet, power supply, etc.<br>Test detectors at AGS.<br>Build additional detectors. |
| 1983 | Install initial detectors in magnet.<br>Tests with first ISA beam. |
| 1984 | Begin research program.<br>Take initial data.<br>Install more complete detectors. |

In the ISABELLE proposal all buildings are scheduled to be completed by 1981. This provides adequate time for the magnet to be assembled in its building before ISABELLE operation begins, as in the above schedule. There is not time for much delay, however, and consequently such a plan requires funding for the lepton detector soon after funding for ISABELLE.

G. Space Requirements for 1975 Summer Study Design

The space requirements are set by the needs to get calorimeter modules in and out of the magnet structure. The magnet is hexagonal, so that there would be 12 hadron calorimeter modules if they are divided at the middle and installed through the open end. If the

total weight is 550 tons this gives 47 tons per module. A strong support system will be needed for sliding modules in and out. Outside they can be lifted by crane. A 40-ton crane would limit the module to a smaller size, so a 60-ton crane is preferable.

The magnet extends 5 meters from the central line, and the calorimeter module is about three meters long. For a high-luminosity insertion the free space is ± 13 meters, which provides a reasonable amount of extra space except for the need to provide for future "end caps". The consensus was to postpone the design of the end cap till after the initial detector is working since the early physics results may strongly influence the final design.

H. Possibility of Measuring the Di-Muon Continuum -- A Rough Rate Calculation

As part of the 1976 Workshop on the Lepton Detector, we considered the possible experimental program for the detector in addition to discovering the W. This note considers the rough rates for a measurement of the cross section $p + p \rightarrow \ell^+ + \ell^- + X$ as a function of $m_{\ell\ell}$ using the present design of the lepton detector.

We use as a starting point the scaling function $m_{\ell\ell}^3 \, d\sigma/dm_{\ell\ell}$ vs $s/m_{\ell\ell}^2$ as shown in Fig. 2 (originally Fig. 4, of Ref. 1).

We consider the case of ISABELLE running at 200 GeV x 200 GeV with a luminosity of $10^{32}$. The lepton detector has a minimum muon momentum cutoff of $\approx$ 8 GeV/c. For practical considerations, this implies a minimum di-muon mass of 20 GeV, corresponding to $s/m^2 = 400$. From Fig. 2, $m^3 \, d\sigma/dm$ is roughly flat down to $s/m^2 = 40$ and then falls off rapidly. (Since $d\sigma/dm$ decreases as the cube of the mass, we will not consider $s/m^2$ smaller than 40 in much detail.) $s/m^2 = 40$ implies $m_{\mu\mu} = 65$ GeV.

The counting rates assuming $\Delta\Omega/4\pi = \frac{1}{2}$ are shown in Fig. 3. We note with some distress that measurements above $m_{\ell\ell} \sim 70$ GeV become

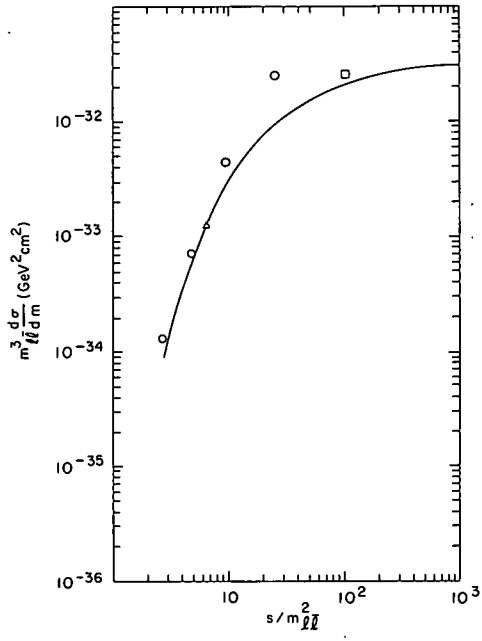


Fig. 2. The scaling function integrated over the entire range of Y. (From ISA Summer Study 1975.)

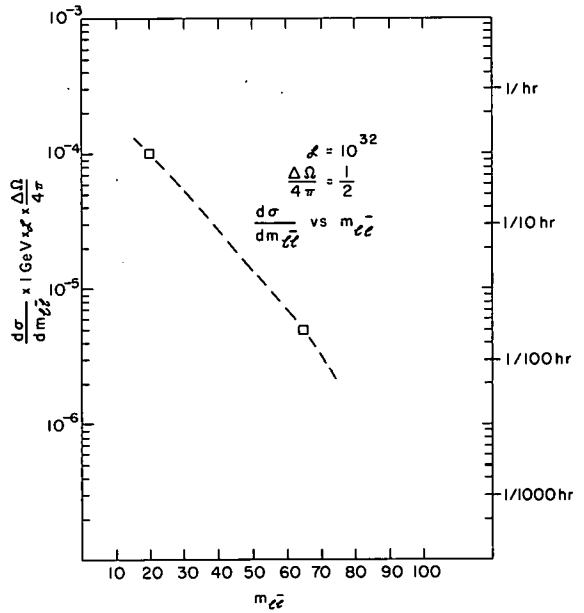


Fig. 3. Counting rates as a function of mass.

extremely difficult -- even with a detector as massive as the lepton detector.

In order to have 10 events in the highest mass bin (60 → 70 GeV), how long a run is required? Since the momentum resolution is ~ 12%, $\Delta m/m \sim 15\%$. Thus, the bin size is ~ 10 GeV in mass. The counting rate in this bin is therefore

$$\frac{d\sigma}{dm} \times 10 \text{ GeV} \times \frac{\Delta\Omega}{4\pi} \times \mathcal{L} = 5 \times 10^{-5} \quad \text{(at 65 GeV)}$$

Therefore in 2 days, one would expect 10 events. A one-week run would produce ample statistics. We note that at 20 GeV, $\Delta m = 3$ GeV,

$$\frac{d\sigma}{dm} \times 3 \text{ GeV} \times \frac{\Delta\Omega}{4\pi} \times \mathcal{L} = 3 \times 10^{-4}$$

or approximately 60 events in a 3 GeV bin. This level of statistics would be sufficient to differentiate between the various quark predictions -- we note that the introduction of color reduces the estimate by a factor of 3. Newer data on the scaling function leads one to expect the lower curve, with the reduction of 3 to be more realistic. The possible results of a 2-day run are shown in Fig. 4. It therefore appears quite reasonable to measure the di-muon continuum with the lepton detector.

## III. OPTIONS AND NEW IDEAS

### A. Reduced Scale Option

#### 1. General Concept

Since the magnet represents a large fraction of the total cost of the initial detector, we considered reducing the size of the inner detector modules so that the magnet could be smaller. In the reduced scale option we propose that the inner detector elements no longer have the capability, in each sector, to identify electrons

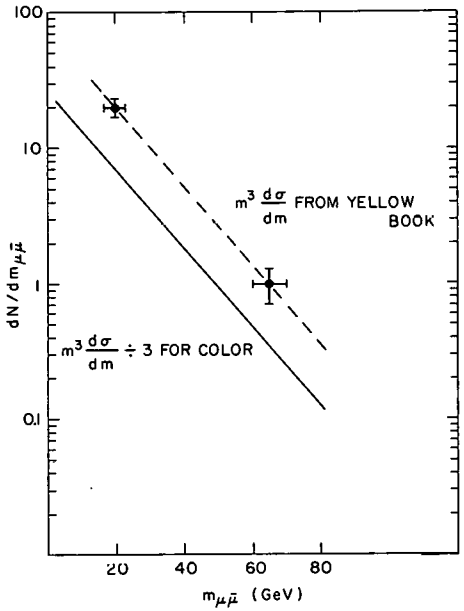


Fig. 4. Results for a two-day run.

and have the full electron and hadron calorimeters. There would be two different types of modules. One would contain the transition radiators and the electron calorimeter and the other would contain only the electron and hadron calorimeters. We can consider an initial experiment comprised of alternating types of modules. In detecting the muonic decay of the W, there is no loss of solid angle in this reduced version compared to the original design, while for the electronic decay we lose a factor of 2. Clearly any $\mu e$ correlations are also reduced by a factor of 2 in this initial configuration. Depending on the early performance of the detector and the early physics results, one always has the option of changing the modular configuration.

If we were optimistic we could believe the calculations for W production and then ask if we could do physics without any transition radiation modules. Filling all the sectors with an electromagnetic calorimeter followed by the hadronic calorimeter would still give us hadron rejection against electrons of at least $10^2$. Taking the W cross sections literally, we would have a $\pi$ background of less than 10% in our electron sample, which still allows us to clearly see the W, without any loss of solid angle in comparison to the large-scale detector. Clearly one can fill half the sectors first with calorimeters and make the final decision concerning what goes in the other half after the initial run. Since this is more speculative than our general approach, we will do the cost estimate assuming two different type modules as described previously. The cost estimate using all calorimeters would be about $400 K more than the estimates that follow.

2. Cost and Space Requirements

The cost of the magnet scales approximately as the volume of the iron, which is estimated to be 62% of the original in the reduced scale design. There is a saving of 38% in both magnet and power

supply, etc. This is 0.38 x 4220 = $1600 K.

Since the transition radiation unit would only occupy three sectors instead of six, a reduction of $100 K is estimated.

The number of hadron calorimeter modules would also be reduced by a factor of two and the size of each would be reduced. There is a saving in construction, supports, and electronics, totalling $1300 K. There is, however, no significant reduction in the cost electron calorimeters.

The drift chambers will be smaller in size, with fewer wires. This will lead to a reduction in cost of about $200 K, including electronics. These reductions are summarized below:

Cost Reduction with Reduced Scale
($ in thousands)

| | |
|---|---|
| Magnet and power supply | 1 600 |
| Transition radiation unit | 100 |
| Hadron calorimeter total | 1 300 |
| Drift chambers | 200 |
| Total Reduction | 3 200 |
| Resulting Cost Estimate | 4 552 |

The overall result is to reduce the cost estimate from $7 752 000 to $4 552 000. This alternative might, therefore, prove to be an attractive one since it does not rule out any of the kinds of experiments for which the lepton detector would be built.

No detailed consideration was given to the schedule for implementation of a reduced scale design, but it was thought that there ould not be any significant change in times required from those of the larger version.

The space requirements would, on the other hand, clearly be less for the reduced scale version. The difference is small enough to be within the uncertainties of the discussions held. There was some feeling that the experimental hall dimensions in the 1976 Proposal would be adequate for the reduced scale design but not for the full scale. If so, the reduced scale would be advantageous for that reason also.

An extra option that was briefly considered for the scaled-down version was an inner toroid magnet creating a field concentration around the beam. This would allow one to determine the sign of the electrons. It would however cut down on the acceptance and raise the cost of the detector. More design work would be necessary before one could decide if this was a feasible option.

B. Alternative Modular Magnet Assembly

The inner detectors were designed in a modular fashion to allow some flexibility for future innovation resulting from both technology advances and the early physics results. An attempt was made with a similar motive to see if one could conceive of the large magnet as being composed of module sections.

1. Hexagonal Configuration

A scheme was envisaged for assembling a hexagonal magnet in two layers with the outside edge 4.2 m from the beam line with blocks of iron with individual windings built into each of the blocks. A sketch of the individual blocks is shown in Fig. 5 and the assembly is shown in Fig. 6. The magnetic circuit goes around the hexagon as in the original design. The unit construction means that it could be enlarged by adding blocks, and additional iron shells could be added with a similar construction.

The outer hexagon has 54 rectangular blocks and 6 corner fillers, while the inner one has 24 and 6. For simplicity in assembly the

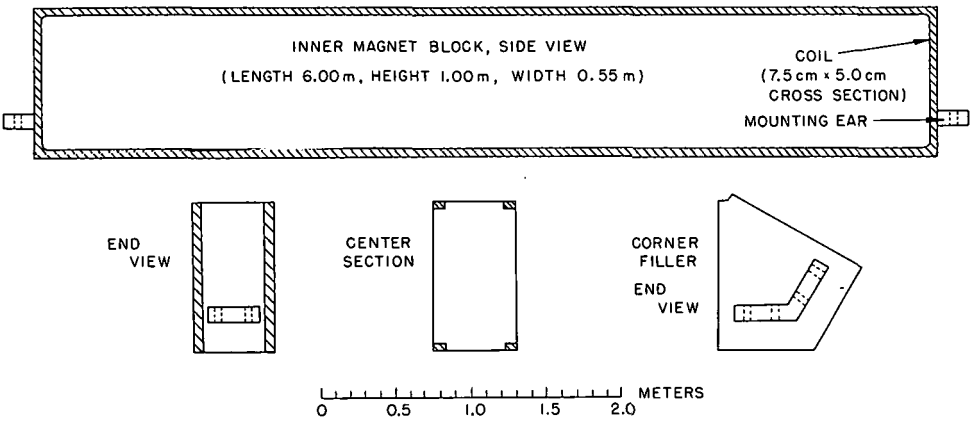


Fig. 5. Sketch of an individual block used in the hexagonal assembly.

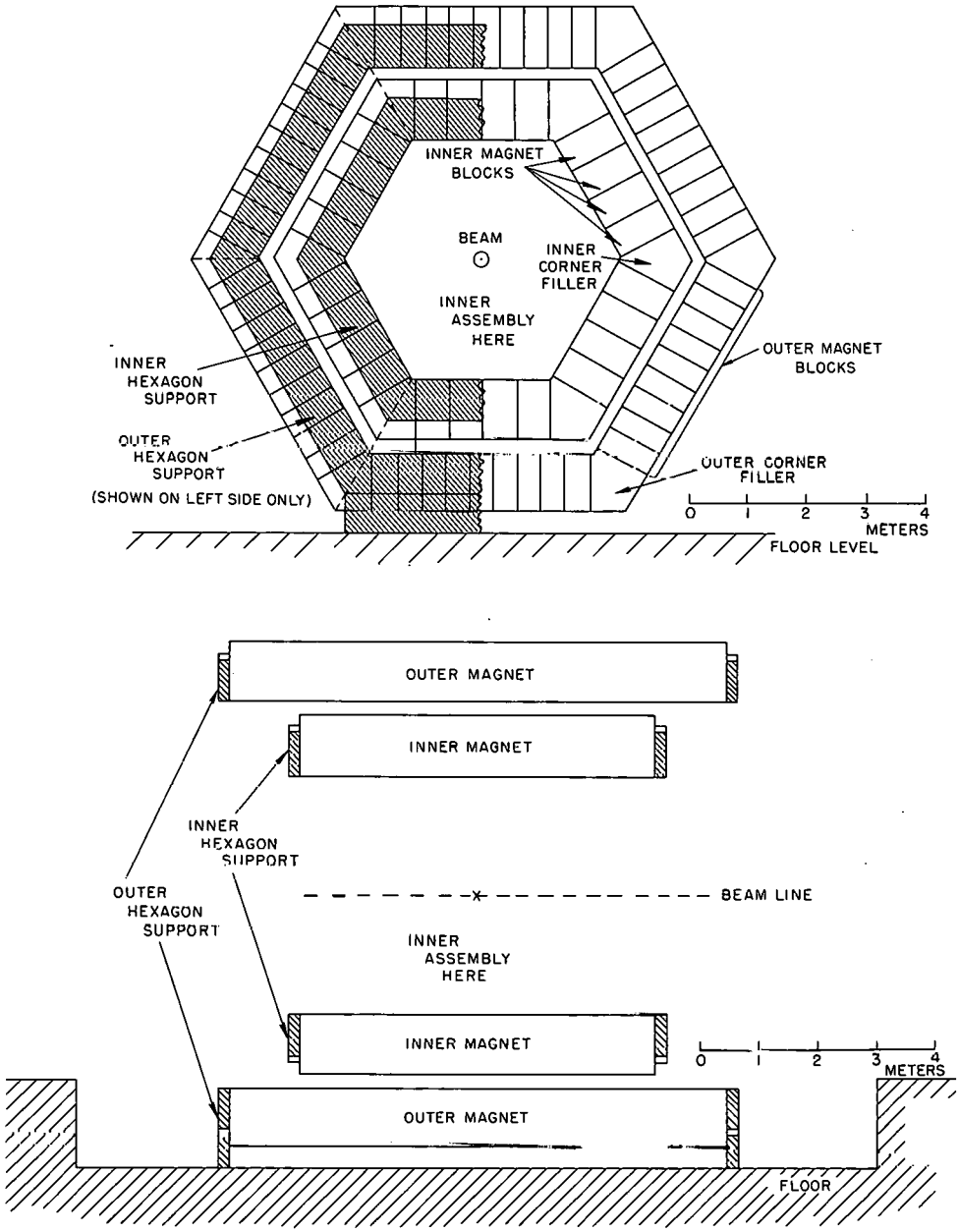


Fig. 6. Assembly for hexagonal magnet using module blocks.

top and bottom blocks have no coils. The magnet blocks weigh about 30 tons, so a 40-ton crane should be adequate. Each hexagon is supported by an end frame which is a heavy channel to which the magnet blocks are bolted. The end frame is 8.4 m high, so it would have to be welded together in the building. The supporting framework is shown cross-hatched. The outer hexagon is supported from the floor and the inner hexagon is supported from the outer hexagon. For the bottom half, the outer hexagon is assembled first, then the ıer, while for the top half the inner is done first, then the outer.

Bus bar and cooling manifolds mount to the supporting frame in the areas that have magnet windings.

It would seem appropriate to have a pit extending the full width of the building somewhat longer than the detector, but the rest of the building floor could be higher, at a level permitting the drift chambers between magnets to slide in from the ends. This would keep the height of supports and scaffolding reasonable. Trucks could drive in at this level, so no separate loading platform would be needed. The lowest drift chambers would slide under the magnet from the side, in the pit. They come in pieces about 4 x 4 m, presumably. Probably the total building width should be about 20 m, since the hexagon is about 10 m. The 16-m width in the '76 proposal seems a bit skimpy.

In some cases it might be useful to remove upper magnet blocks to get at the inner detector assembly, which would not be impossible to do.

2. Free Form Magnet Assembly

An alternative way of energizing the iron that avoids the ⁻ːcessity of constructing the full iron magnet at the beginning and so allows new arrangements of the iron at a later time is presented. The iron hexagon is made up of square blocks with a thickness

suitable for lifting with the crane. Blocks stacked together to give the desired thickness, say 1 m, would then be energized as a single toroid, with the magnetic field perpendicular to tracks at large angle to the beam. For example, a 5 m X 5 m block would have a 30-cm hole cut in the center. Each corner would be cut off (0.6 m X 0.6 m X 0.5 area) so as to provide a reasonable approximation to a circle. A coil would run from the center to each corner. The loss of area due to the missing corners and the hole in the center is approximately 3% of the total area. The width of a toroid would be chosen to correspond to one side of the iron hexagon, and thus two toroids side by side would be necessary to give the desired length along the beam. Thus the iron hexagon in the original proposal or any fraction of it could be constructed out of these iron toroids with a loss of coverage of only 3%.

C. Comments on the Central Solenoid Option

The merits of the solenoid magnet have been considered in the 1975 ISABELLE Summer Study.[1] This note concerns 3 potential drawbacks of the solenoid:

- Inferior on-line hadron rejection in the single electron trigger.
- High rates in the magnet chambers at $L = 10^{33}$.
- What to do with the flux return ?

1. Hadron Rejection

We consider an on-line hadron rejection of $\sim 10^{-4}$ as a very desirable feature. The lepton detector with no solenoid has hadron rejection factors of 1/400 from the transition radiator sections and at least 1/10 from the calorimeter section. The overall factor of 1/4000 makes an excellent trigger.

As discussed in the 1975 Summer Study, the electron trigger with the solenoid option would rely on the longitudinal shower

development criterion alone, which is a rather loose trigger. Using the CCR formula, and an $e/\pi \sim 10^{-4}$, we have at $L = 10^{33}$ roughly 0.2 direct electrons per sec. A trigger with only 1/100 hadron rejection would give a rate of 20/sec, which is high, although not completely prohibitive. Additional off-line rejection is available by comparing the energy measured in the shower with the momentum measured in the magnet. For example, a requirement that the $E_{shower}/p_{magnet}$ be larger than 0.9 provides a hadron rejection of at least 0 at 5 GeV.[2-4] While the solenoid's momentum resolution deteriorates with increasing energy, the shower counter improves. A more detailed calculation of the hadron rejection vs energy should be made.

However, the combined on-line and off-line hadron rejection is still not at the $10^{-4}$ level. Therefore, we consider the possibility of putting transition radiator modules inside the solenoid magnet along with the position measuring drift chambers. Suppose there are only 3 pairs of drift chamber planes, each requiring $\sim$ 5 cm radially. To leave maximum space for transition radiators, we contemplate curved drift chambers, as well as curved TR modules. Then of the $\sim$ 60 cm available inside the magnet, 15 cm are allotted to the drift chambers leaving 45 cm, perhaps 2 short modules, or one long module interrupted by the central drift chamber planes. Further study is clearly needed. Hopefully a hadron rejection of 1/50 to 1/100 could be obtained which would provide a fairly good trigger ($10^{-3}$) and should certainly give a final rejection of better than $10^{-4}$ in the off-line analysis.

---

2. J.S. Beale, F.W. Büsser, L. Camilleri, L. DiLella, G. Gladding, A. Placci, B.G. Pope, A.M. Smith, B. Smith, J.K. Yoh, E. Zavattini, B.J. Blumenfeld, L.M. Lederman, R.L. Cool, L. Litt, and S.L. Segler, Nucl. Instrum. Methods 117, 501 (1974).

   W.J. Willis and V. Radeka, Nucl. Instrum. Methods 120, 221 (1974).

4. J.A. Appel, M.H. Bourquin, J. Gaines, D.C. Hom, L.M. Lederman, H.P. Paar, J.-P. Repellin, D.H. Saxon, H.D. Snyder, J.M. Weiss, J.K. Yoh, B.C. Brown, C.N. Brown, J.-M. Gaillard, J.R. Sauer, and T. Yamanouchi, Nucl. Instrum. Methods 127, 495 (1975).

An important feature of an electron trigger is a pulse height measurement directly after the beam pipe to guard against electrons from $\gamma$ conversions and $\pi^0$ Dalitz decays. Presumably this would be achieved with a barrel of narrow scintillators. With a solenoid, these would have long light guides and P.M.'s mounted outside the solenoid end cap. If the bake-out restrictions are met by leaving a gap between the pipe and the innermost detectors, the barrel might be at $R \sim 10$ cm, and so might have $\sim 60$ 1-cm staves.

2. Rates

It is somewhat questionable whether data collected at luminosity $10^{33}$ in a central track detector can be analyzed. At $L = 10^{33}$ the interaction rate is

$$10^{33} \times 40 \text{ mb} = 4 \times 10^7 \text{ (25 nsec/event)}$$

assuming no rise in total cross section from ISR energies. Supposing the multiplicity on the central rapidity plateau is $dN/dy \sim 1.5$, there will be $\sim 3$ particles/event in the lepton detector ($\Delta y = 2$ for $\pm 45^\circ$). We consider the innermost drift chamber, located at R = 10 cm. Suppose we use 100 cells, so that the cell length is only + 3 mm. The drift time is then $\sim 75$ nsec (assuming 200 nsec/cm). During this 75 nsec, on the average 3 additional beam-beam interactions occur, yielding 9 additional tracks in the detector.

These background tracks can be largely eliminated if the pairs of drift chambers are offset ½ cell (needed for left-right ambiguity resolution in any case) by noting the sum of the transit times for a track in the 2 struck cells. For in-time events the sum is 75 nsec, while for out-of-time events it is less. Timing accuracies of $\pm$ 5 nsec could then eliminate $\sim 90\%$ of the background events. This rejection is somewhat less for low-momentum tracks which strike the chambers at an angle.

However, if a cell contains two tracks, the timing trick of background rejection fails, and the data is lost. With 9 background tracks, the probability of any cell containing one is 9/100. The failure probability is actually 3 times this probability, so the chance of failure is $\sim$ 27% per real track. Thus a system of ± 3 mm cells, requiring 1500 cells in all, would still be subject to a 30% reconstruction failure. This conclusion may be a bit gloomy, but undoubtedly merits further thought.

Note that the transition radiator MWPC's, with 1 mm spacing, are not subject to so much trouble as extra hadron tracks do not destroy the electron signal unless they fall within one pulse-height-analyzed subunit. This should be only a few percent at $L = 10^{33}$, due to overlaps in the scintillator barrel.

3. Flux Return

The flux return scheme presented in the 1975 Summer Study may be the best.

Assuming a solenoid radius of 0.75 m, the total area of the field is 1.8 $m^2$. If the field is 10 kG, and the flux in the iron is also taken to be 10 kG, the iron must have a cross section of 1.8 $m^2$ everywhere. For example, if the return path is a hexagonal shell at R = 2.5 m (after the hadron calorimeter) its thickness must be 10 cm. If the flux is carried from the solenoid to the shell at R = 2.5 by a disc end cap, the cap must be thicker at the center to maintain constant 1.8 $m^2$ cross section. In particular, at R = 0.75, $1.8 = 2\pi\ (0.75)\ T$ or T = 38 cm. Each end cap would weigh approximately 32 tons which would have to be easily movable to obtain access to the inner detector elements -- an interesting engineering problem. A view of this configuration is shown in Fig. 7.

Recall that the direction of the magnetic field in the flux return is perpendicular to that in the outer muon magnet. If the hadron calorimeter is to have magnetized iron (same direction as the

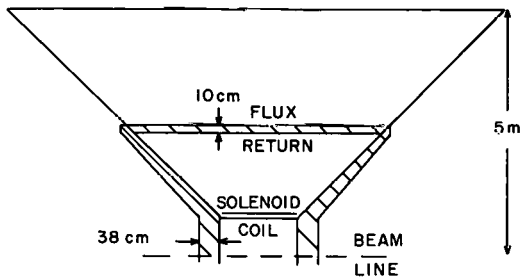


Fig. 7. Return flux for central solenoid option.

muon magnet), it may be best to have the flux return entirely separate from the calorimeter, a loss of 10 cm for active elements of the detector.

We consider some alternative configurations that might allow the end cap to remain in place except for access inside the solenoid itself. This might be obtained by dedicating a certain fraction of the azimuth of the outer detector to the flux return.

In the region of the electron calorimeter R goes from 0.8 to 1.3 meters. The azimuth needed is given by:

$$A = \phi \frac{(R_{max}^2 - R_{min}^2)}{2} = 1.8 \text{ m}^2$$

$$\phi = 3.6 \text{ radians} = 200^\circ .$$

This seems excessive, corresponding to an end view shown in Fig. 8a.

In the region of the hadron calorimeter R goes from 1.3 to 2.7 m. This time $\phi = 40^\circ$ which is not too implausible. One can contemplate the two configurations shown in Figs. 8b and 8c. However, the thin flux return in one dimension must be compensated by a large other dimension to keep the total cross section 1.8 $m^2$. So instead of 38 cm, the end cap must be $38 \cdot 360^\circ/40^\circ = \underline{3.4 \text{ m}}$, and a side view is shown in Fig. 8d.

## IV. CONCLUSIONS AND FUTURE PLANS

### A. Size of Detector

The smaller version of the lepton detector system was preferred because it would be significantly lower in cost and easier to build and its capabilities for muon detection were the same as those of the larger size. Electron and hadron energies can be measured as well as with the larger detector, the only sacrifice being in the solid angle for electron

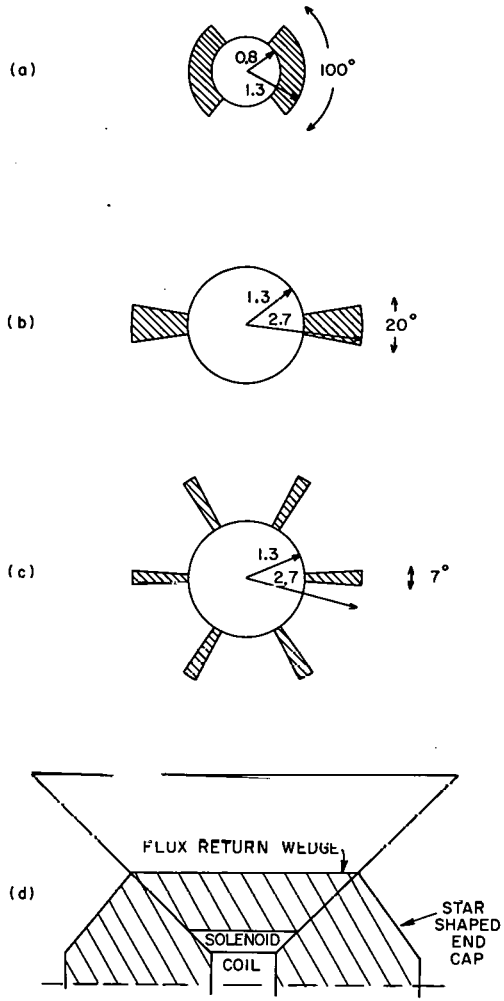


Fig. 8. Some alternative approaches to the return flux problem fo the central solenoid option.

and hadron detection when they are to be done at the same time. The solid angle is still a large one and seemed satisfactory for an extensive program of experiments.

For the present, therefore, further work on the design of the detector and experiments using it should be done with the smaller version.

B. End Caps

The detection of small-angle particles by means of end caps should be left to a later phase of the experimental program. Initially, the lepton detector would concentrate on particles of high $P_\perp$ and relatively large angle, without attempting to observe all secondary particles or achieve overall energy or momentum balance. Design of end caps to accomplish this might eventually be undertaken, but only after a first round of experiments in which the lepton detector would cover angles within $\pm$ 45° of the 90° direction, and initial information on small-angle particles would come from experiments at other insertions with equipment designed for that purpose.

C. Cost Estimates

The cost estimates made during the workshop are very rough ones and may be substantially different from the final cost of an operational system. To arrive at more accurate cost estimates a conceptual design for the major components needs to be worked out in engineering terms and costs derived from it. A definite estimate should be possible for the magnet, which is the most expensive item, since it is of conventional construction though unusual configuration. For the detector modules the uncertainties would be somewhat larger, but estimates could be prepared that would be adequate for a proposal for funding. This should be done in the near future.

D. Feasibility of New Ideas

Two ideas were put forward that involve qualitative changes in design: the self-contained magnet blocks for the muon analyzing magnet, and the toroidal interior magnet for analysis of electrons and hadrons. The duration of the workshop was not adequate for a careful evaluation

of these ideas, so this needs to be done from two viewpoints. In the first place, do these ideas have real advantages from the high energy physics viewpoint; do they make better measurements or better experiments possible? In the second place, are they practical from an engineering viewpoint; would they be cost-effective to build and operate, and reliable and convenient in operation?

## E. Need for a Working Design Group

A working design group is needed to prepare a proposal for the construction of a lepton detector system during the next 18 months. If a definite design and proposal are needed by the spring of 1978, this could be done in two phases, with an evaluation of the new ideas for magnet construction and design of the detector system carried out by summer of 1977, including reliable cost estimates. At that time a further workshop or summer study could review this information, and arrive at a decision concerning which ideas, if any, to incorporate, and resolve further questions concerning the conceptual design. Using this further input, the working group would determine further details and prepare a proposal for submission the following spring.

To do this would require a major fraction of the time of a mechanical engineer with design and drafting support, and part-time participation of physicists familiar with the types of detectors used (drift chambers, Li transition detectors, liquid argon calorimeters) and also superconducting magnets. In addition, the design must be compatible with the details of ISABELLE insertion and experimental hall, and members of the high energy physics community interested in lepton physics at ISABELLE should be kept informed of the progress of the working group.

In conclusion, there is a substantial amount of work that still has to be done on the preliminary design. Considering the various options and alternatives that have been discussed, a possible artist's concept of the detector is shown in Fig. 9.

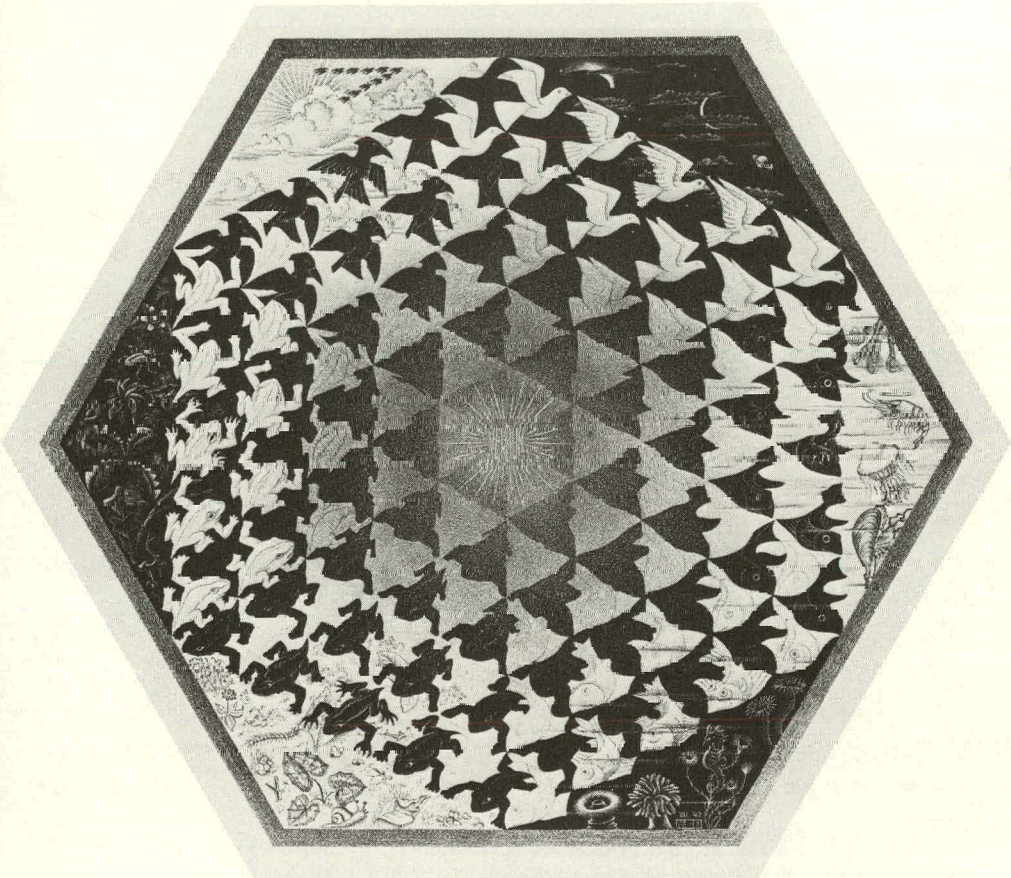

Fig. 9. This could be considered an artist's conception of our Lepton Detector. We thank the Escher Foundation, Haags Gemeentemuseum, The Hague, for permission to copy the work "Verbum" by M.C. Escher.

# LARGE HADRON SPECTROMETER WORKSHOP SUMMARY*

D. Hywel White
Cornell University

## I. INTRODUCTION

In July 1976 a large hadron spectrometer workshop was held at Brookhaven. In 1975 there had been a summer study, and one group had produced a design which is reported in the proceedings.[1] Although this certainly seemed viable to us, the participants in the workshop became enthusiastic about an alternative approach which we describe here. The mandate for the workshop was to propose a design for a spectrometer system that could be used soon after the turn on of ISABELLE to exploit the potential that there would be for exciting physics inherent in the energy that would be available in the c.m. system. In common with all projects that are scheduled for completion in the far future, we had the difficulty that our flights of fancy could easily outstrip reasonable bounds and that rather than try to demonstrate the potential for complexity, we should at least be sure that we would have the most exciting physics at our disposal. We felt that a primary motivation for ISABELLE at the present time stemmed from the potentialities for seeing weak interaction effects, and in particular, for observing the intermediate vector boson both in its charged and neutral states. In the design of this spectrometer system we have used this physics as an example to guide our thoughts.

---

*D. Edwards, A. Etkin, W. Frisken, B. Gibbard, E. von Goeler, M. Good, J. Humphrey, M. Kramer, P. Kunz, T. Kycia, D. Leith, W. Love, D. Nygren, S. Ozaki, R. Palmer, E. Platner, J. Russell, J. Sandweiss, A. Seiden, W. Selove, D. Smith, J. Thompson, A. Walenta, E. Willen, W. Willis.

1. L. Rosenson, S. Ting, J. Russell, W. Selove, S. Lindenbaum, W. Lo R. Louttit, S. Ozaki, F. Paige, E. Platner, and S. Protopopescu, Proc. 1975 ISABELLE Summer Study, Brookhaven, BNL 20550, p. 52.

Starting in the 1975 study a group[2] concentrated on the design of a lepton detector in which the ability for detecting and identifying muons and electrons was optimized. The W is expected to decay $\sim 10\%$ of the time into a lepton and a neutrino and these high transverse momentum leptons should be a clear signal of W production.

In our approach we concentrated on the problem of detecting the charged particles, with identification, and also measuring the energy the photons from hadron decay. Given a high efficiency of detection, the transverse momentum of the neutrino is a good signature of a weak decay and we have investigated this approach here. We note that if the W is produced moving slowly in the laboratory then both the charged lepton and the neutrino will generally have high transverse momentum and may be separable from the hadrons in the production process. Knowledge of these two momenta allows the calculation of the charged W mass directly.

A more difficult but also attractive possibility is to see the W decay into hadronic jets, and therefore, measure the branching ratio, $R_W$. It is not at all clear if these jets can be distinguished from "normal" hadronic jets by their angular distribution and by their invariant mass distribution, but we have also borne this possibility in mind in designing the spectrometer system we describe here.

Apart from the intermediate vector boson, there is the field of charmed particle spectroscopy that beckons at ISABELLE. At high production energies in nucleon-nucleon collisions the J/ψ has been identified at the ISR and at FNAL through the two lepton decay mode, but not, as far as we are aware, directly by decay into hadrons. The higher mass charmed bosons couple less strongly to lepton pairs, and if the spectroscopy is to be pursued, the decays into hadrons must be

---

R. Burnstein, W.C. Carithers, M. Duong-van, R. Imlay, M. Kreisler, U. Nauenberg, C. Rubbia, L. Sulak, G. Snow, H.H. Williams, E. Paschos, M. Sakitt, C.L. Wang, and L.L. Wang, Proc. 1975 ISABELLE Summer Study, Brookhaven, BNL 20550, p. 9; Y.H. Chiang, R. Imlay, S. Iwata, S. Jacobs, R. Kraemer, M. Kreisler, K. McDonald, P. McIntyre, M. Sakitt, J. Thompson, A. Thorndike, A. Walenta, C. Wang, L.L. Wang, these Proc.

seen. The straightforward method of looking for the two particle decays of the D meson e.g., at FNAL[3] by two spectrometers, was not successful and a more constrained set of events are probably necessary. The large acceptance and good momentum resolution of the spectrometers we describe below would provide a good handle on the multiparticle decays of charmed particles. We note that the excited particles are all expected to be produced in the central region with a momentum distribution dominated by the x values of the antiquarks in one of the incident protons.

Although we have made specific suggestions on the physics that we have used to guide the spectrometer design, we are aware that a program of "conventional" hadron physics is necessary and it is our belief that a large range of that physics can be done with an apparatus like this one, using it as a multiparticle effective mass spectrometer system.

## II. FUNCTIONAL DESCRIPTION

During the workshop we have become quite impressed by the difficulties of operating a large and complicated spectrometer system even when access is readily available. Since experience at a storage ring leads us to believe that access will be limited, we have tried to make the design modular and to restrict the interdependence of the components of the system. In Fig. 1, we show a block schematic of a spectrometer system. In the forward direction we expect to measure the high momentum hadrons in the forward angle tagging spectrometers FATS 1 and FATS 2. The nomenclature is meant to imply that functionally, as well as operationally, we can differentiate between the disintegration products of the incident protons and the particles that are produced in the central region. These two spectrometers can measure momenta of charged particles and the energy of the neutrals that are emitted within the cone of acceptance, without necessarily using any equipment

---

3. D. Bintinger, R.A. Lundy, D.D. Yovanovitch, C.W. Akerlof, P. Alley, D. Koltick, R.L. Loveless, D.I. Meyer, R. Thun, W.R. Ditzler, D.A. Finley, F.J. Loeffler, E.I. Shibata, and K.C. Stanfield, Phys. Rev. Lett. 37, 732 (1976).

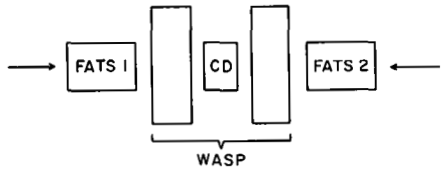


Fig. 1. Spectrometer system consisting of forward angle tagging spectrometer, FATS, wide angle spectrometer pair, WASP, and central detector, CD.

inboard of their main deflection magnets. These are expected to have improved momentum resolution when the knowledge of the vertex position provided by the central device (CD) is used, but this coupling is not essential. The measurement of inclusive particle production within a fairly extensive forward cone can be accomplished by these two spectrometers in a stand alone running mode.

The particles that are produced at wide angles in the central region are measured by a wide angle spectrometer pair, (WASP) in a way similar to FATS. Neutral detectors will measure energy, and the charged particles have their momentum measured with the particle type identified. In our present design the ISABELLE beams pass through WASP. This is not essential, although as we have drawn the overall device in Fig. 2 it has been necessary to remove the neutral detection in the cone of acceptance of FATS. There were many ideas offered at the workshop for ingenious and technically advanced detectors to occupy the area around the interaction region itself. We have labelled it functionally as the central detector (CD) and we feel that apart from assuming that the vertex position will be measured by this device, we should not constrain it further at this time, and we mutter imprecations like transition radiation, photosensitive chambers, time projection chambers, calorimetry and the like. This block is substantially uncommitted in our design, therefore, although we feel that it is essential to any realistic approach to particle detection in the central region.

## III. HARDWARE

The overall layout of the detector is shown in Fig. 2. At 200 GeV/c the angles of the emergent particles are all small, $\sim$ milliradians, the magnetic field is the principal source of transverse momentum available to deflect particles out of the vacuum chamber. We describe the two magnetic spectrometers below.

### A. FATS

These spectrometers have a single bending magnet with a peak field integral of 60 kG-m. It was thought that in the design of these magnets every effort would be made to restrict the fringing field from extending

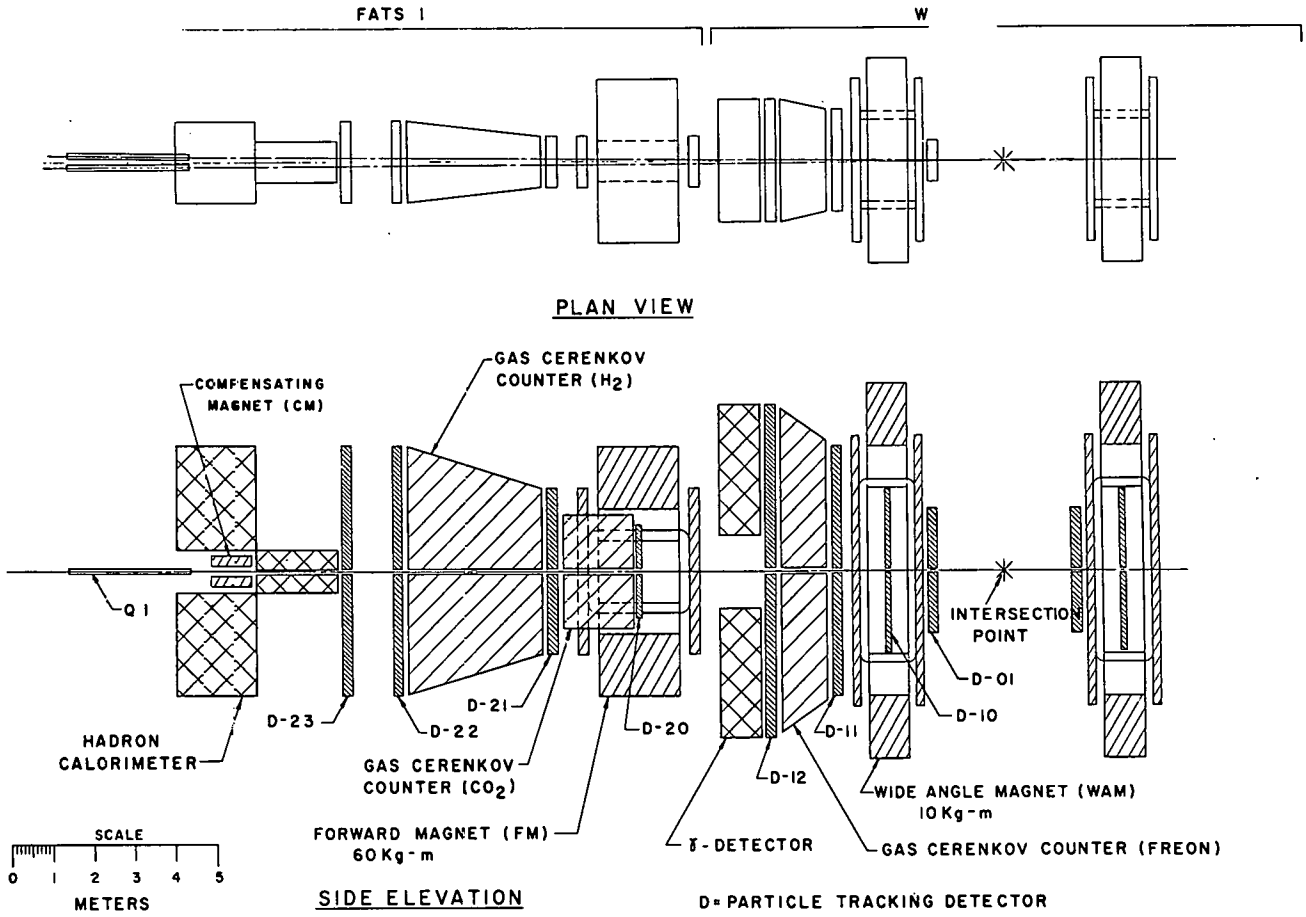


Fig. 2. Plan and elevation views of spectrometer system.

far from the magnets themselves. The idea behind this is that we wish to reconstruct straight line tracks as far as possible, making for simplicity in the software. The bending is in a vertical plane for reasons expressed in the 1975 summer study. We have used $\Delta x = 100\ \mu$ as the spatial resolution to be specified for the drift chambers (D in the figure), again the simplicity of track formation in the field free region leads us to expect that we can accomplish this ambitious goal. This gives us a resolution of $\Delta p/p^2 \sim 0.5\ \Delta x$ ($\Delta x$ in meters, p in GeV/c) which at 100 GeV/c and $\Delta x = 10^{-4}$ is 0.5 GeV/c. This figure is typical of the magnitude of the charged particle momentum uncertainty that we can expect. Multiple scattering in the material of WASP and FATS together gives $\Delta p/p \sim 5 \times 10^{-4}$ so this becomes the dominant error below 10 GeV/c. If the vertex is not measured any better than the beam spot size, these resolution numbers become worse by about a factor of 3.

B. WASP

The principal of operation of these two spectrometers is identical to FATS in that the detection is all downstream of the bending magnet. There is provision for Cerenkov counters, and they are discussed in some detail below. The neutral detection is likely to be expensive in the volumes envisaged, and we feel that it may be necessary to look for interim solutions to the problem of measuring the neutral energy roughly in the early stages. The $\int Bd\ell$ of each magnet is 10 kG-m giving $\Delta p/p^2 \sim 20\ \Delta x$ without the interaction point and $\Delta p/p^2 \sim 4.8\ \Delta x$ with a measurement of the interaction point to the same spatial precision as elsewhere. (As before, $\Delta x$ is in meters, p in GeV/c.) Using this more precise number, below 3.8 GeV/c the material ahead of the spectrometer will dominate the momentum resolution keeping it to 0.5%. The large aperture magnet is of conventional type, if large in size, and no prob are foreseen. The geometry of the WASP system, symmetric about the interaction point, reflects our present prejudice that the angular correlation of the hadron jets will be a noticeable limitation in the

acceptance of a wide angle system, and also that the production at low x will enhance the yield of the symmetrical pair. In the limit of correlation of the lepton pair from the neutral vector bosons, this correlation in the acceptance will be important. For W → lepton-neutrino, there also should be a high potential for observing the particle in coincidence with the lepton to establish the low interaction rate of the neutrino.

C. CD

The central detector is not specified except that it should define a vertex and must be self-compensating magnetically for the rest of the spectrometer work. Otherwise it is independent of the other two spectrometer systems. The absence of specifications for this device should not be taken as evidence for a low priority in our design but only as appreciation of the large number of options presently available. A list of major components is shown in Table I.

TABLE I. Major Items

| | | |
|---|---|---|
| (2) FATS Magnet | 60 kG-m | 1.5m x 1m · gap |
| (2) WASP Magnet | 10 kG-m | 4m x 2m · gap |
| 2 each Cerenkov Hodoscopes | | $H_2$, $CO_2$, Freon 114 |
| Drift Chambers, total no. of wires | | 50 K |
| "Major" on-line computer with preprocessors | | PDP KL10 |
| 2x Hadron Calorimeter | | 6 $m^2$ |
| 2x Photon (LA) Calorimetry | | 25 $m^2$ |
| Central Device | | |

D. Vacuum chamber

The combination of FATS, WASP, and the compensating magnet is to restore the circulating beam to its normal angle and position after traversing the apparatus. The beam gymnastics are not trivial, especially, in the situation that the energy of the two beams differs from the

maximum available. In this condition we would prefer that WASP remains at the nominal full field, since the momenta of the particles in the central region are not changed, and that FATS and the compensating magnets are set to restore the beam conditions. We expect that this problem will be studied further.

E. Cerenkov Counters

We have outlined a design of the counters based on the following principles:

1. The geometry adopted by the 1976 Summer Workshop was adhered ...

2. Since the counters are of awkward shape, gases at atmospheric pressure have been used as radiators.

3. In general, multibody final states will be involved, so a compromise has been chosen which will permit the identification of kaons down to $\sim$ 11 GeV/c. As we show later, this limits the momentum of fully identified kaons to $\simeq$ 40 GeV/c. Separation of pions plus kaons from protons can be extended to higher than 120 GeV/c by the use of He in the third Cerenkov counter.

The gases chosen are freon 114 for counter #1, $CO_2$ for counter #2, and $H_2$ for counter #3. The absolute thresholds for these gases at $0^\circ$ C, 760 mmHg are $\gamma \approx 20$, 33 and 60 respectively. In order to separate kaons, pions and protons, two counters are required. Table II outlines the logic requirements for the combinations C1 + C2, C2 + C3.

In addition, since we plan an A/D converter for each photomultiplier tube, one can use the pulse height information from counter #3 to extend the range of particle separation. By determining the number of photoelectrons, one can separate pions from kaons even though both are above threshold. This technique will work up to $\approx$ 40 GeV/c. This principle can also be used in counter #2 to ensure good overlap of the momentum range selected by the two pairs of counters.

TABLE II. Particle Selection by Cerenkov Counters

| Particle Selected | Logic | Momentum Range GeV/c |
|---|---|---|
| C1 + C2 | | |
| pion | $C1.C2$ | 3 - 17 |
| kaon | $C1.\overline{C2}$ | 11 - 19 |
| proton | $\overline{C1.C2}$ | 11 - 19 |
| + C3 | | |
| pion | $C2.C3$ | 10 - 30 |
| kaon | $C2.\overline{C3}$ | 19 - 30 |
| proton | $\overline{C2.C3}$ | 19 - 30 |

IV. SOFTWARE

There appear to be two major problems in software design and operation in the large spectrometer systems presently in use. The first derives from the overall complexity of the system, and the second from the large computing power that is needed. We consider the modularization of the system to be a probable advantage in problem one, particularly, given the prospect of powerful minicomputers, or even specially built processors handling parts of the system. The need for reduction in the interaction between elements, particularly in the debugging phase, makes it interesting to explore a distributed computer network as a way to solve this problem.

The second problem leads us to believe that the minicomputer offers the potential of much less expensive computing per cycle of the C.P.U., so that the fixed task aspect of some of the computing is conceivably best done in a distributed fashion. Moreover, the simple algorithims that we imagine will cope with straight line track recognition and subsequent momentum calculation, should also lend themselves to distributed computing.

## V. W PRODUCTION

We have used the paper of Palmer et al[4] as a model for estimating rates for production of the intermediate vector boson as well as to understand the kinematical region in which production will occur. Fig. 3 shows the production cross section of the W in p-p collisions from this paper. For rough calculations, provided we are above the "knee" of this curve at $S/m^2 = 10$ then we can suppose that the W production cross section is $\sim 10^{-33} cm^2$. Willis[5] has reported running a detector with extensive liquid argon devices at the ISR at a luminosity of $10^{31}$ $cm^{-2}$ $sec^{-1}$. Optimistically we assume that we expect to use $10^{32}$ $cm^{-2}$ $sec^{-1}$ at ISABELLE, and then the rate of W production is about 10/min, $10^4$/day. Even allowing for inadequacies in solid angle coverage, and a branching ratio into lepton pairs of 0.1, we can expect a substantial data rate. We show in Fig. 4 the distribution of W momentum according to the model used in references 5 and 6. It is clear that the W is produced at small laboratory momenta, leading us to propose the large aperture centered at $x = 0$ represented by WASP. We note that the lepton pair is produced with a center-of-mass angular distribution of $(1 + \cos^2\theta)$, and the same distribution is expected to hold for the hadronic jets from W decay. We intend to pursue the calculation of the acceptance of the central detector in detail, and we consider that the WASP configuration is only typical of a number of geometries that we can envisage.

The basic strategy for detecting the W in a high acceptance, good energy resolution apparatus follows. First a large ($\sim$ 20 GeV/c) transverse component of momentum must be missing, corresponding to the

---

4. R.B. Palmer, E.A. Paschos, N.P. Samios, and Ling-Lie Wang, Phys. Rev. D14, 118, 1976.
5. W. Willis in a talk given at the workshop.
6. Dr. Ling-Lie Wang has kindly calculated these distributions for us.

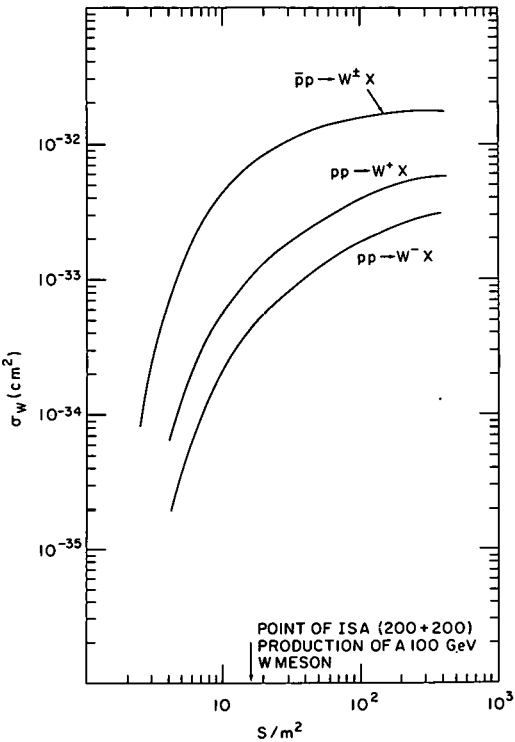


Fig. 3. Production cross sections for the reactions (a) $\bar{p}p \rightarrow W^{\pm}X$, (b) $pp \rightarrow W^{+}X$, and (c) $pp \rightarrow W^{-}X$.

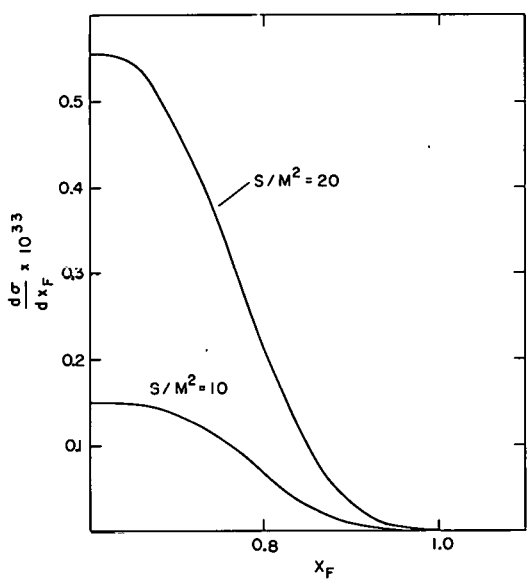


Fig. 4. Cross section for W production as a function of $X_F = 2P_\ell/\sqrt{s}$.

neutrino. There will often be missing momentum of this magnitude in any detector at a storage ring, but the direction will be predominantly down the vacuum box, an area where detection is difficult. Look for a charged particle outside the forward cones with high transverse momentum comparable to the missing neutral. This particle is identified as the charged lepton. The mass of the charged W is the invariant mass of the neutral missing momentum and the charged lepton, and the rest of the detected particles give the motion of the W in the lab. Extra constr: such as the W angular distribution in its center-of-mass system shoul establish the credibility of this scheme.

We have generated events with a reasonable distribution of momenta for the particles in the final state and calculated the missing momenta. The plot is shown in Fig. 5. The missing momentum is the sum of the momenta of all $K_L^o$, n, and $\bar{n}$ formed, of all $\pi^o$ pointing into the aperture of FATS, and all leading particles lost down the vacuum pipe. Note that the longitudinal momentum clusters in two groups, depending on whether a leading particle escapes, and also that the total $p_\perp$ rarely exceeds 2 GeV/c. We feel that these missing values of $p_\perp$ are small enough to leave the credibility of our scheme intact. The hadronic decay is significantly more difficult to establish, and serious claims for its detection must await detailed calculations. The essence of the scheme, however, is that all particles of substantial transverse momentum must be measured and any large transverse missing momentum should occur in a direction where the detection efficiency is high.

Although we have concentrated on the W as a particle whose properties have been predicted,(including production characteristics) we are sensitive to the opportunities for new particle spectroscopy and we believe many of the same identification techniques will apply. Namely, we need an effective mass spectrometer of good energy resolution with the dominant uncertainties coming from the neutral component. This design attempts to establish a balance between charged particle measurement and identification and the difficulties of neutral particle reconstruction. At the luminosity of $10^{32}$ $cm^{-2}$ $sec^{-1}$ we do not anticipate

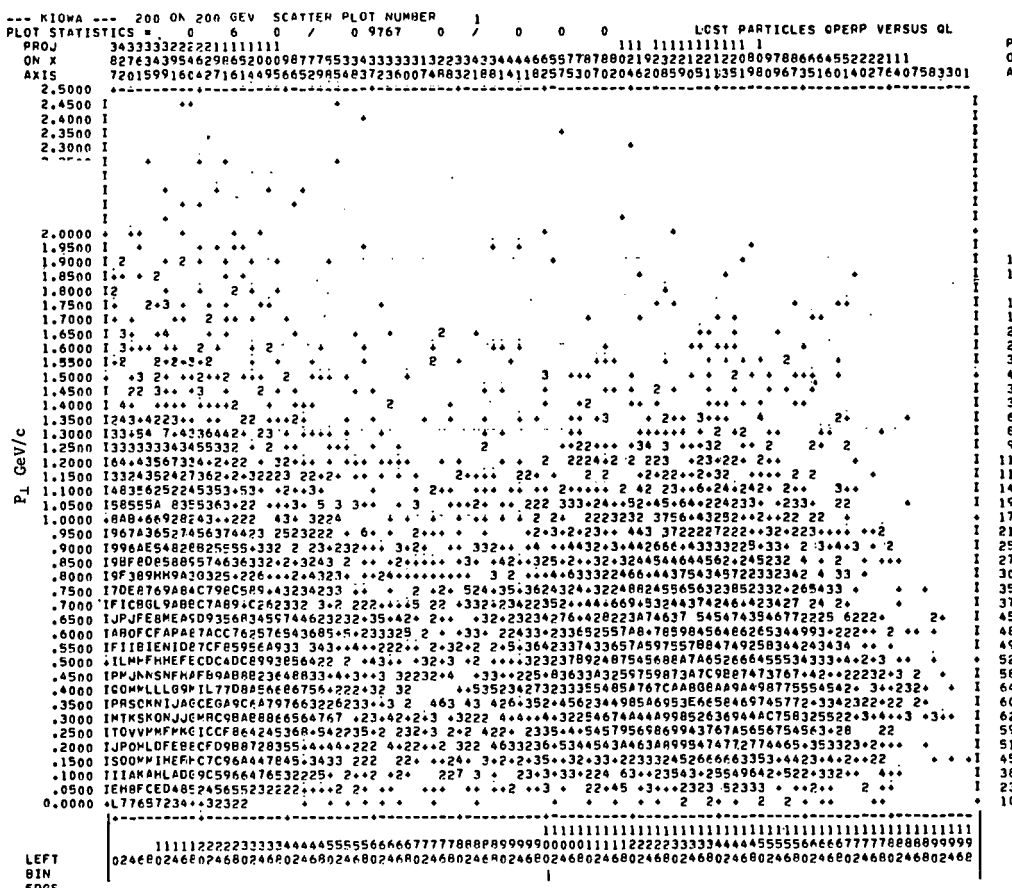


Fig. 5. Scatter plot of missing momentum for Monte Carlo simulation.

difficulties with rate of production, but care must be taken with the design of the computing system to cope with the large data flow.

# THOUGHTS ON LARGE ACCEPTANCE SPECTROMETER DESIGN IN LIGHT OF EXPERIENCE AS A SPLIT FIELD MAGNET USER

Abe Seiden and Dennis B. Smith
University of California at Santa Cruz

The authors, both former users of the Split Field Magnet, have been requested to comment on what they learned about how such a facility should esigned and realized. This memo assumes some familiarity with the SFM. we ieel that, despite a relatively slow start of operation, the SFM is a very useful facility.

## I. Magnet Design

The SFM is very convenient for looking at relatively high momentum ( $\geq$2 GeV/c) particles produced in the forward direction (e.g. by diffractive processes). However, the constant magnetic field in the forward direction changes over to a quadrupole field at large angles with respect to the incident beams. The analysis of particles which pass through the intermediate region is awkward. Consequently, the trajectories of particles of a few hundred MeV/c momentum are not easily parametrized for track finding. (Note: The length of time to fully process an event is about 1 sec of CDC 7600 time.)

Because of its one-meter gap, the magnet has the valuable feature of being well suited for use with a wide variety of external detectors.

There are several additional considerations that seem not to have been suggested in time to be put in the design:

a) Design of shims to allow operation with unequal beam momenta.

b) Incorporation of small holes in the magnet to allow probing the magnetic field in the magnet iron which then could be used for magnetic lysis of high energy muons (as Sam Ting's group was considering).

## ... Detector Design

Since wire chamber technology has advanced the idea of 70 000 MWPC wires would probably be revised. If drift chambers were used, the drift space length would have to be varied depending upon the anticipated rates

in the chambers in different parts of the magnet. The positive high voltage read-out proved difficult to use reliably so perhaps one should consider more wire planes (which would also help in track recognition).

The detector layout is a difficult problem, "playing off" quick chamber access (for repairs) against reasonably full acceptance and good momentum resolution. (A minimum of four wire planes hit by each track would help track recognition.) More flexibility in the mounting of the chambers (e.g. when attaching the chambers to the magnet use a grid of bolt-holes rather than fixed nails) would be desirable.

The layout of the SFMD also favored the study of diffractive processes. There were consequently some losses in acceptance for low momenta ($\leq 2$ GeV/c) particles both in azimuthal and dip angle. Another result of this rigidity of layout was difficulty in forming MWPC triggers using roads in the detector (and "DC Logic") for certain particles corresponding to nondiffractive processes (e.g. wide angle high $p_\perp$) even where their trajectory's curvature was sufficiently small.

Because delta-ray spirals often obscure tracks' intercepts with a given plane, it might be worth considering orienting the chambers so that their gaps don't contain any significant length of individual magnetic field lines.

In addition to track recognition and momentum determination, many users wanted particle identification so the detector (and possibly magnet) design should probably allow for some Cerenkov, dE/dx, and TOF counters.

III. Software

Overall we were very happy with the SFM software. The software lost some generality because of the initial user orientation towards the diffractive processes. Because the initial detector was oriented along some area of symmetry of the magnet, there was a tendency to code programs without allowing for all chamber orientations.

To conclude, the authors would like to stress that one of the best aspects of doing experiments at the SFM facility was the very extensive help given by the support groups, both hardware and software. Both authors received support from CERN and one (DBS) from the IN2P3 (CNRS) and the Swedish Atomic Research Council.

# SUMMARY OF LONGITUDINAL INSTABILITIES WORKSHOP*

R. Chasman

Brookhaven National Laboratory

A five-day ISABELLE workshop on longitudinal instabilities was held at Brookhaven August 9 - 13, 1976. About a dozen outside accelerator experts, both from Europe and the USA, joined the local staff for discussions of longitudinal instabilities in ISABELLE. An ɜnda of talks was scheduled for the first day of the workshop (Apɪdix I). Later during the week, P. Channel gave a presentation on the subject "A more rigorous treatment of Landau damping in longitudinal beam instabilities".

Because the number of participants was not unduly large, it was possible to proceed with the preparation of reports and very informal discussions among small groups of individuals. A few progress meetings were held in which disagreements regarding calculations of coupling impedances were clarified. A summary session was held on the last day.

Heavy emphasis was put on single bunched beam instabilities in the microwave region extending above the cut-off frequency of the ISABELLE vacuum chamber. During the 1975 Summer Study[1] it became clear that the prevention of longitudinal microwave instabilities might indeed be one of the most difficult design problems in ISABELLE. This conclusion was based on recent observations of such instabilities at both the ISR and the PS (CERN) and, further, on theoretical work explaining their behavior quantitatively. The effect seemed most hazardous for the AGS bunches during their acceleration from the injection orbit to the stack. It could cause a blow up of the longitudinal phase-space area of the bunches thus limiting the total current in ISABELLE

---

*J. Channel, A.W. Chao, E.D. Courant, A. Garren, R.L. Gluckstern, S. Giordano, H. Hahn, H. Hereward, J.C. Herrera, D. Johnson, L.J. Laslett, E. Messerschmid, D. Möhl, M. Month, G. Parzen, R.F. Peierls, E.C. Raka, F.J. Sacherer, P. Wilson, B. Zotter.

1. W. Schnell, Proc. 1975 ISABELLE Summer Study, Brookhaven, BNL 20550, p. 126.

to a value below the design intensity of 10 A. To avoid these instabilities the longitudinal coupling impedance (Z/n) of each ring will have to be of the order of a few ohms.

The workshop was asked to address itself to three major aspects of the above problem: Further understanding of the mechanism governing the instability and calculations as well as measurements of the longitudinal coupling impedances in the ISABELLE rings.

Regarding the mechanism of the instability, theory was further extended at the workshop to include the dependence of the threshold current on not only the coupling impedance but also on the quality factor (Q) of the parasitic resonator whose induced voltage is the cause of the instability. Two main contributions to this subject were made.

Numerical calculations performed earlier by Messerschmid and Month[2] had indicated that the single bunch microwave instability was determined by the local Keil-Schnell criterion for resonator bandwidths of the order of the bunch width but that higher threshold currents were obtained for increasing Q-values. Messerschmid and Month[3] carried out further computations during the workshop and also formalized a theory trying to explain the observed results in a quantitative way. Their continued computer simulation showed that for sufficiently high Q values, corresponding to a bandwidth equal to the spacing of individual normal ring modes, the single bunch instability was determined by the ordinary coasting beam threshold criterion. Moreover, it was found that there was a transition region for intermediate values of Q where threshold currents lie between those predicted by the two criteria.

The theory put forward in connection with these results assumes that the instability takes place on a much faster time scale than the

---

2. E. Messerschmid and M. Month, Nucl. Instrum. Methods 136, 1 (1976).

3. E. Messerschmid and M. Month, these Proc.

synchrotron motion. On this basis the latter is ignored and the ordinary coasting beam theory is applied. An effective impedance, $Z_{eff}$, is introduced describing the response of a resonator with impedance Z to a normal mode perturbation superimposed on the unperturbed charge distribution of the bunch. It is shown that this combination, for low Q values, excites a series of modes, equal to 1/B in number, where B is the bunching factor. The effective impedance is ıal to the sum of the impedances of these modes which equals to ). In this way the local Keil-Schnell criterion is obtained. As Q increases the number of excited modes decreases, and when a single mode remains, the ordinary coasting beam criterion applies.

Sacherer[4] also treats the single bunch microwave instability theoretically. According to his earlier theory on longitudinal bunched beam instability, the single bunch mode is stable to first approximation. However, he concluded during the workshop that instability can occur due to coupling of adjacent multipole modes when the beam induced voltage becomes comparable to the applied rf voltage. If the bandwidth of the resonator is smaller than the spacing between the normal ring modes only one spectrum line at most contributes to the instability. For growing bandwidth the resonator will cover more and more lines until it reaches a value of $1/\tau$. Here $\tau$ is the bunch width and also the width of the overlap of two adjacent multipole charge distributions. This leads to the same dependence of threshold current on the Q of the resonator as was found both on a simulated computation and theoretically by Messerschmid and Month.[3] Work is in progress to determine the exact threshold duration.

Theoretical estimates of actual impedances seen by the beam got a a great deal of attention. A more detailed summary of this subject .s prepared by Zotter[5] during the workshop.

Relative contributions from cavities in the form of vacuum ports, etc. and from the connecting vacuum tube sections at frequencies where

---

4. F.J. Sacherer, these Proc., p.

5. B. Zotter, these Proc., p.

the pipe can support propagating modes were discussed. Cavity contributions (resonance impedances) have been calculated in the past and are known to yield rather high values. (A procedure similar to that used at the ISR will have to be used in order to de-Q these cavities and to lower their coupling impedances by several orders of magnitude.)

The vacuum chamber contributions were evaluated in several ways. Impedance calculations based on field matching, put forth by Month and Peierls[6] prior to the workshop, indicated extremely sharp resonance and high values for Z/n. During the workshop it was concluded that these findings were a result of neglecting the wall resistivity of the pipe sections. Gluckstern[7] developed a different approach in which the periodic cavities were viewed only as means of bringing the phase velocity of propagating mode close to the beam velocity. The effect of the discontinuity region is characterized by two parameters related to the reflection and transmission coefficients of the discontinuity alone. Revised results from the field matching calculations[8] and those obtained by Gluckstern now yield a comparable value of several ohms for Z/n of the pipe sections in ISABELLE. (This also agrees with earlier estimates by Faltens and Laslett,[9] viewing the pipe section themselves as resonance cavities.)

In view of this, the ISABELLE vacuum chamber material is now being reconsidered. Changing from aluminum to stainless steel would reduce Z/n of the rings by a factor of seven, bringing the contributions of the tube sections down to the order of one ohm.

The subject of different techniques of impedance measurements was only briefly dealt with. In addition to the measurements of the dis-

continuities mentioned in the previous paragraph, the pros and cons of more conventional methods of determining resonant impedances of parasitic cavities were discussed.

---

6. M. Month and R. Peierls, "Coupling Impedance Structure above the Tube Cutoff Frequency" to be published.

7. R.L. Gluckstern, these Proc.

   M. Month, private communication.

   A. Faltens and L. J. Laslett, Proc. 1975 ISABELLE Summer Study, Brookhaven, BNL 20550, p. 486.

## APPENDIX I

### Workshop on Longitudinal Instabilities

August 9 - 13, 1976

### Agenda

The Workshop will begin at 9:30 in Bldg. 923.

| | | |
|---|---|---|
| Opening Remarks | J. Sanford | 9:30 |
| Introduction | R. Chasman | |
| General Comments on Microwave Instabilities | M. Month | |
| Longitudinal UHF Instability in a Bunch | H. Hereward | |
| Bunched Beam Longitudinal Instabilities and their Extension to High Frequencies | F. Sacherer | |
| Numerical Simulation of the High Frequency Longitudinal Instability of Bunched Beams | E. Messerschmid | |
| Lunch | | 1:30 |
| Calculation of Longitudinal Coupling Impedance of Rings of Arbitrary Shape | R. Peierls | |
| Longitudinal Coupling Impedances in a Periodically Loaded Guide above Cutoff | R.L. Gluckstern | |
| Comparison between Calculations and Measurements of Longitudinal Coupling Impedances (Experience from the PEP Design with very Short Bunches) | P. Wilson | |
| General Discussion | | |
| Coffee | | 3:30 |
| Organization of Working Groups | | |

# THE EFFECTIVE COUPLING IMPEDANCE AND THE "MICROWAVE" INSTABILITY

E. Messerschmid
University of Freiburg
and
M. Month
Brookhaven National Laboratory

troduction

Recent observations on the growth of beam density fluctuations[1,2] have demonstrated the existence of longitudinal instabilities of individual bunches at very high frequencies. It was suggested[1,2] that a quantitative description could be obtained by treating the different sectors as if each was a distinct coasting beam and applying the usual coasting beam theory,[3-5] while substituting local values of current and energy spread for the separate segments. This ad hoc procedure can be justified if the underlying source of the bunched induced instability was a combination of low Q, high frequency resonators.[6] The underlying agreement is that these conditions imply such a fast wakefield that communication between bunch sectors is weakened, thereby allowing them to behave independently of each other. The fast growth rate implied by the high frequency unstable oscillations allows the instability to evolve to significant proportions within a small part of a synchrotron cycle. From this it can be inferred that a single bunch could develop an unstable condition in spite of the damping character for unstable waves propagating along the top of a bunch.[6]

---

1. D. Boussard, CERN Report Lab II/RF/Int. 75-2 (1975).
. S. Hansen and A. Hofmann, CERN ISR Performance Report, ISR-TH/RF-AH/SH, 25.6.1975 and A. Hofmann, ISR-TH/AH/amb, 10.12.1975 (private communication).
3. V.K. Neil and A.M. Sessler, Rev. Sci. Instrum. 32, 256 (1961).
4. A.G. Ruggiero and V.C. Vaccaro, CERN Report, ISR-TH/68-33 (1968).
5. E. Keil and W. Schnell, CERN Report, ISR/TH/RF/69-48 (1969).
6. H.G. Hereward, Proc. 1975 ISABELLE Summer Study, Brookhaven, BNL 20550, p. 555.

The dependence of the threshold impedance and growth rate on the local characteristics of a bunch was qualitatively confirmed by numerical simulation[7] of a particle bunch interacting with high frequency resonators of low quality factor (i.e. low Q). However, when the quality factor of the resonant objects was changed, while keeping the frequency of the resonators fixed, a very strong impact on the results was observed, thus indicating that the simple picture of local bunch segments behaving independently is incomplete.

Here we present the main results of a theory[8] for the fast bunch blow-up. The predictions of this theory are consistent with both computational and experimental observations.

The Effective Coupling Impedance

The basic postulate for the fast instability of a single bunch is that a single azimuthal beam mode, say $n_o$, can excite fields at all modes, n. The limit of this coupling is determined by the bunch spectrum, i.e. the bunch length. The coupling strength between a field mode n to a beam mode $n_o$ is assumed to be given by the usual coupling impedance of mode n. Writing

$$\ell = n - n_o \quad ,$$

and denoting the coupling impedance of mode n by $Z_\ell$, it can be shown that the effective coupling impedance for Gaussian bunches is given by

$$Z_{eff} = \sum_{\ell=-\infty}^{m} Z_\ell \, e^{-\ell^2 \theta_{rms}^2} \quad , \qquad (1)$$

7. E. Messerschmid and M. Month, Nucl. Instrum. Methods 136, 1 (1976).

8. The original paper is to be submitted to Nucl. Instrum. Methods.

where the exponential term represents the "weighting" of the impedances $Z_\ell$ due to the bunch spectrum. The bunch length is represented in units of the azimuthal angle $\theta_{rms}$.

In a rough way the Gaussian distribution function can be approximated by a double step of the same area and unit height, resulting in a cut-off mode number

$$\ell_c = \frac{1}{2B} = \frac{\sqrt{\pi}}{2} \frac{1}{\theta_{rms}} \quad ; \tag{2}$$

$B$ is the bunching factor defined by the ratio of bunch length to bunch separation. Thus we approximate $Z_{eff}$ by

$$Z_{eff} = \sum_{\ell=-\ell_c}^{\ell_c} Z_\ell \quad . \tag{3}$$

In the resonance case, the effective impedance is purely resistive, since the reactive component averages to zero. Thus, writing $Z_R$ as the peak resistive impedance (i.e. at resonance), we have for $Z_\ell$

$$Z_\ell = Z_R \frac{1}{1 + [(2\ell/n_o)Q]^2} \quad , \tag{4}$$

where Q is the cavity quality factor. In this case $Z_{eff}$ is given by

$$Z_{eff} = Z_R \left\{ 1 + 2\, a^2 \sum_{\ell=1}^{\ell_c} \frac{1}{a^2 + \ell^2} \right\} \quad , \tag{5}$$

where $a = n_o/2Q$ is the damping time constant. In the limit of high Q the effective impedance becomes $Z_R$, and in the limit of low Q it becomes $Z_R/B$ for small bunching factors B.

In terms of the effective coupling impedance, as discussed above the threshold criterion is found to be

$$\left| \frac{Z_{eff}}{n_o} \right| \leq F \frac{E}{e} \frac{|\eta|}{I_o} \left( \frac{\Delta E}{E} \right)_h^2 \tag{6}$$

where $E$ is the particle energy

$\eta$ is the energy slipping factor equal to $\gamma_t^{-2} - \gamma^{-2}$, where $\gamma$ is the energy in proton mass units, and $\gamma_t$ corresponds to the transition energy,

$I_o$ is the dc current,

$(\Delta E/E)_h$ is the relative full energy spread at half maximum in the center of the bunch, and

$F$ is a form factor, depending on the nature of the energy distribution function.

The growth rate may be obtained from

$$\alpha = \frac{f_o e I_o}{(\Delta E)_h} Z_{th} \left[ 1 + \left( \frac{Z_{eff}}{Z_{th}} - 1 \right)^2 \right]^{\frac{1}{2}} \sin \theta \qquad (7)$$

where

$$\theta = \tfrac{1}{2} \arctan \left( \frac{Z_{eff}}{Z_{th}} - 1 \right)$$

$f_o$ is the revolution frequency of a central particle and $Z_{th}/n_o$ is given by the rhs of Eq. (6).

Numerical Example

The real part of the coupling impedance, corresponding to $Z_R$ as introduced in Eq. (4), for a cylindrical cavity resonating at the $TM_{010}$ mode, is found to be[9]

$$Z_R = Q\, G(x)$$

where $G(x)$ for relativistic particles only depends on the number x equal to the length to diameter ratio of the cavity:

$$G(x) = 128\, \frac{\sin^2(1.202x)}{x}\ \Omega \ .$$

If we conjecture that the coupling impedance is dominated at high frequencies by resonators, it is not improbable that the sum of many such "low" Q elements can be simulated by a single strong "very low" Q resonator. Then the total coupling impedance is the sum of the single, say m, impedances. For x = 1 we find

$$Z_R = 111.4\ mQ\ \Omega \ . \qquad (9)$$

---

9. E. Messerschmid, BNL Report, ISA 75-14 (1975); and E. Keil and B. Zotter, CERN Report, ISR-TH/70-30 and 70-33 (1970).

With Eq. (9), the effective impedance for the Gaussian bunch spectrum becomes

$$\frac{Z_{eff}}{n_o m} = 55.7 \times \frac{1}{a}\left[\, 1 + \sum_{\ell=1}^{\infty} \frac{e^{-\pi(\ell B)^2}}{1 + (\ell/a)^2} \,\right] \quad .$$

This impedance is plotted in Fig. 1 (full lines) and compared, as function of 1/a, with the impedance for the case of a single rectangular bunch spectrum (dashed lines).

$$\frac{Z_{eff}}{n_o m} = 55.7 \times \frac{1}{a}\left[\, 1 + 2 \sum_{\ell=1}^{\ell_c} \frac{1}{1 + (\ell/a)^2} \,\right] \quad . \qquad (10)$$

It is obvious that the latter becomes a valid approximation for $\ell_c = 1/2B > 1$. The interesting feature of this impedance is that for large $\ell_c$ it does not change very much over a wide range of values of the parameter of 1/a. For large values of 1/a it becomes independent of the bunching factor and for decreasing values of 1/a it becomes a linear function of 1/a. A comparison of the effective impedance in the limit of small 1/a with the impedance for the case of an "unbunched" beam (that is $\ell_c = 0$) yields the bunching factor, in other words

$$\frac{Z_{eff}(\ell_c = 0)}{Z_{eff}(\ell_c = \frac{1}{2}B > 1)} = B$$

as is evident from Fig. 2.

For the numerical example used in references 7 and 8, where an ISR bunch was simulated ($\ell_c = 3$), Fig. 2 shows the effective impedance derived from the numerical simulation and compared with the effective impedance as obtained from Eq. (10). We have also included the results for a very short bunch ($\ell_c = 27$), and for a coasting beam ($\ell_c = 0$) having the same rms energy spread as the bunched beam. The corresponding growth rates of the simulated bunched beam instabilities are otted in Fig. 3 as a function of the inverse damping time constant a and compared with Eq. (7).

## Discussion of the Results and Some Conclusions

We have presented here the results of a theory for the fast longitudinal blow-up of individual particle bunches. The dispersion

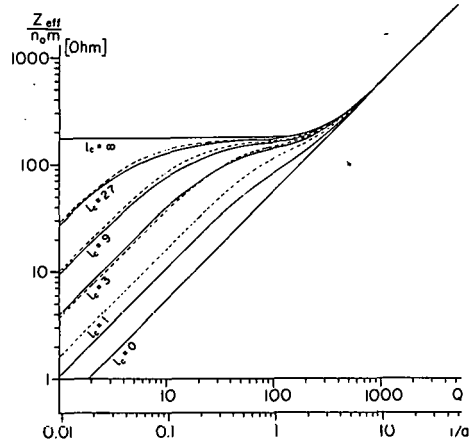


Fig. 1. Effective coupling impedance of a single resonator, as function of the damping time constant 1/a, for various values of $\ell_c$.

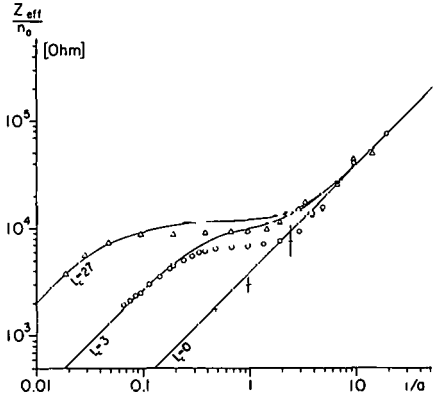


Fig. 2. Effective impedances, obtained from theory and numerical simulation, as a function of 1/a.

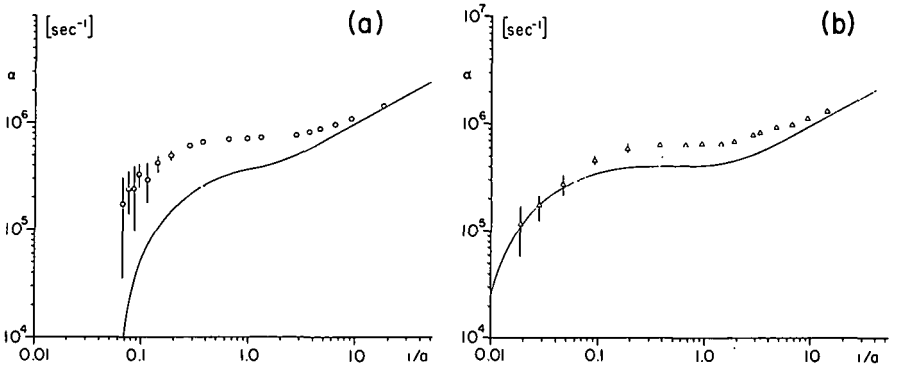


Fig. 3. Growth rates, obtained from theory and numerical simulation, as a function of 1/a. The parameters underlying the simulations were: $\gamma = 27.7$, $\eta = 0.011$, $f_o = 318$ kHz, peak rf voltages 8.27 kV ($\ell_c = 3$), 410 kV ($\ell_c = 27$) and 0 (for coasting beam), rf frequency = $30 \times f_o$ = constant, $m = 70$, $n_o = 6300$, $I_o = 0.18$ mA per bunch, elliptic distribution function of $(\Delta E/E)_h = 2.75 \times 10^{-4}$.

relation turned out to have an exceedingly simple form. It has a form like the coasting beam dispersion relation except with the usual coupling impedance for a particular frequency replaced by a quantity which we have termed the effective coupling impedance and which we have denoted by $Z_{eff}$.

There are in particular two properties of the bunch-environment interaction system which have allowed us to arrive at such a simple picture. First, the rapid evolution of the unstable oscillation modes means that phase motion can be neglected. That is, synchrotron motion is negligible and only direct energy loss by the bunch to the cavity plays a significant role in the dynamics. Second, we recognized that for this type of high frequency interaction, a given beam mode may couple to many field oscillation modes and that the range of such coupling was determined by the bunched character of the interacting beam. Thus we arrived at the concept of an effective coupling impedance, essentially a sum of the usual impedance function over the bunch frequency spectrum. The novel nature of this $Z_{eff}$ is that, to completely define it, we must include not only the properties of the resonators but also the characteristics of the bunched beam.

The theory was tested using a computer simulation model. A comparison of the theory with the simulation experiments has yielded remarkably good agreement. There are slight discrepancies in the range of intermediate values of the damping time constant. For large bunching factors, it is clear that the dominant inaccuracy is due to the small number of lines in the beam spectrum (low $\ell_c$). This is confirmed by the observation that the agreement of the results is better for small bunching factors.

The general solutions of the dispersion relation for instability thresholds and growth rates appear consistent with experimental observations of the fast instability of proton bunches. Since electrons and protons are equivalent on the time scale for the fast instability, it might be of interest to test our theory against the bunch lengthening observations made in electron storage rings.

Acknowledgments

We would like to thank H. G. Hereward, F. Sacherer and B. Zotter for the many stimulating discussions we had during this workshop on Longitudinal Instabilities.

# SINGLE-BUNCH LONGITUDINAL INSTABILITY

F.J. Sacherer

CERN

It has long been recognized that a bunch can oscillate in various modes: dipole, quadrupole, sextupole, etc. In each case the line densi $\lambda(t)$ can be viewed as the sum of two parts, the stationary distributio plus the oscillating perturbation:

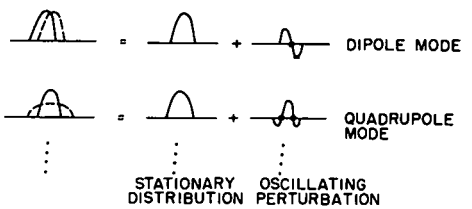


Fig. 1. Bunch oscillation patterns.

The oscillating charge distribution is approximately sinusoidal, and a little thought shows it to be a standing wave with fixed nodes. The modes can be labelled by the number of nodes, m = 1 for dipole, m = 2 for quadrupole, etc.

In the normalized phase plane with circular orbits, mode m has an m-fold symmetry of rotation, and the pattern is carried around with the synchrotron motion. The circular wave moving around the bunch can be viewed as two travelling waves, one moving to the left and the other to

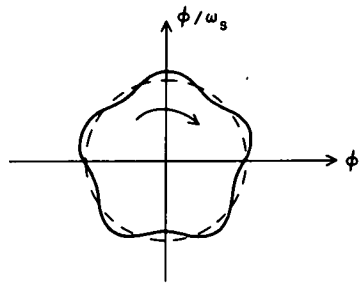


Fig. 2. Phase plane for mode m = 5

the right. The sum or projection $\lambda(t)$ is a standing wave, and such patterns are intrinsically stable. This can be shown by the following argument due to Hereward.[1] A coasting beam supports two independent travelling waves, one near the top and one near the bottom of the stack. If one grows (fast wave), the other is damped at the same rate. Thus for a bunched beam, whatever grows along one side of the bunch is damped on the other, with no net growth after one synchrotron period. There are other ways of showing this also.

If this were the whole story, it would be difficult to explain the recently observed microwave instability, and it also runs counter to our expectation that in the limit of long bunches and fast growth-rates, the coasting-beam stability criterion should apply to bunched beams. In fact, the above standing-wave modes are valid only in the limit of low intensities, when the frequency shift due to wake fields is considerably smaller than the synchrotron frequency. For larger frequency shifts, the standing-wave modes are coupled, and since the sum of two standing waves has a travelling-wave component, single-bunch instability is possible.

Mode-mode coupling means that the wake field due to one mode influences the others. The mathematical procedure[2] starts with the

1. H. Hereward, Proc. 1975 ISABELLE Summer Study, Brookhaven, BNL 20550 p. 555.

2. F. Sacherer, CERN/PS/BR 76-20.

Vlasov equation and results in a matrix M; the diagonal elements give the effect of a mode on itself, while the off-diagonal elements give the mode-mode coupling. Which modes are coupled depends on the frequency and bandwidth of the resonator or coupling impedance that produces the wake.

For a purely reactive impedance (no losses), the matrix is Hermitian, and all modes are stable. If losses are included, instability occurs ab a certain threshold. The threshold arises because the different modes h different natural frequencies ($\omega_s$ for the dipole mode, $2\omega_s$ for the quadrupole mode, $3\omega_s$ for the sextupole mode, and so on) which must be overcome by the coupling terms.

As an example, consider a narrowband resonator that couples only dipole and quadrupole modes. The eigenvalues are given by

$$\begin{vmatrix} \omega - \omega_s + M_{11} & M_{12} \\ M_{21} & \omega - 2\omega_s + M_{22} \end{vmatrix} = 0 \qquad (1)$$

where M is real and antisymmetric, $M_{12} = -M_{21} = \alpha$. Let $\omega_1 = \omega_s - M_{11}$ and $\omega_2 = 2\omega_s - M_{22}$ be the low intensity solutions. Then in general

$$2\omega = \omega_1 + \omega_2 \pm \sqrt{(\omega_1 - \omega_2)^2 - 4\alpha^2} \qquad (2)$$

and the threshold for instability is $\alpha = \frac{1}{2}|\omega_1 - \omega_2|$ .

Several points can be noted. 1) The instability need not be in the microwave region. 2) The dipole and quadrupole modes often appear to be coupled in practice, although this might also be due to the nonlinearity of the RF bucket. 3) The usual Robinson beam-loading criterion assumes rigid bunches and therefore neglects this coupling. 4) This might also explain the threshold observed for turbulence and bunch lengthening in electron storage rings.

The qualitative features of the microwave instability can be derived

from the form of M,

$$M_{mk} \propto j \sum_{n=-\infty}^{\infty} \frac{Z(n)}{n} \tilde{\lambda}_m^*(n)\tilde{\lambda}_k(n) \qquad (3)$$

which involves a sum over the mode spectra $\tilde{\lambda}_m(n)$ and the coupling impedance Z(n).

The spectrum for mode m is peaked near the frequency $(m + 1)/2\tau$ and has an extent $1/\tau$ corresponding to a sinusoidal wave $\lambda_m(t)$ with m nodes and $(m + 1)/2$ wavelengths and duration $\tau$ seconds, where $\tau$ is the bunch length. It is a line spectrum with frequencies $nf_0 + mf_s$ where $f_0$ is the revolution frequency and $f_s$ is the synchrotron frequency. The spectra of adjacent modes overlap, but the overlap for modes further apart can be neglected. As a result, only the main diagonal and the diagnoals immediately above and below need be considered in M.

Because of the even and odd symmetry of the modes, only the reactive part of Z contributes to the main diagonal, and only the resistive part to the diagonals on either side. Furthermore, the normalization of $\tilde{\lambda}_m$ can be chooseu so that M is real and antisymmetric.

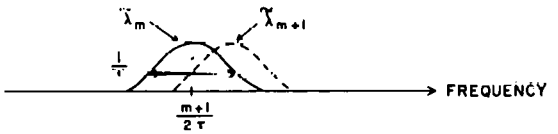


Fig. 3. Spectra for modes m and m + 1

Now consider a resonator with fixed shunt impedance $R_s$ but variable frequency and bandwidth $\Delta f$. If the bandwidth is smaller than the spacing between lines, $\Delta f < f_0$, only one spectrum line at most contributes to the sum (3). The worst case occurs when the resonator is centered on a line as shown in Fig. 4. In this case, obviously the matrix element $M_{m,m+1}$ is independent of the resonator bandwidth provided $\Delta f < f_0$.

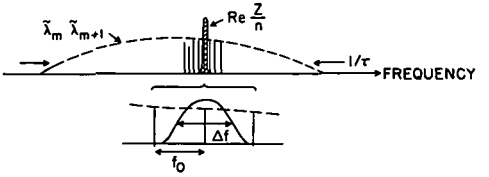


Fig. 4. Narrow band resonator that overlaps only one line

For larger bandwidths, the resonator overlaps more lines, and the matrix element grows, in proportion to the area under the resonance curve. The growth stops when the bandwidth exceeds the width $1/\tau$ of the $\tilde{\lambda}_m \tilde{\lambda}_{m+1}$ envelope. The number of lines contributing in this case is about $1/\tau$ divided by $f_0$ or $T/\tau = B^{-1}$, where B is the bunching factor.

The overall behaviour of $M_{m,m+1}$, and presumably the threshold $\propto M^{-1}$, is sketched in Fig. 5. A similar threshold dependence has been found in the computer simulation of Messerschmid and Month.[3]

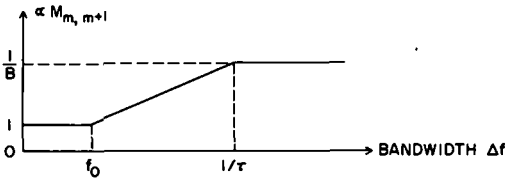


Fig. 5. Overall behavior of matrix element.

3. E. Messerschmid and M. Month, these Proc.

In summary, one expects a threshold proportional to impedance $R_s$ in the limit of very large or small resonator bandwidths, with the threshold lower by the bunching factor for the large bandwidth case. For intermediate bandwidths, the threshold should be proportional to the area under the resonance curve, so de-Qing resonators will have little effect in this region. It remains to compute explicitly the matrix M and find the exact threshold relation. This work is in progress.

# THE COUPLING IMPEDANCE OF A CIRCULAR TUBE WITH PERIODICALLY WIDENED REGIONS

B. Zotter
CERN

## I. Introduction

Because of the stringent requirements on coupling impedance for beam stability (in ISABELLE $|Z|/n$ should be less than a few ohms), a number of models have been discussed during the workshop which yield an estimate of the actual impedance seen by the beam. Special emphasis was given to the frequency region of a few gigahertz, where the tube can support propagating modes.

## II. Comparison of the Various Models

The comparison of the various approaches is complicated by the fact that they do not calculate the same quantities, and hence yield different results. Calculations of the coupling impedance made at CERN several years ago,[1] using field matching and subsequent matrix inversion by computer, indicate a behavior of the coupling impedances as shown in Fig. 1. This model will be discussed further in the next section. The same approach with different geometric subdivisions[2] is reported to have better convergence properties which simplifies the matrix inversion considerably.

In an extension of the first method,[3] which converts the matrix equations into an integral equation, the surprising result appeared that there exists a set of narrow spaced resonances above cut-off, with extremely high Q-values. This result can be explained by the fact that the "tube wall" resistivity was not included, and long sections of the tube wall were only damped by small resistive surfaces of adjacent cavities.

---

1. E. Keil, B. Zotter, CERN-ISR-TM/70-30 and 33 (1970); E. Keil, B. Zotter, Particle Accel. 3, 11 (1972).
2. H. Hahn, private communication.
3. M. Month, R. Peierls, Nucl. Instrum. Methods, 137, 299 (1976).

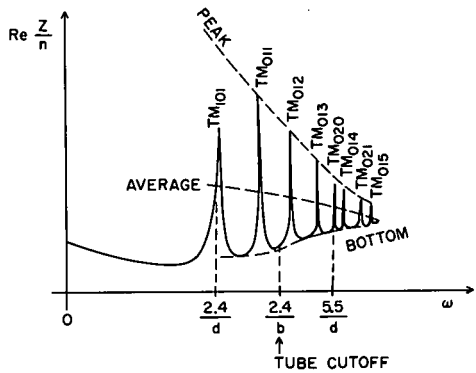


Fig. 1. Coupling Impedance vs Frequency.

Another model developed recently[4] calculates the impedance of a single cross-section step with infinite pipes on either side. This model yields no resonances, but the averaged impedance, and is therefore independent of the wall resistivity to first order.

During the workshop, a model was developed[5] which disregards resonances and considers the periodic cavities only as a means of bringing the phase velocity of the propagating mode close to the beam velocity. To my understanding, this model will essentially yield the bottom part of the impedance curve between the resonant peaks, and yields indeed much lower numerical values.

Two more ambitious approaches attempt to calculate impedances for quite general wall configurations.[6,7] If the cross-section changes are small, perturbation methods can be used to yield approximate results. However, I suspect that the numerical evaluation will become difficult or impossible in the resonant region, if the solutions are not expressed in terms of the eigenmodes of the cavities.

The rectangular cross-section variation assumed for the first two models may appear unrealistic for many accidental cavities such as bellows convolutions. However, the rounding of the edges has usually not a strong influence on the Q-values of the lowest modes, and the model should be better than it looks at first glance. This could be checked with the computer program "Superfish".

## III. Field Matching

The field matching approach leads to infinite matrix equations that can be solved numerically if the matrices may be truncated to a reasonable size. This means that the mode number should not be

---

4. H. Hereward, CERN-ISR-DE/75-47 (1975).
5. R. Gluckstern, Longitudinal Coupling Impedances in a Periodically Loaded Guide Above Cut-off, these Proc.
6. R. Peierls, these Proc.
7. E. Courant, private communications.

too high, i.e. the period length should be much smaller than actual machine circumferences. This may usually be assumed if the tube connecting the cavities is below cutoff, unless the cavity spacing is smaller than the distance in which the evanescent modes decay (usually about one tube diameter). The same assumption can be made above cut-off, if the cavity spacing is larger than the attenuation length of the mode under investigation in a tube of a given wall material.

For the case where these assumptions are not fulfilled, the cavities are strongly coupled and can no longer be treated independently. The problem is changed as one can now get a certain phase relation between adjacent cavities, which was excluded in the original field-matching approach with the assumption of strict periodicity. However, this case has also been treated several years ago[8] and yields the result that the coupling impedance of N equal cavities is at most N times the single cavity impedance, depending on the particular mode, while it is strictly N times the single cavity impedance for negligible coupling.

If the cavities in the ring are not geometrically equal, it is still possible that some of their modes have a strongly overlapping frequency response and should be treated by the methods valid for equal cavities. This is specially applicable when the cavities are strongly damped, and have low Q-values. If this is not the case, they can be treated quite independently and the total impedance is just the sum of the contributions which resonate at different frequencies.

## IV. Conclusions

From earlier work at CERN, one finds that the coupling impedance of a circular tube with periodically widened sections has resonant peaks essentially only at the resonances of the widened sections ("cavities"), independent of whether the frequencies are

8. E. Keil, B. Zotter, CERN-ISR-TM/71-15 (1971).

below or above cut-off of the connecting tube. The tube itself, enclosed between two adjacent cavities, may also be considered a resonator. However, three different mechanisms act together to reduce its coupling impedance: a) the long length and small diameter give a low R/Q, b) the small diameter and the open ends lead to a low Q*, c) the long length yields an unfavorable transit time factor. The result of all this seems to explain the fact that tube resonances can be neglected, and that the important contributions to the coupling impedance are due to the resonances of real or accidental cavities.

---

* Q is approximately the tube radius divided by the skin depth, reduced by a factor which depends on the amount of energy leaking out at the ends.

# Longitudinal Coupling Impedance Structure in Terms of Green's Functions

Ronald F. Peierls
Brookhaven National Laboratory

## I. Introduction

In discussing the longitudinal instability problem for a ›asting beam in a conducting ring, an important consideration is the electromagnetic self coupling of a particular frequency component of the beam due to the presence of the conducting walls. This is parametrised by the longitudinal coupling impedance, which is the average voltage change, per unit amplitude of beam current at this frequency, experienced by a beam particle in one turn.

A number of calculations[1-3] have been made to determine the value of this impedance under specific circumstances, each calculation involving a specific assumption about the shape of the conducting surface, the location of the beam, etc. Evidently many of the gross features of the results do not depend on the details of the assumptions and some general inferences can be made as discussed by Zotter[4] in his summary.

The purpose of this note is to point out that by using a more general formulation of the problem in terms of Green's functions instead of electric fields, it is possible to understand the origins of these general features before specifying a particular configuration and to lay a convenient framework for carrying out detailed calculations in some more complicated cases. In particular, the relationship is clarified between the impedance roperties of cavities, pipes, and other components in isolation nd when combined into a realistic machine.

---

1. E. Keil and B. Zotter, Particle Accelerators 3, 11 (1972).
2. M. Month and R. Peierls, Nucl. Instrum. Methods 137, 299 (1976).
3. E. Courant, these Proc., R. Gluckstern, these Proc.
4. B. Zotter, these Proc.

## II. Formalism

We make the usual assumption that the curvature of the ring is negligible, and take its closed nature into account by imposing periodic boundary conditions

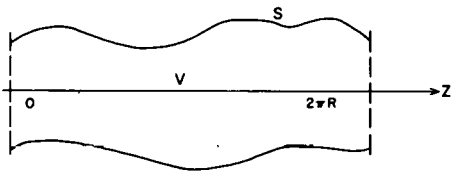


In other words, the structure we consider is a conducting tubular surface of arbitrary shape surrounding the z axis, with the plane $z = 0$ equated to the plane $z = 2\pi R$. V denotes the interior of the structure and S its surface. Considering a component of the beam current of frequency $\omega$, having current density

$$\vec{j}(\vec{r})\ e^{-i\omega t}$$

and resulting in an electric field

$$\vec{E}(\vec{r})\ e^{-i\omega t}$$

the longitudinal coupling impedance is

$$Z(\omega) = \frac{1}{I^2} \int_V \vec{j}^{*}(\vec{r}) \cdot \vec{E}(\vec{r}) d^3\vec{r} \qquad (1)$$

I being the magnitude of the beam current at this frequency.

The usual procedure is to expand $\vec{E}$ in terms of an appropriate set of functions. The boundary conditions at the walls of the structure and at the beam impose constraints resulting in a linear set of equations for the components of $\vec{E}$. The resulting matrix equations can be solved straightforwardly, possibly requir-

ing extensive computer analysis; Z can then be calculated. Care has to be exercised near resonances when the equation becomes singular (or nearly singular if the resistivity is nonzero), and the expansion functions have to be chosen with care to get reasonable convergence.

The field $\vec{E}(\vec{r})$ is linearly related to the current density $j(\vec{r})$:

$$\vec{E}(\vec{r}) = i\omega\mu \int_V \underline{\vec{G}}(\vec{r},\vec{r}') \cdot j(\vec{r}') d^3\vec{r}' \tag{2}$$

where $\underline{\vec{G}}(\vec{r},\vec{r}')$ is the Green's function for the field,[5] satisfying the same boundary conditions as $\vec{E}(\vec{r})$ at the wall of the machine. $\vec{G}$ is a dyadic, since it yields a vector when dotted into a vector. If we choose an appropriate set of vector functions $\vec{\psi}(\vec{r})$, orthonormal in a region R which completely includes V; so that

$$\int_{\mathcal{R}} \vec{\psi}_i(\vec{r}) \cdot \vec{\psi}_j^*(\vec{r}) d^3\vec{r} = \delta_{ij} \tag{3}$$

$\vec{G}$ can be expanded:

$$\underline{\vec{G}}(\vec{r},\vec{r}') = \sum_{ij} G_{ij} \vec{\psi}_i(\vec{r}) \vec{\psi}_j^*(\vec{r}') \tag{4}$$

so that the impedance is given by

$$\left.\begin{aligned} Z(\omega) &= i\omega\mu \sum_{ij} \gamma_i \gamma_j^* G_{ij} \\ \gamma_i &= \int_V \vec{j}(\vec{r}) \cdot \vec{\psi}_i(\vec{r}) d^3\vec{r} \end{aligned}\right\} \tag{5}$$

($\vec{\ }$, $\vec{E}$, $\gamma$, $\vec{G}$ all contain $\omega$ as a parameter).

The problem of finding the matrix coefficients $G_{ij}$ is essentially equivalent to that of finding the coefficients of the field

5. P.M. Morse and H. Feshbach "Methods of Mathematical Physics" McGraw-Hill, New York (1953): Chapters 7 and 13.

$\vec{E}$, and again results in a matrix equation. There are several advantages to this representation.

First, the coefficients $G_{ij}$ depend only on the characteristics of the tube, not the beam, so that once a solution is obtained, the effects of varying the shape or location of the beam are easily seen.

Secondly, there exist a large body of general properties of Green's functions, which allow what would otherwise be tedious manipulations to be carried out more simply. In particular, the resonance structure appears in a very simple way.

We use two properties of the Green's functions. First of all, suppose that $G^0$ is the Green's function satisfying boundary conditions for a perfect conductor on a surface $S_0$ surrounding a volume $V_0$, and G is the Green's function satisfying the same condition on a surface S surrounding a volume V where V lies within $V_0$

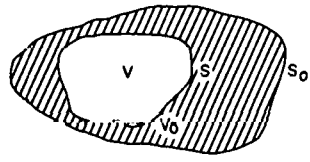


Then the Green's function G can be expressed* in terms of $G^0$ by a matrix equation.

*The derivation follows straightforwardly by applying the vector form of Gauss' Theorem, and will be given elsewhere. (No guarantee is made for the accuracy of the formulas in this note: its purpose is to develop the qualitative conclusions, and show the potential advantage of Green's function techniques.)

When $V_0$, $S_0$ are replaced by $V_i$ $S_i$ (V lying within $V_0$):

$$\left.\begin{aligned} G_{ij} &= G_{ij}^{\,0} + \sum_{k\ell} G_{ik} W_{k\ell} G_{\ell j}^{\,0} \\ W_{k\ell} &= \int_{\Delta V} \left\{ \omega^2 \vec{\psi}_k^{\,*} \cdot \vec{\psi}_\ell - \vec{\nabla} \times \vec{\psi}_k^{\,*} \cdot \vec{\nabla} \times \vec{\psi}_\ell \right\} dV \end{aligned}\right\} \qquad (6)$$

ere $\Delta V$ is the region between S and $S_0$.

Similarly, let G be the Green's function for the electric field in a region V bounded by a perfectly conducting surface S, and G' the Green's function for the same region but with a resistive surface: then

$$\left.\begin{aligned} G'_{ij} &= G_{ij} + \sum_{k\ell} G'_{ik} V_{k\ell} G_{\ell j} \\ V_{k\ell} &= \int_S \xi (\hat{n} \times \vec{\nabla} \times \vec{\psi}_k^{\,*} \cdot \hat{n} \times \vec{\nabla} \times \vec{\psi}_\ell) dS \\ \xi &= (1-i) \sqrt{\frac{\mu_0}{2\omega\sigma}} \end{aligned}\right\} \qquad (7)$$

$\sigma$ being the conductivity of the surface (not necessarily constant), and $\hat{n}$ being the inward normal unit vector to S.

Thus by using (6) and (7) in succession the Green's function, and hence the impedance, of an arbitrarily shaped region can be determined. The choice of function $\vec{\psi}_i(\vec{r})$ and of the reference region $V_0$ can be made to greatly simplify the calculation. If $\Delta V$ is a small region then perturbation methods, equivalent to those iscussed by E. Courant,[3] can be used. Since $\sigma$ is large for cases f interest, $\xi$ is always small and a perturbative solution to (7) is always possible.

III. Resonance Structure

For any enclosed region there exist a discrete set of resonant modes. The fields corresponding to the modes form a complete

set and the Green's function can be expressed[5] in terms of them in the form

$$G(\vec{r}|\vec{r}') = \sum_n \frac{\vec{e}_n(\vec{r})\vec{e}_n^*(\vec{r}')}{\omega^2-\omega_n^2} \qquad (8)$$

where $\vec{e}_n$ is the normalised field associated with resonant frequency $\omega_n$. If we use these fields as expansion functions, the matrix G takes the simple form:

$$G_{nm}(\omega) = \frac{\delta_{nm}}{\omega^2-\omega_n^2} \qquad (9)$$

Equation (6) has the form

$$G = G^0 + G\,W\,G^0 \qquad (10)$$

(We have suppressed the explicit matrix indices.) This has the formal solution

$$G = G^0[1 - W\,G^0]^{-1} \qquad (11)$$

G, $G^0$ and W all being matrix functions of $\omega$. Resonances will occur at those frequencies $\omega$ at which

$$\det[1 - W\,G^0] = 0 \qquad (12)$$

We are interested in the case when W is small; we write $W = \lambda\bar{W}$ and consider what happens when $\lambda \to 0$. Then writing $G^0$ in the form (9) we have the condition

$$\det\left[\delta_{nm} - \frac{\lambda\bar{W}_{nm}}{\omega^2-\omega_{n0}^2}\right] = 0 \qquad (13)$$

For small $\lambda$, it is well known that

$$\det(1 - \lambda A) \simeq 1 - \mathrm{Tr}\lambda A \quad ; \qquad (14)$$

thus

$$\det(1- W G^0) \approx 1 - \sum_n \frac{\lambda}{\omega^2-\omega_n{}^{02}} \cdot \bar{W}_{nn} \qquad (15)$$

This expression passes through all real values in the neighborhood of $\omega = \omega_n{}^0$; and hence must vanish at some point in that neighborhood. To first order in $\lambda$, therefore

$$\omega_n{}^2 = \omega_n{}^{02} + \lambda \bar{W}_{nn}(\omega_n{}^0) \qquad (16)$$

(The result is true as $\lambda \to 0$, provided $\bar{W}$ is a sufficiently slowly varying function of $\omega$, even though the expansion (15) breaks down for $|\omega^2-\omega_n{}^{02}| \ll \lambda$).

Now write G in the form

$$G_{nm} = \sum_k \frac{\theta_{nk}\,\theta^*_{km}}{\omega^2-\omega_k{}^2} \qquad (17)$$

where $\theta_{nk}$ is the overlap between the perturbed modes and the original ones:

$$\theta_{nk} = \int_{V_0} \vec{e}_n^{\,0*}(\vec{r}) \cdot \vec{e}_k(\vec{r}) dV \; . \qquad (18)$$

Equation (6) becomes

$$G_{nm} = \sum_n \frac{\theta_{nm}\theta^*_{km}}{\omega^2-\omega_k{}^2} = \frac{\delta_{nm}}{\omega^2-\omega_m{}^{02}} + \sum_{kj\ell} \frac{\theta_{nk}\theta^*_{km}}{(\omega^2-\omega_k{}^2)} \frac{\lambda \bar{W}_{j\ell}\,\delta_{\ell m}}{(\omega^2-\omega_n{}^{02})} \qquad (19)$$

Equating the residues of the poles at $\omega^2 = \omega_k{}^2$, we obtain

$$\theta^*_{km} = \delta_{km} + (1-\delta_{km}) \frac{\lambda \bar{W}_{km}}{(\omega_k{}^{02}-\omega_m{}^{02})} + O(\lambda^2) \qquad (20)$$

Substituting in (19) we obtain, finally

$$G_{nm}(\omega) = \frac{1}{(\omega^2-\omega_n^{02})}\left\{\frac{\delta_{nm}+\lambda\bar{W}_{nm}}{(\omega^2-\omega_n^{02})} + \lambda^2\sum_{k\neq n}\frac{1}{(\omega_n^{02}-\omega_k^{02})}\right.$$

$$\left.\left[\frac{\bar{W}_{nk}\bar{W}_{km}}{\omega^2-\omega_n^{02}} + \frac{\bar{W}^*_{nk}W_{km}}{\omega^2-\omega_k^{2}}\right]\right\} \qquad (21)$$

Hence we see that the perturbation represented by W has two effects

(1) there is a shift in the resonant frequency

(2) G is no longer diagonal in the original representation, the nm element coupling to all resonant frequencies, with a residue of order $\lambda^2$ for $k \neq n$.

Since we made no use of the properties of the matrix W, the same conclusions apply to Eq. (7) only in this case the frequency shift is complex.

IV. Example: perturbed smooth tube

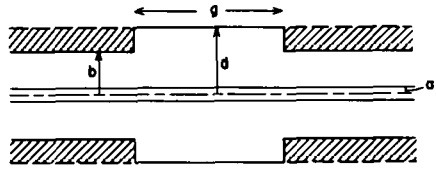


As an example, let us consider a case discussed in a previous calculation[12]: A circular tube of radius b, widening to radius d over a distance g.

For the initial unperturbed region $V_0$ we choose a conducting circular cylinder of radius d. Then, using the normal modes of such a region (with periodic boundary conditions as discussed in Sec. II) we can substitute in ( 5 ) and ( 9 ) to obtain

$$Z(\omega) = i\omega\mu\sum_a \frac{|\gamma_a^0(\omega)|^2}{\omega^2-\omega_a^2} \qquad (22)$$

where

$$\gamma_a = \frac{1}{\Sigma} \int_{V_0} \vec{j}^{*}(\vec{r}) \cdot \vec{e}_a(\vec{r}) d^3V \qquad (23)$$

Here $\vec{e}_a(\vec{r})$, $\omega_a$ are the resonant fields and frequencies for the mode labelled by a.

If the current density $\vec{j}(\vec{r})$ is uniform with radius a, and purely axial, then using cylindrical coordinates $(r,\theta,Z)$:

$$\vec{j}(\vec{r}) = \hat{z}\, I \frac{\theta(a-r)}{\pi a^2} e^{i\frac{nz}{R}} \qquad (24)$$

We consider a single current harmonic n. The frequency associated with this current component is

$$\omega_n = \frac{\beta c n}{R} \qquad (25)$$

$\beta c$ being the particle velocity. This current component is orthogonal to all modes except the axially symmetric TE modes. These are labelled by two integers: $a \equiv m,\alpha$. The fields and frequencies are

$$\left.\begin{aligned} e_{ma}(r) &= N_{m\alpha}\, e^{\frac{imz}{R}} \left[-i\left(\frac{md}{Rj_\alpha}\right) J_1(j_\alpha r), 0, J_0(j_\alpha r)\right] \\ N_{m\alpha} &= \frac{\chi_a}{\pi\sqrt{2R}\; d\omega^0_{m\alpha} J_1(j_\alpha)} \\ \chi_\alpha &= \frac{j_\alpha}{d} \\ J_0(j_\alpha) &= 0; \quad \alpha = 1,2.... \\ \omega^{02}_{m\alpha} &= m^2/R^2 + \chi_\alpha^2 \end{aligned}\right\} \qquad (26)$$

Hence

$$\gamma_{m\alpha}(\omega_n) = \delta_{mn}\, 2\pi R\, N_{m\alpha} \left( \frac{J_1(\chi_\alpha)a}{\chi_\alpha a} \right)$$

and

$$Z = i\omega\mu \sum_\alpha \left( \frac{4\pi R^2 N_{m\alpha}^2}{\chi_\alpha^2 + n^2/\gamma^2 R^2} \right) \left( \frac{J_1(\chi_\alpha a)}{\chi_\alpha a} \right)^2 . \qquad (27)$$

Thus we see that although the impedance has the appearance in (22) of a sum of resonances, the residues all vanish. The sum over $\alpha$ in (27) gives the usual smooth wall capacitative impedance, though clearly this is not the most convenient representation to evaluate it!

Note that below cutoff, i.e., for $\omega < \chi_\alpha$, resonances can not be excited because the denominator does not vanish. Above cutoff they do not appear because the residue vanishes, and this is due to the fact that each mode field $\vec{e}_n$ involves only one harmonic in z. This follows from the uniformity of the cylinder.

If we now use the results of Sec. III we see from Eq. (21) that perturbing the boundary shape so that the cross section varies mixes in other modes. From Eq. (21) we can see that all the resonances can now be excited: that corresponding to the mode $k\beta$ giving a contribution to Z of the form

$$Z_n^{(k\beta)} \approx \frac{j\omega\mu}{\omega^2 - \omega_{k\beta}^2} \sum_\alpha \frac{|\gamma_{n\alpha}|^2 |W_{n\alpha\, k\beta}|^2}{(\omega^2 - \omega_{n\alpha}^{0})^2 (\omega_{n\alpha}^{02} - \omega_{k\beta}^{02})}$$

where $\omega_{n\alpha}^0$ is given by (26) and

$$\omega_{k\beta} \approx \omega_{k\beta}^{\,0} + W_{k\beta\, k\beta}(\omega_{k\beta}^{\,0}) \quad .$$

The matrix W is just that given by (6) with the function $\vec{\psi}$ replaced by the mode function $\vec{e}_n$ defined in (27) and the integration region

is the shaded annular region shown in the figure.

Hence a perturbed, perfectly conducting closed ring has an impedance which exhibits a number of closely spaced resonances whose frequencies are given by

$$\omega = c\sqrt{\frac{m^2}{R^2} + \frac{j_\alpha^2}{d^2}} + W_{m\alpha m\alpha} \qquad \begin{matrix} m = 1,2,\ldots \\ \alpha = 1,2,\ldots \end{matrix}$$

When the walls become resistive, the major effect is that each resonance frequency acquires an imaginary part. If the imaginary part of the resonant frequency is much larger than the resonance spacing then no resonant structure will be visible but the real part of the impedance will be dominated by the value of the residue at the nearest pole. This is in qualitative agreement with the results calculated previously and will be spelled out in detail elsewhere.

V. Coupling of cavities due to the tube: effects of attentuation.

In the last section, we discussed the case of very small cavities regarded as a perturbation on the tube. In this section we consider the opposite case: cavities of appreciable size, where the tube acts as the perturbation which shifts the resonant frequency of the cavity and couples different cavities together

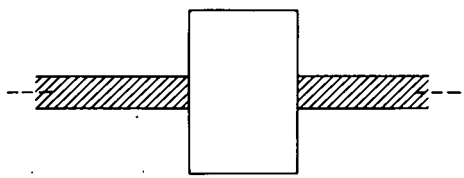

For a single cavity, the problem is straightforward: the perturbation is treated essentially as in the previous section but now the expansion functions are those of a conducting cavity and the region $\Delta V$ needed to construct the perturbation matrix W is the shaded

part of the tube. Once again, the frequency shift can be explicitly calculated.

Now suppose that we have two identical cavities separated by a distance S

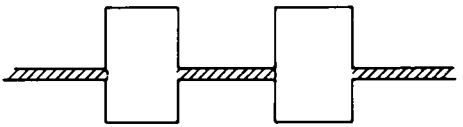

Using the same general approach as before, the unperturbed problem consists of two independent cavities: the unshaded area in the figure. The effect of the tube perturbation is to pick some particular linear combination of the independent resonances

$$\vec{e}_m(\vec{r}) \approx \theta_1(\vec{r}) e_m^0(\vec{r}) + e^{ik_m s}\theta_2(\vec{r}) e_m^0(\vec{r})$$

where $\theta_1(\vec{r})$, $\theta_2(\vec{r})$ vanish unless $\vec{r}$ is in the first or second cavity respectively, and $k_m$ is the propagation constant for the $m^{th}$ cavity mode in the Z direction. Inserting this into (5) and (9) we see that

$$Z = 2Z_1[1+\cos k_m s]$$

where $Z_1$ would be the impedance of a single cavity leading to the natural conclusion that the cavities interfere constructively or destructively according to their separation. Note that this mixing of levels and thus the interference is possible only if the cavities are identical so that their resonances overlap.

The effect of multiple cavities can be taken into account in just the same way, the impedance acquiring a factor

$$\left| \sum_r e^{ik_m S_r} \right|^2$$

$S_r$ being the distance of the $r^{th}$ cavity from the first.

In practice, attenuation will prevent the coupling of more than a few adjacent cavities. Putting resistive losses in the walls gives the resonance frequencies an imaginary part, leading in turn to an imaginary part for $k_m$, and a behaviour

$$e^{-\mathrm{Im}k_m \cdot |Z-Z'|}$$

for the Green's function, so that there is little coupling between current elements at distances large compared with $(\mathrm{Im}k_m)^{-1}$.

## VI. Conclusions

In this note we have sketched a description of coupling impedance in terms of Green's functions. The problem has been defined as a stationary one, dealing with fixed frequency components of a coasting beam. Exactly the same kind of treatment can be given to a nonstationary situation by using a time dependent Green's function

$$\vec{G}(r,t|r',t')$$

which may be of use in understanding the way instabilities grow.

# LONGITUDINAL COUPLING IMPEDANCES IN A PERIODICALLY LOADED GUIDE ABOVE CUT OFF

R.L. Gluckstern
University of Maryland

## I. Introduction

A bunched circulating proton beam will cause electromagnetic fields to be generated in a metal wall vacuum structure. For a structure with constant cross section, the waves generated will be those associated with waveguides, and the modes which propagate will have phase velocities greater than the velocity of light. As a result, the interaction of these waves on the particle bunch will average to zero, and not cause any undesirable effects.

When there are regions of the vacuum pipe which have different geometrical properties, such as vacuum ports, probe regions, clearing electrode regions, etc., it is possible for the beam to excite modes which can travel, as in a periodically loaded waveguide, with the velocity of the beam bunch. In this case, a longitudinal beam instability can be set up, limiting the current which can be circulated. This limit is related to the "coupling impedance" of the electromagnetic structure and the purpose of this note is to calculate this coupling impedance approximately.

Keil and Zotter[1] have calculated the coupling impedance for a particular geometry of periodic discontinuities in a ring, in essence solving the complete electromagnetic field problem primarily at frequencies below the cut off frequency in the main part of the vacuum pipe. Month and Peierls[2] have reformulated the analysis for frequencies above the cut off, but also treat the complete electromagnetic field problem. In the present calculation, the main fields are considered to be present in the guide region, rather than in the discontinuities, and the effect of the discontinuity region is characterized by two parameters related to the reflection and transmission coefficients of the discontinuity. In this way it should be possible to determine these two parameters from simple rf measurements on the

1. E. Keil and B. Zotter, Particle Accelerators 3, 11 (1972).
2. M. Month and R.F. Peierls, Nucl. Instrum. Methods 137, 299 (1976).

discontinuity alone, or from simple mode solutions of the discontinuity using computer routines like SUPERFISH.[3] We shall assume a frequency above the cut off of the $TM_{01}$ band, but below the cut off of the $TM_{02}$ and higher TM bands, so that only one mode is able to propagate. The discontinuity regions will include enough of the vacuum guide so that nonpropagating modes have decayed sufficiently to be neglected at the boundaries. We shall further assume that the beam bunches avel with the velocity of light.

ii. General Calculation of the Coupling Impedance

If one assumes a time-dependence of $e^{-i\omega t}$ and a sinusoidal driving current density of the form

$$J_z = I\, e^{i(\omega/c)z} e^{-i\omega t} \delta(x)\delta(y) \quad , \tag{1}$$

it is possible to solve Maxwell's equations for the electric field generated by this current. If the voltage is defined as

$$V = \int_{ring} dz\; E_z(0,0,z) e^{-i\omega t}\Big|_{t=z/c} \quad , \tag{2}$$

one can obtain an expression for the coupling impedance $Z_{coup} = - V/I$, given by

$$\frac{Z_{coup}}{120\pi\Omega} \cong \sum_{resonances} \frac{i\omega c}{[\omega^2 - \omega_r^2 + i(\omega^2/Q_r)]} \frac{\left|\int_{ring} E_z e^{-i(\omega/c)z} dz\right|^2}{\int E^2 dv} \tag{3}$$

where the integral in the numerator is taken along the beam axis, and the integral in the denominator is taken over the complete volume of the vacuum region, with the factor $e^{-i\omega t}$ being suppressed. The losses have been incorporated in the quality factor $Q_r$ in a form which neglects the small shift in resonance frequency due to finite $Q_r$, but which exhibits the traditional resonance denominator.

Our task is now two-fold. First, we must formulate the mode and ield structure in this ring loaded with periodic discontinuities. Then we must determine the location of the resonant modes, so as to see which resonance modes contribute to $Z_{coup}$ at a given frequency.

---

3. K. Halbach and R.F. Holsinger, Particle Accelerators (to be published).

III. Mode Structure in a Periodically-Loaded Ring

We shall assume a structure like that shown in the figure,

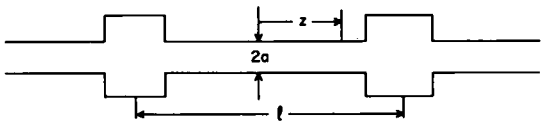


consisting of a ring of length $N\ell$ containing N periodically spaced discontinuities. The rotation frequency is

$$\frac{\omega_o}{2\pi} = \frac{c}{N\ell} \tag{4}$$

and z = 0 is chosen as the midpoint between discontinuities. The voltage integrand in (3) must repeat when z increases by $N\ell$, requiring the driving frequency to be given by

$$\omega = \frac{2\pi nc}{N\ell} = n\omega_o \tag{5}$$

where n is an integer.

Within the pipe, the propagation constant, $\beta$, is given by

$$\beta^2 = \frac{\omega^2}{c^2} - \frac{p^2}{a^2} = \frac{\omega_o^2}{c^2}(n^2 - n_c^2) \tag{6}$$

where $p = 2.405$ is the first zero of the Bessel function for the $TM_{01}$ mode and where the cut off harmonic $n_c$ (not necessarily an integer), is defined by

$$\frac{\omega_c}{c} = \frac{p}{a} = \frac{\omega_o}{c} n_c = \frac{2\pi}{N\ell} n_c \quad . \tag{7}$$

The presence of the periodic discontinuities changes the phase advance in the distance $\ell$ from $\beta\ell$ to $\mu$, the Floquet parameter (which is defined in such a way that it is identical to $\beta\ell$ in the absence of

discontinuities). Because of the ring structure, $N\mu/2\pi$ must be an integer, so that

$$\mu = \frac{2\pi}{N} h \quad , \tag{8}$$

and in the absence of discontinuities

$$n^2 = n_c^2 + h^2 \quad . \tag{9}$$

The behavior of the field $E_z$ can be written, by virtue of the Floquet theorem, as

$$E_z = \sum_{-\infty}^{\infty} \left[ b_m \sin \left( \frac{2\pi m + \mu}{\ell} \right) z + c_m \cos \left( \frac{2\pi m + \mu}{\ell} \right) z \right] \tag{10}$$

where $b_m, c_m$ are the harmonic coefficients caused (for $m \neq 0$) by the periodic discontinuities. The voltage integral in (3) will then be given by

$$\left| \int_{\text{ring}} dz \; e^{-i(\omega z/c)} E_z \right|^2 = \frac{N^2 \ell^2}{4} (b_m^2 + c_m^2) \tag{11}$$

only for that value of the integer m which is given by

$$\frac{\omega}{c} = \frac{2\pi m + \mu}{\ell} \tag{12}$$

or

$$n = mN + h \quad . \tag{13}$$

The tasks which now remain are listed below:

1. We must estimate $b_m$ and $c_m$ for the value of m appropriate to (9) and (13). We shall do this by assuming that the dominant field is the propagating mode in the guide section, with shift of phase $\pm \mu$ between adjacent sections.

2. We must calculate the energy storage term in (3), which we shall also approximate by assuming that the major contributions are from the propagating mode in the guide sections.

3. We must calculate the resonant frequencies of these modes by determining the relationship between $\beta\ell$ [related to frequency by (6)] and $\mu$ by measuring or computing the electromagnetic properties of the discontinuity.

IV. Calculation of Coupling Impedance

In estimating the dependence of $b_m, c_m$ on m, we shall assume that the transverse electric field is given, in the $j^{th}$ waveguide section, by

$$E_r = (V_o^j \cos \beta Z + W_o^j \sin \beta Z) \frac{a}{p} J_1\left(\frac{pr}{a}\right) , \qquad (14)$$

where we shall relate $V_o^j$ and $W_o^j$ in adjacent sections by a 2 x 2 matrix description which parameterizes the effect of the discontinuities. The transverse field $E_r$ can be written equally well near the axis in terms of $b_m$ and $c_m$, analogous to (10), as

$$E_r = \sum_{-\infty}^{\infty} \left(\frac{2\pi m + \mu}{\ell}\right) \left[ -b_m \cos\left(\frac{2\pi m + \mu}{\ell}\right) z + c_m \sin\left(\frac{2\pi m + \mu}{\ell}\right) z \right] \frac{r}{2} \qquad (15)$$

We shall relate $b_m$ and $c_m$ to $V_o^j$, $W_o^j$ by equating these two expressions.*

The matrix transformation for a section of waveguide with characteristic impedance $Z_c$, and with the elements of the vector being $E_r$ and $iZ_c H_\varphi$ is

$$\begin{bmatrix} \cos \beta\ell & \sin \beta\ell \\ -\sin \beta\ell & \cos \beta\ell \end{bmatrix} \qquad (16)$$

The equivalent matrix for the symmetric discontinuity also has unit determinant and equal elements along the diagonal, and can therefore be written in terms of two parameters $\sigma$ and b as†

$$\begin{bmatrix} \cos \sigma & \frac{\sigma \sin \sigma}{b} \\ -\frac{b \sin \sigma}{\sigma} & \cos \sigma \end{bmatrix} \qquad (17)$$

*We match $E_r$ instead of $E_z$ because lumped shunt behavior by the discontinuities will correspond to infinite $E_z$ in the version in (15), but not in (14).

†This matrix corresponds to the discontinuity including enough guide on each side to guarantee decay of evanescent modes, multiplied on each side by the reciprocal of (16) for half the total length of obstacle and guide extensions. In this way (17) corresponds to an element of zero length located at the center of each obstacle.

The parameters $V_o^j$ and $W_o^j$ are then obtained from $(M)^j$, where

$$M \equiv \begin{bmatrix} \cos\mu & \beta_o \sin\mu \\ \frac{-\sin\mu}{\beta_o} & \cos\mu \end{bmatrix}$$

$$= \begin{bmatrix} \cos\frac{\beta\ell}{2} & \sin\frac{\beta\ell}{2} \\ -\sin\frac{\beta\ell}{2} & \cos\frac{\beta\ell}{2} \end{bmatrix} \begin{bmatrix} \cos\sigma & \frac{\sigma\sin\sigma}{b} \\ \frac{-b\sin\sigma}{\sigma} & \cos\sigma \end{bmatrix} \begin{bmatrix} \cos\frac{\beta\ell}{2} & \sin\frac{\beta\ell}{2} \\ -\sin\frac{\beta\ell}{2} & \cos\frac{\beta\ell}{2} \end{bmatrix} \quad (18)$$

I can be written as

$$V_o^j = V_o^o \cos j\mu + W_o^o \beta_o \sin j\mu$$

$$W_o^j = \frac{-V_o^o}{\beta_o} \sin j\mu + W_o^o \cos j\mu \quad (19)$$

After much manipulation, $b_m$ and $c_m$ can be obtained by equating (14) and (15), using (19) and inverting the Fourier series, leading to*

$$b_m^2 + c_m^2 = \left(\frac{\ell}{2\pi m + \mu}\right)^2 \left(\frac{V_o^{o2} + \beta_o^2 W_o^{o2}}{2\beta_o^2}\right) \left[\frac{(1+\beta_o)\sin[(\mu-\beta\ell)/2]}{2\pi m + \mu - \beta\ell} - \frac{(1-\beta_o)\sin[(\mu+\beta\ell)/2]}{2\pi m + \mu + \beta\ell}\right]^2 . \quad (20)$$

It is also necessary to calculate $\int E^2 dv$. Again assuming that the essential contribution comes from the sections of waveguide, one finds

$$\int E^2 dv = \frac{N\ell}{2} \frac{\pi a^4 J_1^2(p)}{p^2} \frac{\omega^2}{\beta^2 c^2} \left(\frac{1 + \beta_o^2}{\beta_o^2}\right) (V_o^{o2} + \beta_o^2 W_o^{o2}) \quad . \quad (21)$$

One then finds from (3), (11), (20), and (21), and $J_1^2(p) \cong 2/\pi p$, that the coupling impedance can be written as

$$\frac{Z_{coup}}{n} \cong \frac{7.5\ \Omega}{p} \sum_{res} \left[\frac{i\omega^2}{\omega^2 - \omega_r^2 + i(\omega^2/Q)}\right] \frac{N^2}{(1 + \beta_o^2)} \frac{h^2}{n^6} \left[(1 + \beta_o)(n + h) \times \sin\left(\frac{\mu - \beta\ell}{2}\right) - (1 - \beta_o)(n - h) \sin\left(\frac{\mu + \beta\ell}{2}\right)\right]^2 \quad (22)$$

*Note that, in the absence of an obstacle $\sigma = 0$, $b = 0$, $\mu = \beta\ell$, $\beta_o = 1$ and (20) vanishes for $m \neq 0$, as it must.

This equation should be understood as follows:

1. The externally chosen frequency is determined from (5) by the particular choice of n. With $n_c$ determined from the geometry through (7), one finds h from (9). It is necessary now to consider several integral values of h in the vicinity of that determined by (9). The only values of h which can contribute are those for which m is an integer in (13). In each case, $\mu$ is determined by (8).

2. The parameters of the discontinuity, $\sigma$ and b, must either be calculated or measured for a particular discontinuity geometry. A possible measurement scheme is discussed briefly in Section VI.

3. One now determines the value of $\beta$ necessary to satisfy (18). From (6), one then determines the resonant frequency $\omega_r$. The parameter $\beta_o$ is also found from (18).

4. The quality factor $Q_r$ is obtained in the usual way from the conductivity, frequency and waveguide radius, since in our assumption the losses are dominated by the waveguide.

5. The coupling impedance is now obtained from (22) as the sum of contributions from each resonance. If the spacing of resonances is such that a single resonance dominates (high Q), the first bracket in (22) will have a maximum value of $Q_r$. Where several resonances contribute (low Q) the bracket will be approximately $\pi\omega/\delta_r\omega$, where $\delta_r\omega$ is the spacing of the resonances,* and where we assume a slow variation of all terms except the resonant term. In this case, approximately $\pi\omega/Q_r\delta_r\omega$ resonances contribute at one time.

## V. Approximate Calculation of Coupling Impedance

It is possible to proceed further, in a very approximate manner, by assuming that each discontinuity can be represented by a low value

*It can be readily shown that the value of $Q_r$ at which several resonances start to contribute corresponds to the attenuation in the guide becoming significant between discontinuities. For low $Q_r$ the discontinuities apparently act independently.

of the shunt susceptance B. This corresponds to $\sigma \to 0$, $b = -BZ_c$ in (18) leading to

$$\cos\mu \cong \cos\beta\ell - \frac{b}{2}\sin\beta\ell \tag{23}$$

which, for small b, gives

$$\mu - \beta\ell \cong \frac{b}{2} \quad . \tag{24}$$

One further finds from (18) that

$$(1 - \beta_o)\,\sin\frac{\mu + \beta\ell}{2} \cong (1 + \beta_o)\,\sin\frac{\mu - \beta\ell}{2} \cong \frac{b}{2} \tag{25}$$

d (22) becomes

$$\frac{Z_{coup}}{n} \cong \frac{25\Omega}{16}\left[\frac{Q}{\frac{\pi\omega}{\delta_r\omega}}\right]\frac{N^2h^4}{n^6}\,b^2 \quad . \tag{26}$$

The spacing of adjacent modes which can couple to the beam corresponds to values of $\mu$ which differ by $2\pi$, and therefore to values of h which differ by N. From (9), this corresponds to a spacing

$$\frac{\omega}{\delta_r\omega} \simeq \frac{n^2}{hN} \quad . \tag{27}$$

If Q is sufficiently small so that $Q < n^2/Nh$, one finds

$$\frac{Z_{coup}}{n} \simeq \frac{25\pi}{16}\frac{Nh^3}{n^4}\,b^2 \quad \text{(low Q limit)} \quad . \tag{28}$$

It should be pointed out, however, that (28) is valid only for extremely low values of Q (< 100 for ISABELLE parameters) which may be quite unrealistic. Thus, the upper term in the bracket in (26) should normally apply.

If b is indeed small, the parameters planned for ISABELLE predict a value of $Z_{coup}/n$ of order 1 ohm or less. However, it should be pointed out again that this corresponds to modes dominated by fields in the waveguide and assumes nonresonant behavior in the discontinuities.

## VI. Determination of Discontinuity Parameters

It should be relatively simple to measure the parameters $\sigma$ and b, by measuring the resonant frequency of a discontinuity containing a known length of guide on each side.

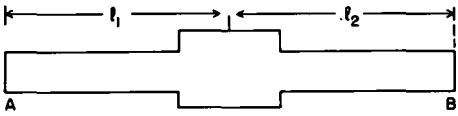


In simplest form, if $\ell_2$ is chosen to be an even number of guide quarter wavelengths ($\beta\ell_2 = j\pi$), the condition for resonance with shorted terminations at A and B is

$$\tan\beta\ell_1 = -\frac{\sigma}{b}\tan\sigma \quad . \tag{29}$$

If $\ell_2$ is chosen to be an odd number of guide quarter wavelengths [$\beta\ell_2 = (j + \frac{1}{2})\pi$], resonance will occur for

$$\tan\beta\ell_1 = \frac{\sigma}{b}\cot\sigma \quad . \tag{30}$$

The parameters $\sigma$ and b are obtained simply from these two measurements.

## VII. Resonant Discontinuities

At those frequencies at which the discontinuities resonate, one must start again with (3). If the discontinuities each resonate at a frequency within the width of a single resonance, one finds that the factors involving E lead to a factor

$$N\frac{R_s}{Q} \tag{31}$$

where $R_s/Q$ is essentially the ratio of shunt impedance per unit length to quality factor for a single resonant discontinuity. If each discontinuity is sufficiently detuned from the others, the factor N in (31, will be absent.

In general, the only resonant frequencies which will contribute are those for which the variation of $E_z$ with z matches the phase factor in (3). Otherwise there will be a rapidly falling transit-time

like factor. This implies contributing resonances which are widely spaced, suggesting the desirability of a major reduction in the quality factor, if practical.

## VIII. Summary

We have tried to estimate the contributions to the coupling impedance in a ring-like structure in which there are periodic perrbing discontinuities. These set up resonant modes above cutoff, edominantly in the waveguide sections, which have components traveling with the beam bunch. Our results are parameterized with the characteristics of the perturbing discontinuities, assumed to be nonresonant. For the ISABELLE parameters, it appears that $Z_{coup}/n$ is well below 1 ohm, and therefore not troublesome.

## IX. Acknowledgments

This work was carried out primarily at the Coupling Impedance Workshop at BNL from August 9-13, 1976. I have profited from numerous conversations with other participants in the workshop, especially R. Chasman, H. Hereward, L.J. Laslett, M. Month, R. Peierls, P. Wilson and B. Zotter.

# SUMMARY OF EXPERIMENTAL INSERTIONS WORKSHOP*

J. Sandweiss
Yale University
and
M. Month
Brookhaven National Laboratory

The last ISABELLE workshop of the summer 1976 series, which was held at Brookhaven August 16-20, focused on the design and utilization of the experimental insertions. The workshop was attended by approximately 30 scientists and engineers drawn from Brookhaven, Fermilab, SLAC, CERN and the University High-Energy Physics Community.

The goals of the workshop, which were somewhat more general than might be suggested by the title, are listed below:

a) Review the ISABELLE proposal from the point of view of experimental use. Especially study aspects related to the experimental program taken in toto rather than as individual isolated experiments.

b) Contribute useful information on the "open questions" in the ISABELLE design principally:

i) Is 8 the correct number of insertions? Should the number perhaps be 6?

ii) What is the optimum configuration of experimental halls?

iii) Are there any new ideas either in physics or technology which would have a significant impact on the ISABELLE design?

c) Develop data for experimental equipment and operating cost estimates.

d) Project a first approximation to ISABELLE operating modes. In essence prepare a reasonable scenario for the first few years of ISABELLE operation.

---

*A. Abashian, R. Chasman, C.Y. Chien, D. Edwards, T. Ferbel, H. Foelsche, A. Garren, H. Hahn, J. Herrera, R. Huson, D. Johnson, V. Kistiakowsky, B. Knapp, T. Kycia, W.Y. Lee, P. Limon, D. Lowenstein, T. Ludlam, R. Majka, M. Month, G. Parzen, J. Peoples, L. Pondrom, E.C. Raka, M. Sakitt, J.R. Sanford, M. Schwartz, W. Selove, R.P. Shutt, L.W. Smith, A. Thorndike, T.E. Toohig, W. Walker, H. Wiedemann, D.H. White, W.J. Willis.

Given the limitations of a one week study, the strategy adopted was to make maximum use of results from previous studies - the 1975 Summer Study, the ISABELLE proposal, and the reports of the various laboratory working groups during the past year — and to focus our efforts on an initial review of the existing design and on the new features addressed in the workshop.

The workshop was organized into five groups:

Scenarios Group - Chairman, A. Thorndike

This group attempted to project the first five years of ISABELLE operation under several different assumptions about funding, manpower, etc.

II. Experimental Design Group - Chairman, J. Sandweiss

This group carried out a physics review and an engineering design of a selected set of experiments chosen from the 1975 summer study.

III. Machine Studies Group - Chairman, M. Month

This group had two general objectives. First to establish the available range of collision region parameters allowed by the ISABELLE lattice design; and second, to determine the relative merits of 6 and 8 insertions with respect to machine performance.

IV. Radiation Studies Group - Chairman, T. Toohig

This group examined the different aspects associated with radiation problems including backgrounds, dumping and scraping systems, effects of magnetic trapping of muons, and possible radiation damage to experimental electronics.

V. Small Diamond Group - Chairman, W.J. Willis

This group studied the possible designs and ways of using a small (~ 5 cm) beam crossing region. In particular, high resolution detectors and imaging Cerenkov counter systems which require a small diamond were studied and evaluated.

There was substantial interaction between the groups and the information developed in one was quite often useful for the work of another. A summary of the results of each group was written by the respective chairman and these are included in the following reports. It would be redundant to summarize these results again here. Nevertheless, it may be useful to make a few general remarks about the results.

a) The proposed ISABELLE design appears to be fundamentally sou All the experiments studied were feasible. There are no inter-experiment interactions of a fatal nature and the design has a remarkable flexibility to adapt to new requirements, as illustrated, for example, by the small diamond modification.

b) This study shows that the choice of the number of insertions (6 or 8) is not a technical one but rather is a fiscal and policy choice. A viable scenario and good machine operation for experiments is possible with 6 or 8 insertions. Of course, with 8, properly funded, the research program will have greater capabilities than with 6.

c) Even a cursory glance at the individual reports reveals that a great many questions remain to be studied in detail. They do not seem to be questions of the sort that would change the conclusions given above, but they must be solved at some point before the machine is fully operational. Many of these would be most usefully addressed at this point by the continuing efforts of the ISABELLE group rather than by workshops or summer studies. Some of them, on the other hand, are still at the stage where periodic attention by a broadly based group - experimenters and accelerator physicists — would be very useful. An example of the latter is the possible standardization of data transfer electronics at ISABELLE.

# SUMMARY OF EXPERIMENTAL DESIGN GROUP

J. Sandweiss
Yale University

The basic goals of the experimental design group were twofold. First, the study was asked to provide information which would be useful in estimating experimental operation and equipment budgets, for ISABELLE. In addition, the study was to check in depth, at least for a few typical experiments, that the ISABELLE design, including insertions and halls was indeed compatible with the successful execution of the experiment.

Given the limitations of a one week workshop, the strategy adopted was to make full use of the previous studies on the experimental utilization of ISABELLE, and especially the rather detailed 1975 summer study. Thus, a small set of experiments, which had previously been written up in the 1975 study were chosen for more detailed investigation. Because there had been separate workshops on the large hadron and lepton detectors, these were excluded from our consideration. One participant addressed the general problems of electronic instrumentation at ISABELLE. The following lists the experimental design efforts carried out during the workshop and described in the individual reports following this summary.

1. Small Angle Single Arm Spectrometer (measurement of inclusive spectra) C.Y. Chien

2. Large Aperture Two Arm Magnetic Spectrometer at ISABELLE (measurement of large $P_\perp$, $\mu$'s and e's) B. Knapp and W. Lee

3. Study of Hadrons at Large Transverse Momentum (two arm magnetic spectrometer for jet studies) J. Peoples

4. Elastic Scattering and Diffraction Dissociation in the Angular Range 0 - 50 mrad P. Limon and R. Majka

5. Some Notes Concerning ISABELLE Electronic Instrumentation

M. Schwartz.

For each experiment studied an attempt was made to carry out the following analysis:

1. Review physics goals in the light of physics developments and the evaluation of the ISABELLE design since summer 1975.

2. Specify magnets, counters, wire chambers, etc.

3. Specify cabling, electronics, control computers, locations o control equipment and of experimenters.

4. Specify the vacuum chamber realistically, allowing correctly for pumping requirements and clearing electrodes.

5. Study rates and backgrounds. Establish luminosity requirements.

6. Estimate time required for

   a) set-up and test
   b) data collection
   c) demount or modify.

7. Compile a "parts" list and if possible, a first attempt at a cost estimate.

8. Study the relative utility of the various ISABELLE experimental halls for the proposed experiment.

The participants were by and large able to carry out this analysis and their results are given in the ensuing reports. These reports are short enough that there is not much point to summarizing them here. It may, nevertheless, be useful to abstract a few general features from them.

1. All of the experiments were indeed feasible and could be successfully carried out with the proposed ISABELLE design.

2. The physics interest has heightened in the experiments as a result of the recent discoveries. As a single example, Peoples notes that the hadronic decay of the W-boson will give rise to high $P_\perp$ jets carrying charm, and if there are more "flavors of quarks", high $P_\perp$ jets carrying the new quantum numbers as well.

3. The complexity (and cost) of the experiments has tended to grow relative to the 1975 summer study estimates. Some of this is due increased capability (as in the case of the high $P_\perp$ experiments) t some is due to the more realistic evaluation carried out in the workshop.

4. Careful consideration should be given to establishing a high degree of standardization in electronics, not only fast electronics modules as is now common, but also the data transfer systems from the experimental halls to the trailers. This latter may be especially useful at ISABELLE given the necessarily static siting of the experiments and "trailer" locations.

5. High ISABELLE luminosities, the use of drift chambers with $\sim 0.5$ $\mu$sec memory time, and the desire to search for "rare" events may lead to a very great utility for ultrafast microprocessor pattern recognition.

6. Computation in general — as it always does — appears to offer some difficulties if present-day state-of-the-art is assumed.

# SCENARIO GROUP SUMMARY*

Alan Thorndike
Brookhaven National Laboratory

## I. ASSUMPTIONS ON GENERAL SCOPE OF OPERATION

The following scenario provides a plausible sequence of events from FY 1980 to 1990. No doubt reality will be quite different. The scenario is based on the construction schedule of the 1976 proposal. Assembly and testing of the accelerator will occur until the end of FY 1983, and the next six years will provide pp interactions for the initial high energy physics research. By 1990 any temporary conditions associated with start-up of ISABELLE should be a thing of the past and all experimental capabilities fully utilized.

The overall scope of the program will be determined primarily by the financial support provided by ERDA. A set of numbers is given in Table I, which corresponds closely to the curves describing the funding plan in "Long Term Strategy for Construction and Operation of High-Energy Physics Facilities", October 10, 1975, prepared by ERDA for OMB. How the realities of the decade of the 80's may depart from this plan we cannot say; it is the basis for the Insertion Workshop scenario. Table I is expressed in 1976 dollars.

The operating funds in 1980 are somewhat higher than those available to BNL at present, and they continue to rise to 1983, at which time a total is reached which is roughly consistent with the cost of $17.5 M to operate ISABELLE (in addition to AGS) quoted in the ISABELLE proposal. It is wise to ascribe uncertainties to these quantities typical of measurements in high energy physics. The curves in the ERDA strategy stop at 1985, and we have extended them in an unimaginative way through 1989.

The equipment funds must cover some rather constant amount of small items, which we set at $2 M per year. This is assumed to cover the needs of AGS research as well (perhaps a doubtful point). The

*A. Abashian, T. Ferbel, H. Foelsche, W.Y. Lee, P. Limon, D. Lowenstein, J. Peoples, L. Pondrom, R. Shutt, L. Smith, and W. Walker.

remaining $41 M over the 10 year period is to equip ISABELLE for research. In the proposal equipment needs were stated to be "nearly $50 M". The schedule in Table I permits building equipment rather early so that a good deal can be ready when ISABELLE starts operation. This is to be contrasted with some past assumptions that complex equipment would be introduced only after a few years of operation. In developing the physics scenario it appeared that major parts of these large devices would be required at the earliest moment. It is moreover easier to install equipment in experimental areas before the beam is on than after, so the present sequence is advantageous from the operational point of view as well.

Table I also includes an estimate of the number of physicists doing high energy physics at Brookhaven during this period. The figures are reduced to full-time equivalent since most university people are at Brookhaven only a small fraction of the time. During the last fiscal year, there were 275 high-energy experimentalists with guest appointments. The main significance of the manpower estimates is the belief that many physicists will want to do experiments at ISABELLE, and that such manpower will not be a limiting factor in determining the scope of the experimental program.

TABLE I SCALE OF EFFORT

| F.Y. | Operating | Equipment | Physicists[a] |
|---|---|---|---|
| 80 | $34 M | $7 M | ~ 90 |
| 81 | 35 | 9 | ~ 90 |
| 82 | 39 | 11 | ~100 |
| 83 | 44 | 9 | ~110 |
| 84 | 44 | 6 | ~120 |
| 85 | 43 | 4 | ~130 |
| 86 | 43 | 4 | ~140 |
| 87 | 43 | 4 | ~150 |
| 88 | 43 | 4 | ~150 |
| 89 | 43 | 4 | ~150 |

[a] Full time equivalent for experimental physicists doing experiments at AGS and ISA, mainly from universities.

## II. THE OVERALL AGS & ISA SYSTEM

The AGS and ISA must be considered together because the AGS is required to provide 30 GeV protons for ISABELLE. The operation of the two must be planned together. In addition, it is very important to have particle beams from the AGS that can be used for testing detector modules and experimental subsystems that are to be used at ISABELLE. Since equipment in the ISA insertions is not accessible when the ISA beams are on, and the beams should not be turned off to suit the convenience of individual experiments, it is necessary for equipment to be much more reliable and more modularized than has normally been the case for AGS experiments. Careful testing of sub-assemblies is necessary to assure this. Consequently, a substantial increase in the number of test beams is foreseen from 1 to 3, as indicated in Table II.

TABLE II NUMBER OF SPIGOTS

| F.Y. | Test | AGS Res | Crossings[a] |
|---|---|---|---|
| 80 | 1 | 12 | --- |
| 81 | 2 | 11 | --- |
| 82 | 2 | 11 | --- |
| 83 | 3 | 9 | ? |
| 84 | 3 | 8 | 4 |
| 85 | 3 | 8 | 5 |
| 86 | 3 | 7 | 7 |
| 87 | 3 | 7 | 7 |
| 88 | 3 | 6 | 7 |
| 89 | 3 | 6 | 7 |

[a]Assuming eight-fold symmetry

There is a corresponding decrease in the number of AGS beams available for research from FY 80 to FY 83, as shown in Table II. In FY 84 some of the ISA crossing regions have experimental equipment installed and ready for taking data. By FY 86 all of them are in service and the ISA research program is in full swing. The resources

available to Brookhaven would not permit this without some diminution of the AGS research program. By FY 89 the number of AGS research beams is reduced to 6 from the 12 available in FY 80. AGS experiments in the 1980's will tend to be long and detailed, with fewer turnovers per beam than at the present time, as well. FY 89 will be the 28th year of research using beams from the AGS and it will be older than many of physicists then using it for their research.

Some increase in the number of experimental support personnel Brookhaven will be required to install equipment in the ISA insertions while maintaining the ongoing AGS program. Especially during FY 82, 83 and 84 there will be much work at the ISA, and new experimental set-ups and new AGS beams will be few during this period. Careful phasing of ISA and AGS programs will be needed to meet experimental needs within constraints of machine schedules and limitations in staff.

## III. EQUIPMENT FUNDS ALLOCATION

The $41 M that is available to provide equipment of long-term usefulness for ISABELLE is distributed as shown in Table III.

TABLE III EQUIPMENT

| F.Y. | Lepton | Hadron | High PT | Misc. |
|---|---|---|---|---|
| 80 | $ 2M | $ 1M | $ 1M | $ 1M |
| 81 | 2 | 2 | 2 | 1 |
| 82 | 2 | 3 | 2 | 2 |
| 83 | 0 | 2 | 1 | 3 |
| 84 | 1 | 0 | 0 | 3 |
| 85 | 0 | 1 | 0 | 1 |
| 86 | 1 | 0 | 1 | 0 |
| 87 | 0 | 1 | 0 | 1 |
| 88 | 1 | 0 | 1 | 0 |
| 89 | 0 | 1 | 0 | 1 |
| TOTAL | 9 | 11 | 8 | 13 |

(These amounts are for major apparatus, in addition to ~ $2 M for small items per year.)

This scenario includes three detector systems of substantial size, the Lepton Detector, Hadron Spectrometer, and a "High PT" system with large acceptance spectrometers on both sides of the interaction region. The Lepton Detector is assumed to have the reduced scope suggested as a possibility in the Lepton Detector workshop. The magnet can be procured early enough for it to be installed before machine testing begins. Similarly, the funds for Hadron Spectrometer and High PT system should make it possible for their magnets that are placed around the vacuum tank to be installed early enough that no interruption of machine testing and initial running would be required. The funds indicated for the Hadron Spectrometer match the scope described in the workshop devoted to it. There is a provision for extensions and improvements during the years 84-89.

The High PT system described during this workshop would not cost as much as the amount shown in Table III. The scenario assumption is that the system would become more elaborate and costly when actually built. Thus three insertions would be occupied early in the experimental program by rather large systems which would provide information on the existence and properties of intermediate bosons as well as other topics.

This allocation would leave about 30% of the equipment support for other magnets, detector systems and perhaps data-acquisisition and on-line analysis systems, that would be of long-term and widespread usefulness. No attempt was made to complete a parts list for these items. As shown in Table III this would provide an initial complement of such equipment, but there is only limited provision for additions and improvements during the years 85-89.

## IV. TIMING OF ISA OPERATION

With the construction schedule of the 1976 ISA proposal, beneficial use of ISA buildings will begin in FY 80 and all will be in service by the end of FY 81. This makes it possible to install experimental magnets and other major pieces of equipment in the experimental halls as the

equipment becomes available. This can go on in parallel with installation of ISABELLE components. To the extent that this can be done ahead of turn-on, the need for interruptions of ISA operation is reduced. In FY 83 beam will be injected into the ISA rings and tests, adjustments, and debugging will be underway for the machine. As this activity permits, installation of experimental equipment will continue, following tests with AGS beams. By the end of the year, the ISA beam will

adequate intensity and stability for tests of experimental equip- and initial data-taking runs will be possible, but infrequent.

During FY 84, ISABELLE operation will become more routine. The luminosity will increase, beam stability improve, and beam will be available for experiments more frequently. Background levels will become more acceptable. Most installed experiments will acquire some useful data.

Installation of equipment will continue during this period to make experiments more complete, and to activate additional insertions. This will consist largely of wire planes and Cerenkov counters, with most magnets and other massive items already installed before turn-on of the ISA.

## V. DUTY CYCLE

The scenario group did not discuss the details of day-to-day scheduling of the ISA experimental program, but there was general agreement that the overall duty cycle would be unlikely to exceed 50%, and that the schedule would have the general properties shown in Table IV.

TABLE IV DUTY CYCLE

| |
|---|
| 2 month shutdown twice a year. |
| Up to 100 days beam per 4 month on-time. |
| Limited access time every day or two |

The shutdown duration of 2 months is set in part by the time required for warm-up and cooldown of the superconducting magnet system. An overall time of about four weeks seems to be necessary, and two months is considered adequate for changes to ISABELLE that require the magnets to be warmed up. This should not happen as often as twice a year. Two months, however, is a reasonable time in which to accomplish major changes in experimental set-ups also, and an average of two such shutdowns per year should permit the necessary work of this sort to be done to meet the changing needs of the research program. During these periods people concerned with the support of the experimental program would concentrate on ISA insertions. During the remainder of the year subsystem assembly and testing, as well as work required in the AGS experimental program could be done.

Each four-month ISA research period contains about 120 days, but there will need to be some days, perhaps even weeks,with the beam off, distributed according to the needs of the ISA and the experimental program. At the beginning these interruptions will be very frequent. When the machine is in routine operation, up to 100 days per research period should be possible, and it may be most efficient to run for one or two weeks between beam-off days.

The duration of circulating beam in ISABELLE will usually be more than 10 hours but less than 100 hours. When the beam is dumped and refilled, some limited access time will normally be provided, allowing minor repairs and adjustment to experimental and machine equipment in the halls and tunnel. The duration will be at most a few hours. This mode of operation is essentially that used at the ISR. Details, of course, will vary according to the needs and capabilities of machine and research program at ISABELLE.

## VI. PROGRAM WITH 8-FOLD CONFIGURATION

### A. Lepton Hall

The magnet for the lepton detector[1] will be installed in 82 and tested. Testing of detectors at the test beam area will go on in

---

1. I.H. Chiang, R. Imlay, S. Iwata, S. Jacobs, R. Kraemer, M. Kreisler, K. McDonald, B. McIntyre, M. Sakitt, J. Thompson, A. Thorndike, A. Walenta, C. Wang, L.L. Wang, these Proc.

parallel and those necessary for a "muon-only" phase of the program will be installed during 83 and ready to use whenever ISA beam is available. Test, calibration, and installation of a partially completed assembly of hadron-calorimeter and electron-identifier modules will continue during 84 and 85. Based on initial results a complete hexagonal inner detector system will be installed and used during 86 and 87 and end caps will be added. The inner detector will be replaced in 88 and 89 with a second version providing magnetic analysis of the electron and hadron tracks.

B. Wide Angle Hall

This hall will house a pair of wide-angle spectrometers at $90^{\circ}$, initially used to measure muon and electron spectra to investigate weak interactions and intermediate boson properties.[2] Magnets will be installed in 82 and the associated detector systems in 83, after the necessary test and calibration. The remaining solid angle will be used for a variety of monopole-catchers. After initial data-taking in 84 and 85, the spectrometers will be modified to emphasize high PT hadrons during 86 and 87. By shifting positions, the angular range will be extended to explore jets and correlation phenomena more completely, with a sequence of experiments extending into 88 and 89.

C. Hadron Hall

It will be important to install the magnets for the hadron spectrometer[3] before the ISA beam is turned on so this will be done during 82 and 83. Testing of wire planes, Cerenkov counters, and calorimeter modules for the complete spectrometer will be actively pursued during those years, with installation during 83 and 84, as permitted by schedule and the experimental support work load. In 84 the effect of spectrometer magnets on the ISA beam will be explored, and operating procedures established. Complete system testing will begin in 85 with extensive data-taking runs in 86 to explore both hadronic states from intermediate boson decay and the dynamics of hadron interactions evidenced by multiparticle correlation phenomena.

---

2. B. Knapp and W. Lee, these Proc.

3. D.H. White, these Proc.

During this period, two central detector systems will be developed by regional consortia of universities which will be installed in alternate years during 87-89. This will provide quite complete information concerning multiparticle states, analysis of which will require increasingly substantial effort.

D. Elastic Hall

The initial experiment in this hall will be the Coulomb interference experiment,[4] installed in 83. During 84, however, machine operation will not be sufficiently stable for reliable results in this delicate experiment. It will continue during 85 while the small angle spectrometer is installed. Inclusive spectra from dissociation processes will be studied in 86. During 87 the $4\pi$ detector system of the $\sigma_{total}$ experiment[5] will be moved to this location. This system will permit more detailed study of Pomeron processes in 88 and 89.

E. Small Angle Hall

The initial experiment in this hall will be the measurement of $\sigma_{total}$ by the observation of secondaries in a "$4\pi$" detector.[5] This will occupy 84 and some of 85. A compatible version of the detector for elastic scattering and diffraction dissociation[6] will then be introduced. This will measure elastic differential cross section, $\sigma_{total}$ by extrapolation, and $\sigma_{total}$ by combining the two methods, during 85 and 86. Going on to Phase III in 87, further study of diffractive processes will continue in 88 and 89.

F. Open Areas

The scenario assumes that the remaining two insertions are implemented as open areas with concrete block shielding around the beam pipe as suggested during the experimental halls workshop. In this eight-fold scenario, the two open areas are near the beam injection points. The suspicion that experimenters in the areas will suffer from special problems due to beam losses at injection could not be entirely laid to rest.

---

4. J.N. Marx and R.D. Majka, Proc. 1975 ISABELLE Summer Study, Brookhaven, BNL 20550, p. 204.
5. S.U. Chung, P. Grannis, and D. Green, ibid. p. 183.
6. R.M. Edelstein and M. Zeller, ibid. p. 234.

During the 1975 Summer Study, a number of very speculative experiments were described in the summary of "New and Unthinkable Ideas".[7] The open areas provide a lot of flexibility to accommodate unexpected geometries, so they are used for experiments of this kind. In fact, the scenario assumes that the unthinkable experiments will look quite different when they are built in 1985 from what was thought in the 1975 summer study.

If, however, a scenario is constructed from the experiments :ribed in 75, one open area would have equipment installed in it in 85 for the "Search for Heavy Leptons via $K_L^o$ Type of Experiments", with the addition in 87 of the "Metastable Neutral Particle Arm". The other open area would have the "New Object Detector" installed in 86, with experimental use and further development in subsequent years. During the first year or so the open areas are not utilized except for possible "nook and cranny" experiments requiring negligible set-up effort.

G. Summary

This scenario has a conservative orientation, as might be expected for a schedule established by a committee. The large systems get started first, and the speculative adventures come later in the sequence. Of course, a scenario is not a prediction of what <u>will</u> happen, nor a value judgment as to what <u>should</u> happen. It is a statement of a plausible set of events, reasonably consistent with initial conditions and determining forces.

The main features of the program with the eight-fold configuration are indicated in Fig. 1.

## VII. OPTIONS

The ISABELLE Proposal mentions four major options: 1) $\bar{p}p$ collisions, ., a muon storage capability, 3) a deuteron storage capability,and 4) ep collisions with an additional electron storage ring. In this scenario only the $\bar{p}$ option is in use before 1990. The necessary

7. L.M. Lederman, <u>Proc. 1975 ISABELLE Summer Study, Brookhaven</u>, BNL 20550, p. 84.

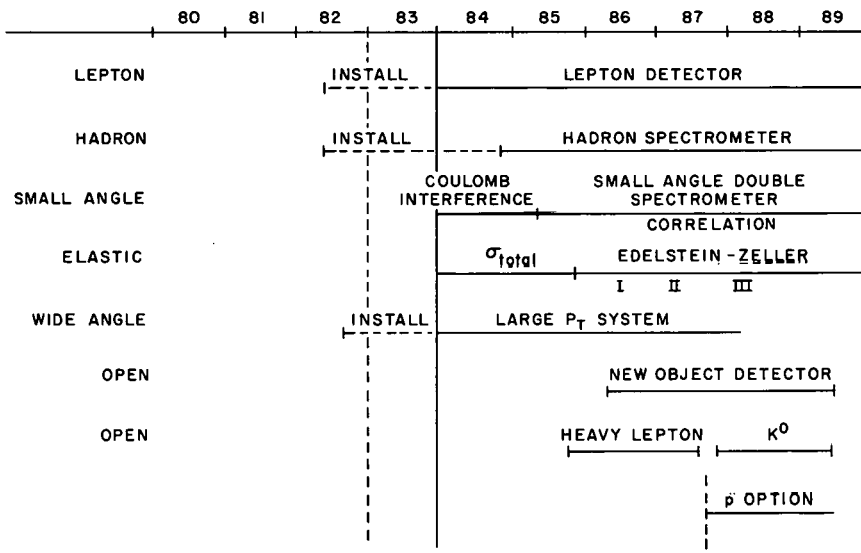


Fig. 1. Eight-fold program.

funds ($3.26 M in the proposal) are considered to become available following completion of the pp machine, with $\bar{p}$ testing in 87 and limited beam for experimental use during 88 and improved intensity by 89.

Many existing experiments could utilize $\bar{p}p$ collisions with little or no modification, so this would be a major part of the intermediate boson studies, the investigation of diffractive processes, and multi-

ticle state work by the end of the period. Comparison of $\sigma_{total}$ ($\bar{p}p$)

h $\sigma_{total}$ (pp) would be of immediate interest, but experiments of the highest precision would not be done until after 1990.

While this scenario does not include the ep option, a number of individuals considered study of ep collisions to have the highest priority. It would be an interesting exercise to prepare an alternative scenario with ep option, perhaps constrained to the same integrated BNL high-energy physics funding to 1990, but with a different allocation, or perhaps with an appropriate increment in funding.

## VIII. PROGRAM WITH 6-FOLD CONFIGURATION

With the six-fold configuration, 5 experimental insertions are available. These were assumed to include four halls and one open area. Again, two of the five areas would be near beam injection points. There would be a single long hall in place of elastic and small angle halls. The scenario development appears as follows:

A. Lepton Hall

The program will develop in essentially the same way as for eight-fold.

B. Wide Angle Hall

The program will develop in essentially the same way as for

ght-fold.

C. Hadron Hall

The initial experiment in this hall will be the program of elastic and diffractive studies (Edelstein-Zeller), which will continue

through 84, 85 and 86. If possible, the final phase of this program would use magnets designed for the hadron spectrometer, which would be installed late in 85. This would permit installing the complete hadron spectrometer in 87 at which time its program would begin, about two years later than with the eight-fold configuration.

D. Small Angle Hall

The total cross section and Coulomb interference experiments would occupy this hall for 84 and 85. By 86 the small angle spectrometer would be installed, and it would soon operate together with the $4\pi$ detector. Due to sharing of space, this work would progress somewhat more slowly than with the eight-fold configuration.

E. Open Area

The open area would be devoted to speculative experiments as before, and it would be necessary to start in 84. The New Object Detector goes in at first, with the Heavy Lepton Search in 86, and the metastable neutrals before 90. All three could be active if a very large and complex shielding enclosure was erected.

This program for the six-fold configuration is indicated in Fig. 2. The reduction from 7 to 5 experimental insertions causes the program to go more slowly, and it is generally consistent with a reduced funding scope. Accomplishment of research objectives would be lagging by about one year out of six. (One year's operation costs $43 M.) Because of the need to pack experimenters into limited space, experimental turnover flexibility is lost and the experimental support task becomes more difficult. (This could be eased by making experimental halls larger and more expensive, so they are more "general purpose".) As a result of these overall considerations, the $\bar{p}$ option is deferred to after 1990 in this scenario.

## IX. MODIFICATIONS IN SCOPE

Explicit scenarios were not prepared for general levels of support higher or lower than those of Table I. It seems clear that a higher level would make it possible to speed the program up somewhat, to push speculative experiments more aggressively and to implement options at an

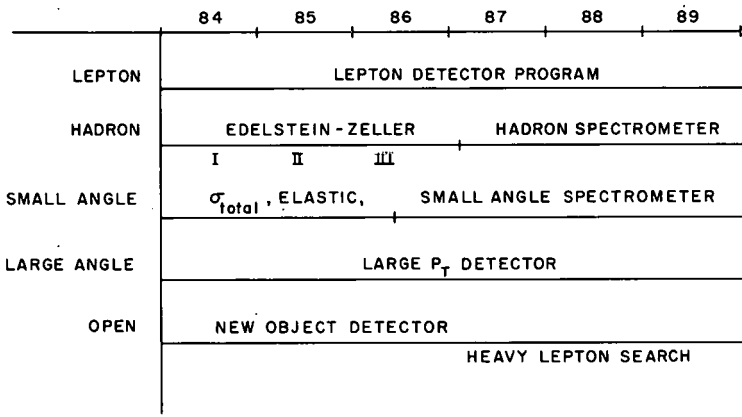


Fig. 2. Six-fold program.

earlier time. The AGS research program might well be continued at a higher level.

Conversely a reduced overall scope would probably involve one or more of the following: a) forced choice of six-fold rather than eight-fold option, b) more drastic reduction of AGS research, c) operation with poorer duty cycle, and reduced beam time per year, and d) failure to implement even the $\bar{p}$ option. Overall this would mean a much smaller output of results per year from the research program.

# TWO SUGGESTIONS TO "IMPROVE THE UTILIZATION OF ISABELLE"

Alan Thorndike
Brookhaven National Laboratory

One of the topics assigned to the Scenario Group was: "Are there any features of the experimental area design which improve the utilization of ISABELLE, but which have been overlooked at present?" There was little discussion of this topic during the week of the insertion workshop. In this note, two suggestions are outlined which are aimed at improving the efficiency of work in experimental areas by improving the information available to experimenters.

## I. COMMUNICATIONS BETWEEN EXPERIMENTAL HALL AND DATA ACQUISITION ROOM

Each experiment will have detectors in the experimental halls and data acquisition electronics in an outside room about 100 feet away. Tests and adjustments frequently require one experimenter at each of these locations with a good way to communicate between them. Lost time and confusion are common in this situation, and it would really pay to have a very good communication system to make work during times when beam is off as efficient as possible. Here are some ideas: 1) It should be a dedicated system that is always on or can be turned on from either position. It should be impossible for the two ends to be on different channels. 2) TV is desirable so each individual can watch what the other is doing to avoid confusion. 3) Slave CRT units would be desirable so both can watch a given waveform or other test signal. 4) It should also be possible to monitor key voltages from either location.

Such needs would seem to be common to most experiments. Standard equipment should be available to meet them.

## II. BEAM INFORMATION VIA COMPUTER

Each experiment needs to know about the beam conditions at its crossing region. It is probable, however, that each crossing will be affected to some degree by conditions in the others. The machine operators, of course, need to know about all of them.

Experimenters probably will spend a lot of time worrying about background, so they will need to know conditions that determine background as well as simple beam parameters like energy, current and

position. The values of these quantities should be available to each experimenter, but that probably will not be enough. If, for example, there is a set of background monitors in the ring, experimenters may need access to readings from all of them to evaluate conditions for their experiments. Perhaps measurements of vacuum will be important. Perhaps magnet currents at other insertions or their fluctuations will be required.

It seems reasonable to imagine that this information would be stored in one or more files on a disc in the on-line computer system. Each experimenter's computer could then get whatever information was desired. Handling the information by computer is straightforward, and more or less standard systems for data-base management should be applicable. Having satisfactory sensors to monitor the information that is needed seems like more of a problem, but they are required in any case.

It is very likely that information from experiments should also be made available to the ISA control room. This could include settings of any magnets or other equipment which might affect beam behavior, trigger rates, measures of background or beam quality from experimental detectors, and other information on the status of the experiment. This would give the machine operator a better idea whether conditions were good or bad for each experiment. (In a few cases experimental information has been relayed to the AGS control room at present. Means for doing so should be built in at ISABELLE.)

This suggestion does not mean that data from which high-energy physics results are extracted would be included in these operational data files. Such data would be stored, or analyzed on-line, as each experiment desired. The operational data files would only include information on the status of the experiment, conditions that might affect the circulating beams, and measures of beam qualities and background that are of general operational interest.

Such information would need to be updated several times an hour, and it might be useful to log some of this operational information from time to time on magnetic tape or other permanent storage medium. This record would be useful to the scheduling physicist and might well eliminate some manual record keeping that is done for administrative purposes. This would be a by-product, however, and the main purpose should be to aid in decisions during normal high-energy physics data-ing and test runs.

# REPORT OF THE RADIATION GROUP ON RADIATION BACKGROUNDS AND DAMAGE IN THE ISABELLE INTERSECTION REGIONS

T. Ludlam
Yale University
V. Kistiakowsky
MIT
and
T.E. Toohig
FNAL

## I. INTRODUCTION

The Radiation Group was charged to examine radiation aspects of the current ISABELLE design and the projected experimental arrangements. Some examples of questions to be addressed were:

1. How does the overall shielding design impact the experimental design?

2. What backgrounds might be expected from the proposed beam scraping, shaving, etc. schemes?

3. What are the radiation damage considerations for experimental electronics near the beam?

4. What backgrounds might be expected in an experiment from operation of another experiment in the same or the adjacent intersection region?

The review was based on the ISABELLE Proposal,[1] The Proceedings of the 1975 ISABELLE Summer Study,[2] and the estimate of ISABELLE shielding requirements by Stevens and Thorndike.[3]

### A. Criteria

Based on more recent operating experience, criteria were adopted for the radiation shield that differ somewhat from Stevens and Thorndike.

---

1. ISABELLE A Proposal for Construction of a Proton-Proton Storage Accelerator Facility, BNL 50519, May 1976.
2. Proc. 1975 ISABELLE Summer Study, Brookhaven, BNL 20550.
3. A.J. Stevens and A.M. Thorndike, BNL Report ISA 76-11 (1976).

1. Site boundary: 5 mrem per year at any point on the boundary. This is ~ 3% of natural background and is very conservative.

2. 1.5 rem per year in accessible regions outside the shielding. This is the PEP criterion.[4] It seems to be reasonable not to adopt more restrictive criteria unless there is a clear reason to do so. In practice the criterion is to be applied alongside the shielding berm where nonradiation workers might reasonably be expected to have ess. In view of many years of experience at BNL and Fermilab, even ual occupancy of the top of the berm during machine operation is so rare as to be nonexistent outside of well-defined crossing points. Applying the criterion alongside the berm is consistent with the design of the BNL North Area Shield.

3. The experimental areas will, in fact, be controlled areas at all accelerators. The allowed radiation level in these areas is that for radiation workers, 2.5 mrem/h. In practice this would be held below 1 mrem/h for continuously occupied areas such as experimental trailers.

B. Approach

As far as possible, experimental data were utilized in estimating the backgrounds and damage to be expected. The older shielding data are summarized in the 1971 review by Patterson and Thomas.[5] More recent data at higher energies and intensities are available from the ISR, SPS, and Fermilab. The Fermilab data are especially relevant as being in the same energy region as ISABELLE. ISR data have a special relevance for considerations of beam manipulation and stacking at high intensities.

---

PEP, Conceptual Design Report, Feb., 1976.

H.W. Patterson, R.H. Thomas, Particle Accelerators 3, 77 (1971).

## II. TYPES & SOURCES OF RADIATION

At ISABELLE energies, serious radiation problems exist with respect to both hadrons and muons.[6] The average multiplicity of hadrons increases as $< n > \approx 3/2 < n \text{ charged} > \approx 3$ lns where $\sqrt{s} \simeq \sqrt{2mE_o}$ for a fixed target machine and $\sqrt{s} = 2\bar{E}_o$ for storage rings; $E_o$ is the energy of the accelerated beam. The average multiplicity of hadrons per collision will increase from $\sim$ 12 at 28.5 GeV (AGS) to $\sim$ 18 at 200 GeV for beam loss (fixed target) and $\sim$ 36 for beam-beam collisions. The average energy per secondary particle will also increase as a function of s so that secondary collisions will in turn be more energetic, producing more particles per collision.[7] All of these particles may contribute to the radiation levels inside the tunnels and experimental halls and to damage to experimental components.

The neutron component of the hadron cascade is the dominant factor with respect to the radiation levels outside the hadron shield.

The muon component of the radiation field, which had begun to be a problem at AGS energies, is the dominant factor at 200 GeV in the forward direction downstream of collision points. The number of muons increases with beam energy as the number of parent $\pi$ and K mesons increases. In addition, the penetrating power of the muons increases approximately linearly with energy. At 200 GeV incident proton energy the shielding in the forward direction required to shield against muons

---

6. cf. e.g. G.R. Stevenson, CERN Rept. 76-4 (1976); K. Goebel, Ed. CERN Rept. 71-21 (1971); A. Rindi and R.H. Thomas, LBL 1721 (March 30, 1973).

7. J. Ranft, Particle Accelerators 3, 129 (1972).

is more than an order of magnitude greater than the shield length required to stop the hadron cascade.[8] The muons contribute to the personnel shielding problem and to the background in the experimental halls. They are not a consideration with respect to radiation damage because the energy loss rate is so low.

Routti & Van de Voorde have summarized[9] the sources of radiation in the ISR and their relative strengths. van Steenbergen and Teng ve projected a similar summary for ISABELLE on which Stevens & rndike base their estimates.[10]

The ISR data throw into relief some of the basic assumptions of the current ISABELLE design. The ISR reports 3% beam loss at injection, which is downstream of a crossing region. This corresponds in integrated loss per day to 10% of what was the allowed targeting at G-10 of the AGS. The residual radiation level at G-10 was the order of 10R at a foot. In the ISABELLE scheme, the injection points are immediately upstream of intersection regions for experiments, on the assumption of zero loss at injection. Careful consideration must be given to whether (a) one is willing to pay the price for the extra aperture required by the present design, and (b) having paid the price whether the pressure to fill the aperture with more beam could be resisted. History seems to be on the side of filling all available aperture with beam. From another point of view the presence of experiments just downstream of

---

8. D. Keefe and C.M. Noble, "Radiation Shielding for High Energy Muons: The Case of a Cylindrically Symmetrical Shield and No Magnetic Fields", UCRL 18117.

9. J.M. Routti and M.H. Van de Voorde, Nuclear Engineering & Design 34, 293 (1975).

10. A. van Steenbergen and L. Teng, Proc. 1975 ISABELLE Summer Study, Brookhaven, BNL 20550, p. 243.

injection may be the ingredient which is necessary to force a restraint on excessive filling of the rings.

A second feature of the present design which is thrown into relief by the ISR experience is the beam injection/abort philosophy. The ISR uses an internal abort system to dispose of the stored beam both for routine disposal and also when the beam begins to get out of control. This is also the practice at Fermilab where even at 400 GeV and $1.5 \times 10^{13}$ circulating protons a 3 mm cross section beam is routinely aborted in 20 to 40 $\mu$sec without any apparent damage to a crude aluminum abort block. These data suggest that at 200 GeV and $7 \times 10^{14}$ circulating protons it may be feasible to use an internal abort in ISABELLE if that were desirable, especially if Be were used. The radiation problems that would be associated with this are illustrated in Fig. 1, which shows the residual radiation pattern downstream of the Fermilab abort dump.[11] Measurements indicate that the dynamic radiation pattern reproduces the residual pattern with a scale factor of $10^1$ - $10^4$ (Ref. 12).

The possibility of internal dumping obviates the strict necessity of extracting the beam in case of problems. In this circumstance the question should be examined of whether one is willing to pay the price of providing extra aperture to ensure that the beam remains within the allowed phase space even when it begins to go out of control, or conversely whether one is willing to restrict the beam to a limited region of phase space which allows it to be extracted under all circumstances. The question should also be examined whether one is willing to pay the price for extraction channel aperture required to match the requirement of

---

11. J.H. McCrary, H.H. Casebolt, Jr., Particle Accelerators 7, 111 (1976).
12. J.H. McCrary, D.D. Yovanovitch, Particle Accelerators 7, 119 (1976).

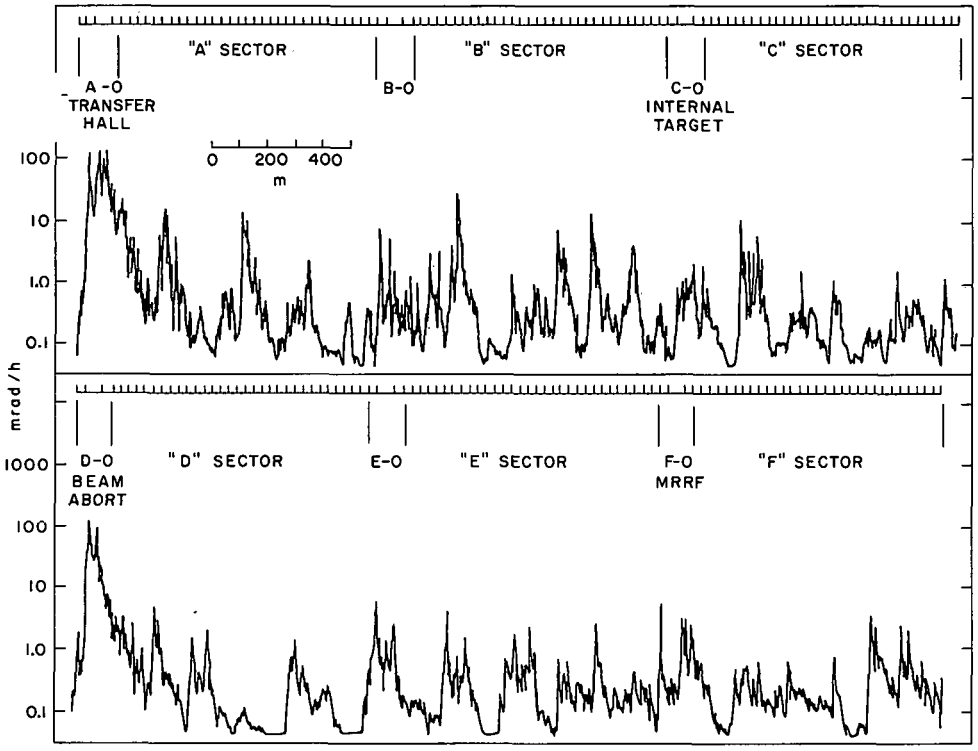


Fig. 1 Radiation levels in the Fermilab ring.

extracting the beam under all circumstances. The channel for extracting well-controlled beam might be of smaller aperture. Since the assumption of disposing of the beam internally is more restrictive and consistent with current practice, it will be adopted for the purposes of this study.

## III. SHIELDING FOR HADRONS

### A. Shielding in Uncontrolled Areas

An order of magnitude argument can be made for the average thickness of the hadron shield to reduce the integrated dose outside the primary hadron shield to the required level of 1500 mrem/yr. For 6000 hours of operation per year this level implies an average dose rate of 0.25 mrem/h outside the shield. From the Fermilab measurements[13] of McCrary and Yovanovitch, the average dose rate in the Main Ring during operations is $\sim 10^3$ mrem/h at 1 meter from the beam. Assuming a falloff as 1/r for the geometrical dependence, plus a falloff of 1 decade per meter of soil, the average shield around the entire ring should be crudely 3 meters of soil for a loss rate of $5 \times 10^{13}$ protons per hour. Using the estimates of Stevens and Thorndike, this is equivalent to dumping all of the accelerated beam in the ring. Since the beam loss is not uniformly distributed around the ring, but is lost mainly on the abort dump, the abort would require more than 3 meters of shield, while the quiet regions would require less than 3 meters. By placing the high loss points in the regions of the machine where the natural contours of the land provide adequate shielding, the above crude argument indicates that 3 meters of shielding is adequate in the quieter regions where the beam must be built up above the existing land contours. When the slope ratio for the berm of 2:1 is kept in mind and applying the 1500 mrem/yr criterion alongside the berm as noted above; 3 meters above the ring should be more than adequate.

---

13. The Fermilab experience is an excellent test of the various Monte Carlo techniques of calculating radiation damage, etc. Before excessive reliance is placed on these calculational techniques, they should be forced to reproduce these data. They have not been particularly useful in Fermilab target and dump design. Indications are that they grossly overestimate the situation.

The shielding above the abort may be obtained from the measured dose above the Fermilab abort dump. McCrary[14] has measured the dose above the abort when $1.5 \times 10^{13}$ protons at 400 GeV were being aborted in $\sim 40$ μsec. The shield thickness in this region is 6.4 meters. No radiation is detected above the dump, but at 25 meters downstream from the abort the level is 0.2 mrad/h at the peak of the spill, which is estimated to convert to 10 mrem/h during the time when the beam is ıg aborted. These data may be interpreted to indicate a requirement $\leq$ 5 meters of dirt downstream of the abort if all the beam is dumped internally.

B. Shielding in the Experimental Halls

The Fermilab experience is that within 1.25 cm of the circulating beam of $1.5 \times 10^{13}$ protons, there is a beam halo of the order of $10^{-8}$ of the circulating beam.[15] Beyond 1.25 cm there is a background due to beam-gas interactions such that at r = 1.5 cm the background is less than $10^{-12}$ of the circulating beam. The Fermilab vacuum under these conditions is $10^{-7}$ Torr. Since the postulated ISABELLE vacuum is $10^{-11}$ Torr, background in the quiet regions of the machine is completely negligible with respect to personnel shielding.

The personnel shielding in the experimental halls when the beams are colliding may be estimated from the Internal Target Area at Fermilab. The beam-jet interaction rate at the ITA is $10^{9}$ interactions per sec, which is comparable to the beam-beam interaction rate at ISABELLE. The residual activity at C-0 is less than 1 mrem/h. Using the appropriate McCrary-Yovanovitch scaling factor of $< 10^{3}$, the dynamic

---

14. Memo J.H. McCrary, "Radiation Levels on Top of the Main Ring Berm," (August 18, 1976).

. F.R. Huson, D.D. Yovanovitch, "Main Ring Halo," Report of the 1976 Fermilab Summer Study.

radiation levels are much less than 1 rem/h. To reduce this to the desired level of less than 2.5 mrem/h in the experimental hall would require 6' of concrete with the outside face of the concrete 6 meters from the circulating beam.

These data raise the possibility of making a more flexible experimental hall arrangement in those areas where the beam height is at or above the natural contours of the land, vid. Wide Angle Hall, Small Angle Hall, and Big Lepton Hall. Such a hall would look like tl original Target Building for the AGS. It would be an industrial type building with appropriate crane coverage. The beams and experimental apparatus would be enclosed by movable concrete blocks[16] much like the old G-10 Area. Note that the interaction rate contemplated for the ISABELLE crossing regions is $\approx 10^{-3}$ the G-10 rate, which translates into 3 meters less of shielding. Fast logic, gas systems, etc. could be located just outside the concrete shield. Personnel, slow logic, etc. might be housed in a trailer sited outside the 1 mrem/h zone.

## IV. SHIELDING FOR MUONS

During the course of the original 200 GeV Design Study, Denis Keefe[17] considered in some detail the problem of muon shielding in the presence of magnetic fields in the machine lattice. The result of this detailed analysis is radically different from the simplified approach of Stevens and Thorndike. It is consistent with the lack of observation of muons outside the shielding berm at Fermilab in the D and E sectors where the berm is at or above the surrounding terrain.

The structure of the ISABELLE magnets is probably more favorable

---

16. A typical concrete roof beam 1.5' x 3' x 36' weighing 12 tons would cost about $600, so this is not a large investment compared with piling up sand.

17. D. Keefe and M. Scolnick, "Trapping of μ-mesons in Magnet Structures", UCID 10143 (September 14, 1965).

than the open C-magnet design of the 200 GeV Design Report for trapping and degrading muons. It is clear that the detailed analysis of Keefe must be repeated for ISABELLE. A preliminary estimate follows.[18]

The requirements for muon shielding around the ISABELLE ring are determined by the behavior of the highest energy $\mu$'s which emerge tangentially in a narrow pencil from a source inside the ring (Fig. 2). The calculations[3] which have led to the present design berm thick-
s (t = 77 m) assume the muons emerge as shown in Fig. 2 with no
_ietic deflection. It appears, however, that the trapping of high energy $\mu$ mesons by the ring magnets may substantially reduce the required amount of shielding. To the extent that such trapping occurs, it may tend to enhance the muon background in experimental halls.

A. Muon Trapping

We rely on the results of Keefe,[17,19] as summarized in the design study for the Berkeley 200 GeV machine. A muon traversing a magnet, once deflected out, may encounter the reversed field of the yoke which will reduce the angle of deflection and in some cases may reverse the sign of the angle of divergence. For a particular magnet geometry this can result in a large fraction of the high energy muons being confined to the accelerator ring, expending their energy in successive traversals of magnet iron. For the Berkeley design Keefe came to the following conclusions after a detailed computer tracing of muons of various production angles and momenta:

(1) The trapping of $\mu^+$ was essentially "complete": The losses

18. This estimate has been prepared by T. Ludlam.
. D. Keefe, Berkeley 200 BeV Design Study (1965).

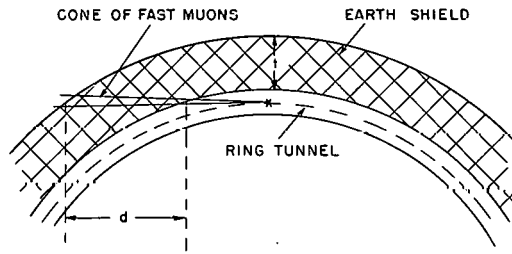


Fig. 2 Muon shield geometry neglecting magnetic dispersion. (Source at x)

from the magnet structure were due primarily to Coulomb scattering, which is small for the high energy part of the path, and (for the Berkeley design) the $\mu^+$ shielding problem was essentially eliminated.

(2) The trapping effect was of no help in degrading the $\mu^-$ within the ring.

Some examples of Keefe's results (taken from Ref. 17) are shown in Figs. 3, 4 and 5. Note that the trapping effect occurs even for only large angles of production: The angle $\theta = 0.5/p_\mu$ corresponds to muons well above the average transverse momentum. Note also the focusing effect which is illustrated in these examples: Rays starting at different production angles eventually come together again, often several times.

For the Berkeley design the $\mu^+$ trapping resulted despite the FOFDOD magnet structure with alternating return yokes of C type magnets. The unfavorable result for $\mu^-$ mesons resulted from the location of the presumed sources (septum magnets) relative to the return yoke orientation. For the ISABELLE magnets, with return fields on either side of the beam (and two sets of magnets side-by-side) the situation may be much better. On the other hand, the presence of quadrupoles may hurt. A detailed study is needed. In the following we have used reasonable (if crude) estimates of what the trapping effects might be in order to assess their impact on the ISABELLE design.

B. Shielding

The muon shielding requirements obtained by Stevens and Thorndike[3] result from the following set of criteria and assumptions:

| | | |
|---|---|---|
| (i) | Maximum allowed level at site boundary: | 5 mrem/yr |
| (ii) | Maximum allowed level on site: | 1000 mrem/yr |
| (iii) | Strength of any source within the ring: | $3 \times 10^{15}$ interacting protons/yr |
| (iv) | Distance to site boundary: | 600 m |
| (v) | Average flight path for decay of pions: | 10 m |

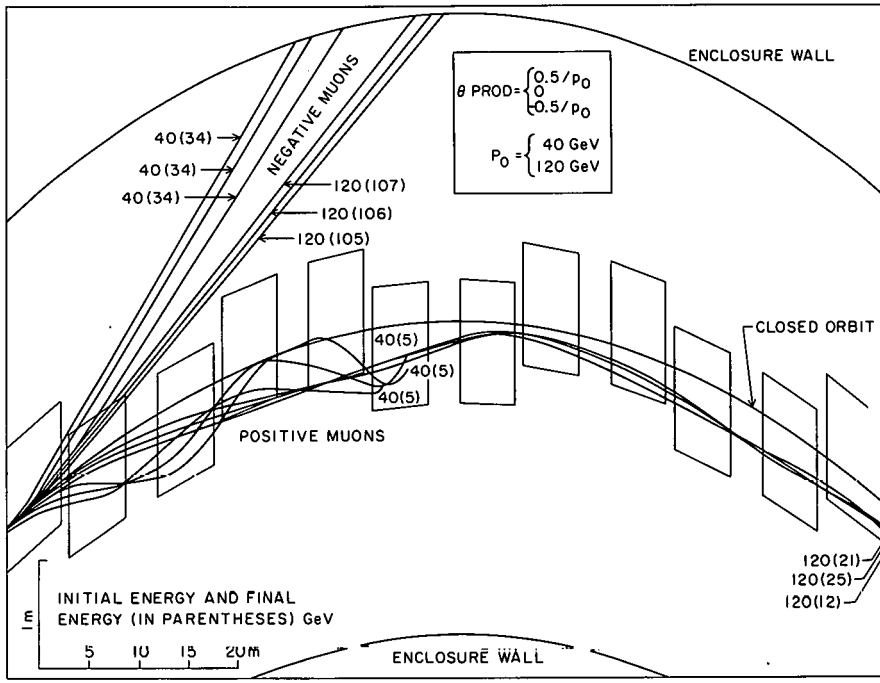


Fig. 3 Muon orbits from Keefe and Scolnick.

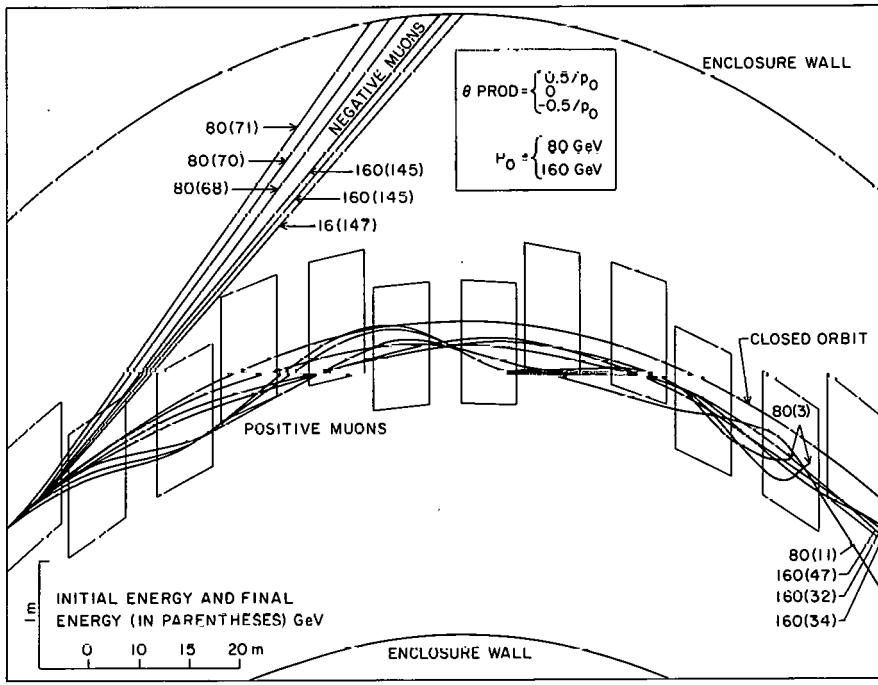


Fig. 4 Muon orbits from Keefe and Scolnick.

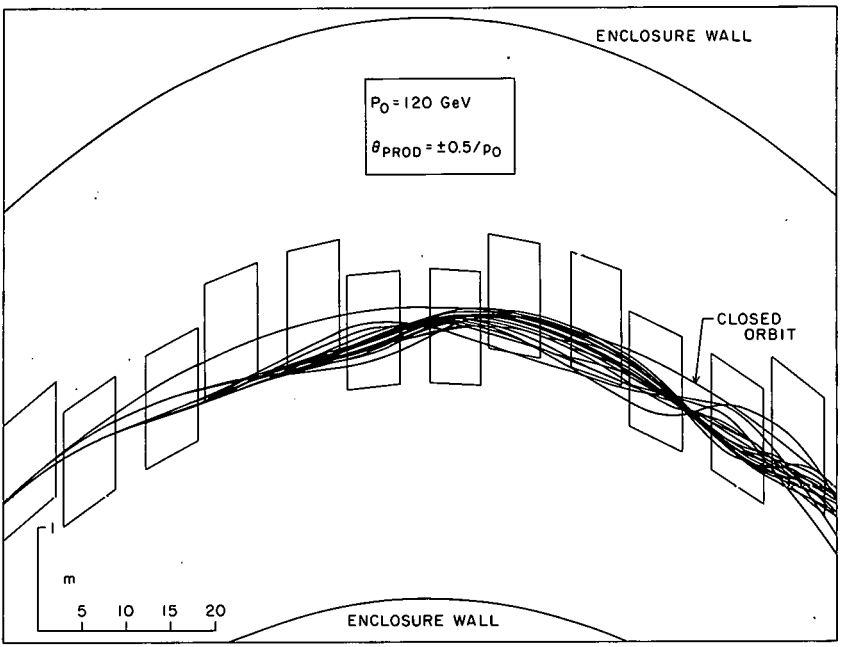


Fig. 5 Muon orbits from Keefe and Scolnick.

With condition (iii), the site-boundary level becomes $5 \times 10^{-11}$ muons per $cm^2$/interacting proton, and the on-site level becomes $10^{-8}$ muons/$cm^2$ per interacting proton.

The figure of 600 m for the distance to the site boundary is appropriate for that part of the ring in the vicinity of the north intersection region, where tangential rays point toward the Wm. Floyd Parkway (Fig. 6). With this figure, the site-boundary requirement determines the shielding thickness -- as detailed in Ref. 3. At oth points around the ring where the site boundary is much farther away, or is protected by the natural contour of the land, the maximum allowable on-site level determines the required shielding thickness. In any case, the most sensitive area for these calculations is the north side of the ring where the beam lies above the existing ground level and an earth berm must be constructed.

The calculation of Stevens and Thorndike (Ref. 3) considers the positive muon flux calculated for $\theta < 1$ mrad using the empirical formula of Wang[20] for pion production ($\pi^+$, and hence $\mu^+$, dominate $\pi^-$ in pp collisions). The procedure is to integrate the muon spectrum above some momentum, find the range, R, corresponding to that momentum, and then apply the appropriate solid angle factor to obtain the flux at the edge of the shield -- assuming shield depth R -- and the flux at the site boundary (600 m).

For clarity, we redo the flux calculation here, as we will need the results in somewhat more general fashion. The Wang formula gives:

$$\frac{d^2\sigma}{d\Omega dp_\pi} = A\, p_M \times (1 - x)\, e^{-Bx^C}\, e^{-Dp_T} \qquad (1)$$

---

20. C.L. Wang, Phys. Rev. D10, 3876 (1974).

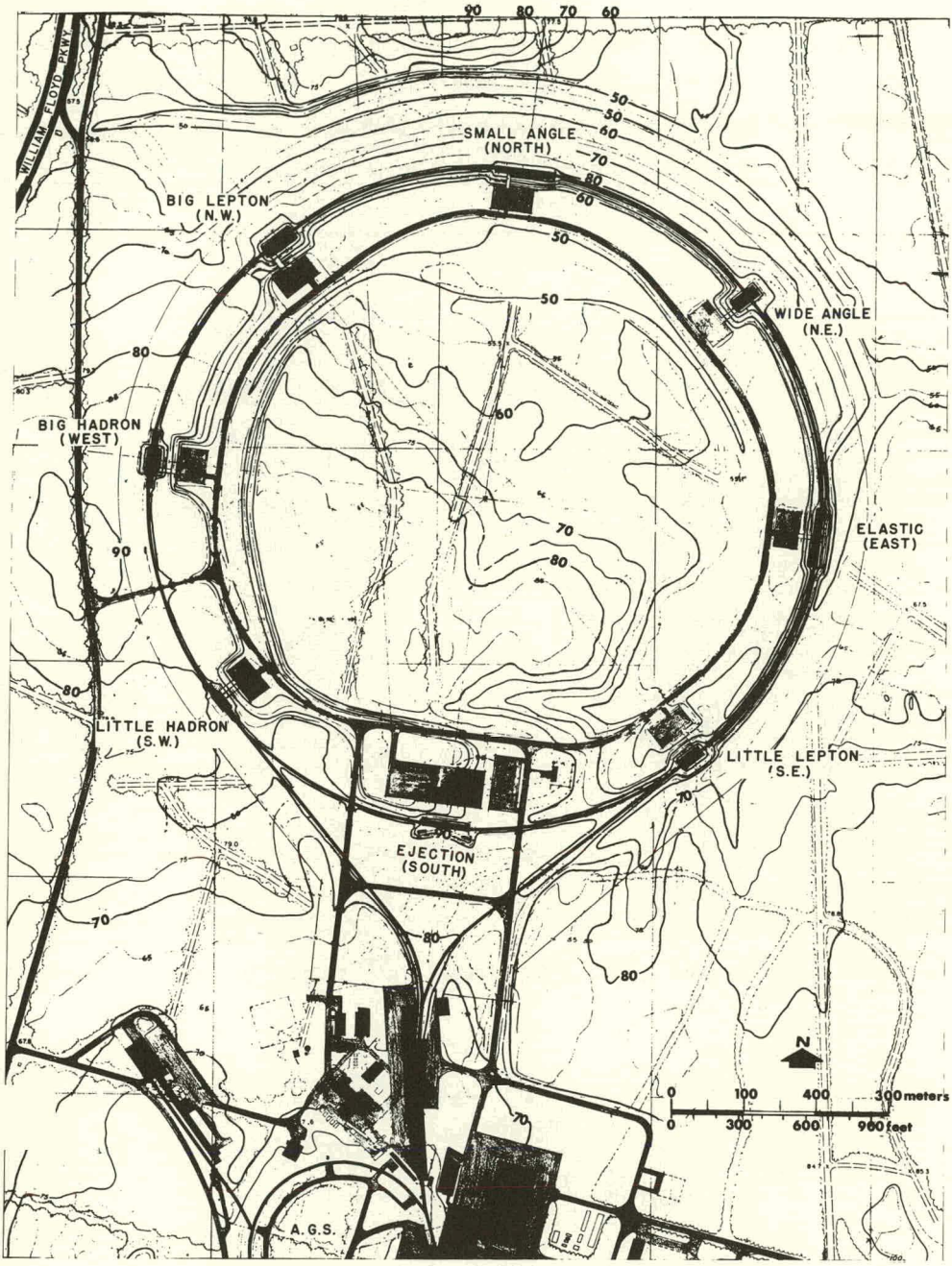


Fig. 6 General site plan.

where the units are mb and GeV, $p_M$ is the maximum pion momentum (200 GeV/c), $x = p_\pi/p_M$, $p_T = p_\pi\theta$, and the coefficients are given in Table I.

TABLE I. Coefficients for Wang formula

| | A | B | C | D |
|---|---|---|---|---|
| $\pi^+$ | 77.793 | 3.558 | 1.333 | 4.727 |
| $\pi^-$ | 51.403 | 5.732 | 1.333 | 4.247 |

Integrating over solid angle (for $\theta < \theta^*$):

$$\left.\frac{d\sigma}{dp_\pi}\right|_{\theta < \theta^*} = \frac{2\pi A}{D^2 p_M} \left(\frac{1 - x}{x}\right) e^{-Bx^C} \left[1 - e^{-Dx^{p_M}\theta^*}(1 + Dx^{p_M}\theta^*)\right] \tag{2}$$

A pion of relativistic momentum $p_\pi$ produces a decay muon according to a flat spectrum with $0.57\ p_\pi < p_\mu < p_\pi$ :

$$\frac{dN_\mu}{dp_\mu} = \frac{L\, M_\pi\, c}{0.43\, p_\pi^2\, c\, \tau_\pi} \qquad \left[0.57\ p_\pi < p_\mu < p_\pi\right] \tag{3}$$

where L is the decay path length

$$\tau_\pi = 7.8 \text{ m}$$

If the pion momentum spectrum is given [e.g. by Eq. (2)], then the muon spectrum is given by:

$$\frac{d\sigma_\mu}{dp_\mu} = 0.042\, L \int_{p_\mu}^{p_o} \frac{1}{p_\pi^2} \frac{d\sigma}{dp_\pi}\, dp_\pi \tag{4}$$

where $p_o$ is the larger of $\frac{1}{0.57}\ p_\mu$ or $p_M$.

Finally, the cross section for producing muons with momentum greater than some minimum value $p^*$ is

$$\sigma_\mu (p_\mu > p^*) = \int_{p^*}^{p_M} \frac{d\sigma_\mu}{dp'} dp' \quad . \tag{5}$$

The results of this calculation, for unit decay path and $\theta < 1$ mrad, are shown in Fig. 7. The resulting fluxes at the site boundary and at the edge of the shield, as a function of shield depth, are shown in Figs. 8 and 9. In these latter figures, following Stevens and Thorndike, an average decay path of 10 m was chosen, and the range measurements of Theriot[21] were employed. (Similar energy loss curves are given by Richard-Serre.[22])

The $\mu^+$ flux at the site boundary determines a shielding depth of $\sim$ 240 meters which, by simple geometry (see Fig. 2) dictates a berm thickness t = 77 meters. The thickness required to satisfy the maximum on-site level (at edge of shield) is t $\simeq$ 30 m (corresponding to a depth d $\simeq$ 130 m).

This is an earthwork of considerable proportions, and so it is appropriate to ask how these results might be affected if the trapping phenomenon is taken into account. The effect will clearly be helpful, as it reduces the highest-energy, most penetrating component. As a crude estimate, we consider substituting the $\mu^-$ for the $\mu^+$ flux. This is likely to be a very conservative estimate, for even in the absence of $\mu^-$ trapping, and with only partial $\mu^+$ trapping, the magnetic fields will provide considerable dispersion -- destroying the simple "search light" geometry of Fig. 2 and introducing large solid angle factors. In any event, for the $\mu^-$ calculation shown in Figs. 8 and 9 the reduction in shielding requirements is substantial. The required

---

21. D. Theriot, FNAL Report TM - 260 (July, 1970).
22. C. Richard-Serre, CERN Report 71-18 (1971).

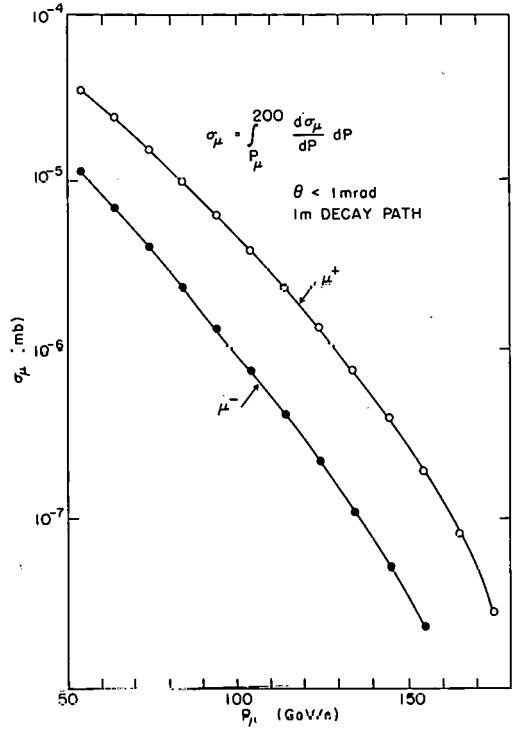


Fig. 7 Effective production cross section for muons.

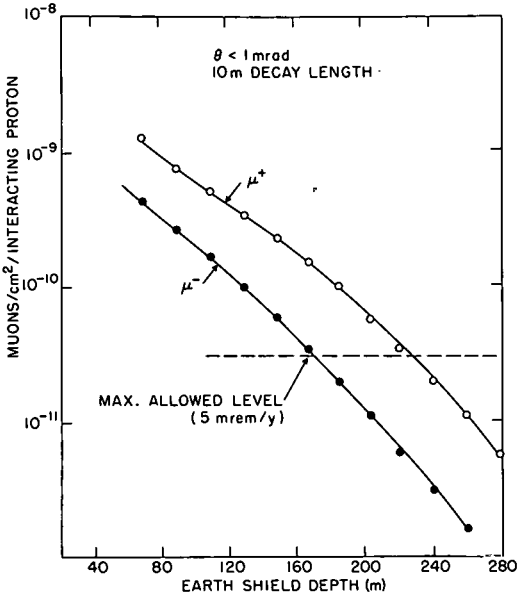


Fig. 8 Muon flux at site boundary.

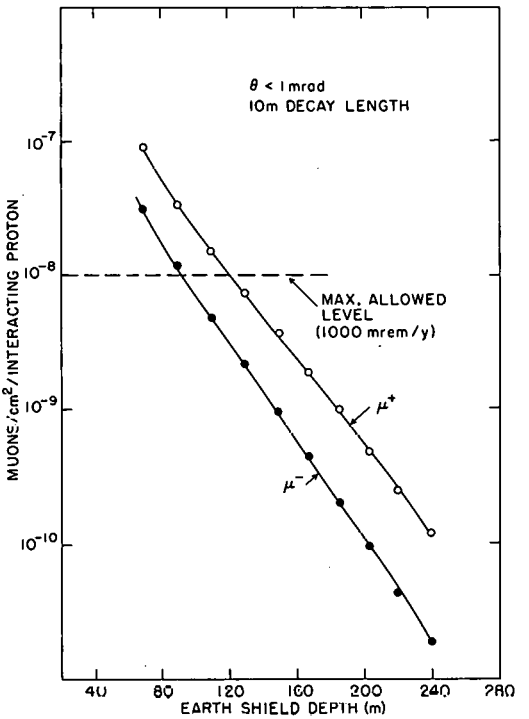


Fig. 9 Muon flux at edge of shield.

depths (d) and berm thicknesses (t) are:

| | |
|---|---|
| Site boundary level at 600 m -- | d = 165 m, t = 40 m |
| on-site level -- | d = 90 m, t = 12 m |

It must be noted that the trapping mechanism is not likely to be effective for muons produced in an intersection region, owing to the long free space. (And, also, that a proton loss at full energy of $3 \times 10^{15}$/yr is not likely to occur at any point on the north side of ring except at an intersection.) If steel shielding is used at the intersection regions, it appears that a berm size sufficient for hadronic shielding would do as well for the muons. The berm might have to be built up some along the tangent to that (small) portion of the ring near the north intersection which "points" to the site boundary at small distance.

The approximate depths of steel would be as given in Table II.

TABLE II. Steel Shielding Depths at Intersections

| | clockwise | counterclockwise |
|---|---|---|
| N.W. (big hadron) | 25 m | none |
| North (small angle) | 25 m | 50 m |
| N.E. (wide angle) | none? | 25 m |
| East (elastic) | none | 25 m? |
| All others | none | none |

Question marks reflect my uncertainty about the existing land contours.

C. Muon Backgrounds

While only a small fraction of the muons produced in an intersection region are likely to be captured in the ring (owing to the long free space), those which are may be transported far enough to provide a background problem in the next experimental hall.[23] As a rough measure of the magnitude of the effect, we assume that all $\mu^+$ which enter the aperture (or coil) of the first main ring dipole (normally 70 m downstream of an intersection) are captured. This corresponds to muons angles up to $\sim$ 1 mrad.

Not all of the trapped muons will make it through to the next intersection. We may assume that there is some value of $p_\mu$ for which muons of lower momentum will be brought to rest or scattered out of the ring well before they have traversed 1/8 of the circumference. For a given guess as to the minimum momentum of contributing muons the background rate (muons/sec) is obtained by reading the corresponding value of $\sigma_\mu$ from Fig. 7 and multiplying by the appropriate decay path length and by the luminosity. We assume L = 70 m and a luminosity of $10^{33}$ cm$^{-2}$ sec$^{-1}$ = $10^{6}$ mb$^{-1}$ sec$^{-1}$.

As a rough estimate we might (for instance) guess that muons must be at least stiff enough so that the bending power of the dipoles in one cell of the lattice is not sufficient to deflect them out of the aperture ($p_{\mu,\min} \simeq 80$ GeV/c). This gives an estimated background rate of

$$(70\text{ m}) \times (10^{6}\text{ mb}^{-1}\text{ sec}^{-1}) \times (10^{-5}\text{ mb/m}) = 700\text{ muons/sec.}$$

Such an estimate must, of course, be multiplied by 2 since these fluxes impinge in each insertion from both directions. The backgrounds we are talking about are perhaps as large as a few $\times 10^{3}$/sec.

---

[23] L. Lederman, private communications.

D. Conclusion

These exercises illustrate that the magnetic trapping of muons in the ring can effect significantly the size (and hence cost) of the required muon shield. Since this is presently an item of $\sim$ \$1 million in the construction budget, it invites careful consideration. The trapping effect will also result in muon backgrounds at the various insertions which, while probably not intolerable, should be borne in mind in the design of experiments. A more detailed study along the lines of the calculations done by Keefe[19] should be carried out in order to put these semi-quantitative results on a firmer basis.

## V. RADIATION DAMAGE

The problem of radiation damage/quenching of the superconducting magnets has been investigated in the 1975 Summer Study[24] and by Kaugerts[25] and will not be considered here.

Some information on the effects of radiation on electronic components and detection devices is presented in this section and the implications for ISABELLE are considered.[26]

There has been considerable research on radiation damage to electronic components for both the space and the nuclear weapons programs. Table III summarizes the results presented in a few selected papers.[27]

---

24. F. Sanger, Proc. 1975 ISABELLE Summer Study, Brookhaven, BNL 20550, p. 626.

25. J. Kaugerts, ISA Technical Note No. 20 (August 3, 1976).

26. This discussion has been prepared by V. Kistiakowsky.

27. We would like to thank R. Chase, Brookhaven National Laboratory, for bringing these to our attention.

Table III. Radiation Damage to Electronic Devices

| Device | Result | Equivalent in rem | Ref. |
|---|---|---|---|
| Bipolar Transistors | Some varieties deteriorate unacceptably at $5 \times 10^{12}$ electrons/cm$^2$ | $1.7 \times 10^5$ | 28 |
| | 10% failure at $\sim 10^4$ rads for some varieties | $1.4 \times 10^6$ | 29 |
| | Amplification changed by $< 10\%$ for $5 \times 10^{12}$ electrons/cm$^2$ for some varieties | $1.7 \times 10^5$ | 30 |
| MOS Devices | Deteriorate unacceptably at $5 \times 10^{11}$ electrons per cm$^2$ | $1.7 \times 10^4$ | 28 |
| Zener Diodes | Not affected at $5 \times 10^{12}$ electrons/cm$^2$ | | 28 |
| Power Transistors | Deteriorate unacceptably at $10^{13}$ neutrons/cm$^2$ | | 31 |
| Logic Circuits | Deteriorate at $7 \times 10^{14}$ neutrons/cm$^2$ | | 32 |


28. W.E. Price and A.G. Stanley, IEEE Trans. Nucl. Sci., NS-22, 2669 (December 1975).

29. W.E. Horne and J.A. Folsom, "Total-Dose Survival Probability for Bipolar Transistors", The Boeing Co., Seattle, Washington.

). W. Poch and A.G. Holmes-Siedle, "A Prediction and Selection System for Radiation Effects in Planar Transistors", RCA Astro-Electronics Division, Princeton, N.J.

31. C. Rosenberg, I. Arimura and A.M. Unwin, "Statistical Analysis of Neutron-Induced Gain Degradation of Power Transistors", The Boeing Co., Seattle, Washington.

32. R.J. Olson, Dr. R. Alexander and R.J. Antinore, "Radiation Response Study of New Radiation-Hardened Low Power TTL Series," Air Force Weapons Laboratory, Kirtland, New Mexico.

The effect of radiation for the bipolar transistors varied considerably by transistor type and even by manufacturer. Price and Stanley[28] report that the 2N2222A's supplied by one manufacturer exceeded the rejection limit and those from another were an order of magnitude below it. References 28 - 32 indicate an extensive literature on component selection and radiation hardening.

Three experiences with radiation damage at high energy acceleration should be mentioned, since they point to possible problems at ISABELLE. The first is the failure rate of the oil-filled capacitors for the beam extraction kicker magnets at Fermilab, some of which must be replaced after a month of use.

These special capacitors of the fast pulser electronics must normally be changed every few months. They sit on the floor just under the kickers to minimize the kicker rise time. The residual radiation level here indicates a dynamic level of $\sim$ 50 rem/h. This datum should be considered with respect to the proposed scheme to put extraction kickers in the ejection/abort region. Secondly, again at Fermilab, a 50% degradation of the resolution of surface layer solid state detectors is observed when they are placed 1 meter from the beam in $C_o$ for a period equivalent to approximately half a year of continuous running at luminosity $10^{32}$ $cm^{-2}$ $sec^{-1}$. Finally, there is the experience of the CERN-Saclay group at the ISR, that integrated circuits deteriorate in approximately a week when they are used close to the vacuum pipe in a location where the radiation level is several times that from a usual intersection region.

A rough estimate of the radiation level 1 meter from a $10^{33}$ $cm^2$ $sec^{-1}$ luminosity intersection region at ISABELLE yields the figure $\sim$ 2 rem/h or $\sim$ 300 rem/week.[33] Thus, MOS devices would seem unsuitable for use in the experimental halls, but in general bipolar transistors are satisfactory. However, previous experience indicates that some care should be exercised in selection of components particularly if integrated circuits are used where amplification levels are important.

---

33. See the discussion in Section III on shielding for hadrons.

## VI. CONCLUSIONS

The present study is necessarily somewhat sketchy because of time and resource limitations. It seems clear that a careful reexamination should be made of various philosophies and underlying assumptions of the present ISABELLE design in the light of current operating experience at the high intensity and high energy machines.

No consideration has been given to the question of ground water vation. This is probably not a serious problem, but with the proximity of the Long Island water table to the surface and the nature of the soil in that area, the question should be considered and resolved.

# INTERACTION REGIONS WITH SMALL SOURCE SIZE

W.J. Willis

CERN

## I. INTRODUCTION

It is often not clear what considerations really determine the size of an experimental apparatus. Spatial resolution in available detectors is often given as the answer; but this may be an oversimplification, since the spatial resolution is itself a function of detector size. The thesis of this note is that an important determining factor is the size of the source of the interactions.

To illustrate this point, we consider the design of a detector using a small axial field magnet and high resolution chambers and an imaging Cerenkov detector. The configuration of the intersection region which provides the necessary small source size has been determined by the machine study group.

## II. A HIGH RESOLUTION CENTRAL DETECTOR

A large scale view of the axial field magnet detector is shown in Fig. 1. The smallest possible vacuum pipe is used in the central region, 35 mm i.d. This, together with a short (100 mm) intersection diamond, allows the design of a magnet consisting of two small coils, generating about 1.5 Tesla on the diamond. This modest field volume is sufficient for the measurement of moderate momenta because of the use of very high resolution cylindrical drift chambers. This detector is contained within a radius of 200 mm, and leaves most of the solid angle unobstructed. Thus, it is possible to surround the inner detector with another system which can itself remain of reasonable size, for example, a calorimeter or Cerenkov detector. In the cases where we wish to have three layers of detectors, such as momentum measurement, Cerenkov, and calorimeter, it is even more useful to keep the first as small as possible to end with a last layer of feasible size.

The detector of Fig. 1 is composed of the following elements:

1. The beam pipe, which is a double wall structure integral with the inner wall of the drift chamber container. The inner

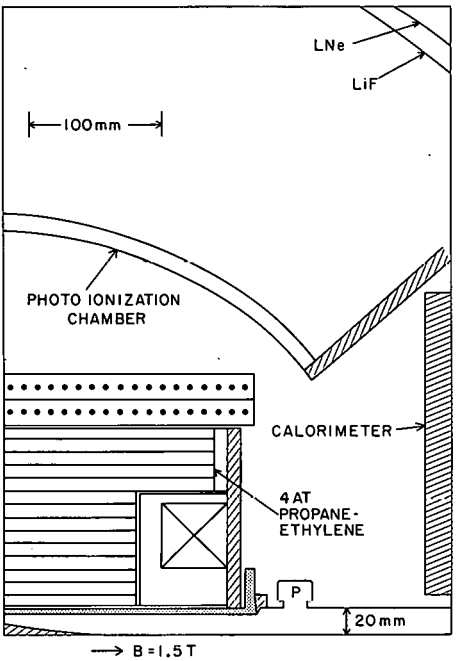


Fig. 1. Central detector unit consisting of compact axial field magnet and very high resolution drift chambers.

vacuum pipe can be quite thin, since it bears no pressure. The space between the two tubes is evacuated and superinsulated, allowing bake-out of the inner tube without disturbing the experiment. The conductivity of the inner tube (0.2 mm Al) is sufficient to allow heating only at the end. The pipe must be flared in the horizontal plane, starting at ± 100 mm from the crossing, to accommodate the crossing angle, which will probably be ~ 50 mrad. Pumps are mounted about 25 cm from the center, giving a safe vacuum condition in the small diameter pipe, according to the calculations of D. Edwards.

2. A set of cylindrical drift chambers with 10 mm drift distance. These are built according to the design of H. Walenta, with four atmospheres of propane-ethylene gas. For these conditions, the resolution has been measured to be ≤ 30 μm, and particle pair resolution is 2 mm. The width of the dE/dx distribution has also been found to be several times smaller than for argon at atmospheric pressure, while the plateau of the relativistic rise is expected to be smaller. All these properties are most valuable for this application. We show 13 layers of drift chamber measurement to ensure adequate pattern recognition and to provide improved accuracy. Each wire has current division readout, which should determine the position along the wire with an accuracy of a few mm. Two layers of orthogonal wires, formed on a polygonal cylinder, are shown as well. These are used to determine the axial coordinate more accurately. Alternatively, the high accuracy cathode strip read out developed by Charpak can be used to achieve this accuracy.

3. Superconducting coils are used to provide the field. Since the stored energy is small, the coils can use intrinsically stable superconductor at a high current density, up to $10^5$ A/cm$^2$ in the overall conductor. In this case, the conductor cross section provided, ~ 8 c$^2$ should be adequate for the current, some $2 \times 10^5$ A-turns, desired, and may, in fact, allow a considerably higher field.

Although detailed calculations have not been performed, the machine group believed that the solenoidal field integral was small enough so that local compensation would not be required.

The magnetic field varies greatly over the volume used in the detector, but it does at least have azimuthal symmetry. This variation is the inevitable price paid for the large open solid angle, and seems well worthwhile.

These items complete the central detector. Before describing the particular detectors chosen as examples of the outer layers, we proceed to analyze the performance of the central detector. A ged track can be represented approximately as three points with tal length of 10 cm in a 1.0 T field and a point accuracy of 20 $\mu$m. In this case, the momentum accuracy for a 1 GeV/c particle is about 6%. For smaller momenta, the error remains roughly constant due to multiple scattering, while for larger momenta there is a linear increase. Thus, the sign of particles is measured up to about 10 GeV. Clearly, this detector is intended to measure the momenta only for low transverse momentum particles, and must be supplemented by a different external detector capable of measuring high momenta, such as a calorimeter or an imaging Cerenkov counter, or both. In the case of a good calorimeter, the accuracy in energy is better than that from the momentum measurement above about 3 GeV, and the combined measurement accuracy in the worst case is less than 15%. In the case of an imaging Cerenkov detector with a threshold of $\gamma \simeq 2$, the worst case accuracy occurs for a proton of $\leq 2$ GeV, and is about 10%.

One consequence of the small detector size which may be important is that the transverse momentum imparted by the magnetic field is comparable or less than that typical of the particles relative to a jet axis. For example, this property, coupled with the small source size, allows the interpretation of the pattern of energy de- ited in a calorimeter without detailed track reconstruction, for ggering purposes. It is also crucial for the optics of imaging Cerenkov detectors, as mentioned later.

Another property of the central detector is the measurement of dE/dx to some accuracy. A relative ionization of 1.2 times minimum should be distinguished from minimum by several standard deviations. This would allow the identification of particles with $\gamma < 1.5$. If there is a Cerenkov detector with threshold around $\gamma = 2.2$, the whole range of $\gamma$ can be covered without the need for a time-of-flight measurement, which becomes impractical in a very compact setup.

It may be noted that the dE/dx measurement might be useful in another way. For a slow, heavy particle, such as a 400 MeV/c proton, the accuracy of the momentum measurement is spoiled by the $1/\beta$ term in the multiple scattering, and that derived from dE/dx is actually more accurate.

A real limitation of such a detector may be the particle pair resolution. Some particles in the core of a jet will not be resolved in these chambers, and must be handled in the outer detectors. These will usually be high-energy particles which were intended to be measured there anyway, but a low-energy particle may get lost this way. The measurement of pulse height on each wire helps to identify overlapping tracks.

The polar angle coverage of the inner detector as shown extends down to $20^{\circ}$ or $30^{\circ}$, depending on the number of hits demanded. The small size means that no particle, even that passing through the coil, passes through so much material that a calorimeter measurement is invalidated. That is, to say that the worst case represents only about 2-3 radiation lengths and a fraction of an interaction length. Thus, a general knowledge of the character of the event can be gained over the full solid angle, while most magnetic detectors lose 30% or more of the solid angle. This is an important feature of the design.

## III. OUTER CERENKOV AND CALORIMETER DETECTORS

We now turn to a description of the further detectors in our sample design. The overall assembly is shown in Fig. 2.

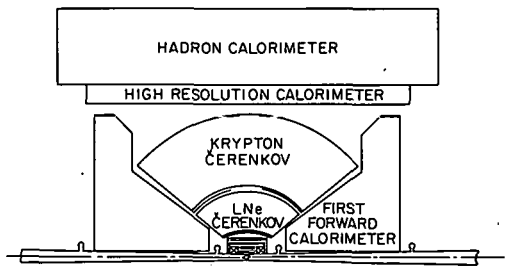


Fig. 2. Overall detector assembly showing outer detectors. (Would extend symmetrically on other side of beam line also.)

1. The next item is an imaging Cerenkov detector design according to ideas of T. Ypsilantis. The radiators are 2 cm of LiF and 4 cm of liquid neon, with thresholds $\gamma = 1.35$ and $\gamma = 2.39$. The Cerenkov light generated in the radiators is reflected from a spherical aluminum mirror of 70 cm radius and brought to a focus at a radius of 35 cm from the center of the source. The Cerenkov photons with an energy of about 8 eV are detected by photo-ionization of benzene in a proportional chamber, with a quantum efficiency of about 50%. There are about 30 detected photons on the circular image. The anodes in the proportional chamber have the form of needles in an array of 2 mm pitch read out with delay lines.

The error on $\Delta\gamma/\gamma$ in such a detector has limitations from spatial resolution, chromatic aberrations, multiple scattering, and other sources, calculated in detail by Ypsilantis. It is found that $\Delta\gamma/\gamma$ is a few percent near threshold and increases as $\gamma^2$. If the momentum or energy is known roughly from measurements in the magnetic field or a calorimeter, this device determines the mass and furthermore can give the most accurate measurement of the momentum over much of the range covered. The accuracy becomes insufficient to determine mass for $\gamma \gtrsim 30$.

2. A second radiator using krypton at atmospheric pressure starts at a radius of $\sim$ 75 cm and ends at a spherical mirror at a radius of 150 cm. It provides a Cerenkov threshold of $\gamma = 28$. The photons are detected in a proportional chamber at a radius of 75 cm. This detector provides $K/\pi/p$ separation up to about 60 GeV, where $\Delta\gamma/\gamma$ for a K is $\sim$ 20%. Note also that $\pi/\mu$ separation can be made up to $\sim$ 10 GeV and that $\pi/e$ separation is obtained below about 15 GeV. These capabilities are most interesting in that other methods of e and $\mu$ identification do not work as well at these momenta, particularly in the case where e and $\mu$ are to be detected simultaneously. The ability to identify muons at a few GeV with very small decay paths seems almost unique. The high accuracy of the measurements very close to the production vertex allows the elimination of most $\pi$-$\mu$ decays by finding discrepancies in the angle or curvature of the track, and the comparison of energy measurement in the magnet and

in the Cerenkov detector eliminates other $\pi$-$\mu$ decays in the intervening region.

In order to obtain the quoted errors on $\Delta\gamma/\gamma$ in the imaging Cerenkov detectors, the optical aberrations due to the finite source size must be sufficiently small. For a point source, the aberration is a combination of spherical aberration and coma, and varies as $\theta^3$. We find that the effect of the source size, $\pm$ S, can be neglected if

$\ll \theta$. For the LNe radiator,

$$\theta = 0.43 \ , \ R = 70$$
$$S \ll 30 \text{ cm} \ ,$$

while for the krypton radiator

$$\theta = 0.036 \ , \ R = 150$$
$$S \ll 5.4 \text{ cm} \ .$$

Thus, we see that condition is easily satisfied for the LNe radiator, while there starts to be effect on the krypton radiator system. These are largely masked by other errors, but it is clear that it would be out of the question to use this detector with a standard intersection region with a meter long diamond. It is also important that the central magnet does not increase the effective source size appreciably, that is, it must be kept sufficiently small and weak.

3. In our example, a third layer of detectors is included, a set of calorimeters covering the full solid angle. This is the most effective element for a selective trigger, and is essential for the measurement of neutral particles. It also covers parts of the solid angle not covered by the central detectors.

One element is a high spatial resolution detector for electromagnetically interacting particles, covering the large angle region. — ; should have a photon pair resolution of < 10 mm. This could be ieved by a calorimeter with 2.5 mm uranium strips with an average density of 10 g/cm$^3$. This detector is at 1.6 m and could not be placed any closer to the source and still resolve neutral pion decays, so that the size of the inner detectors is small enough in this sense.

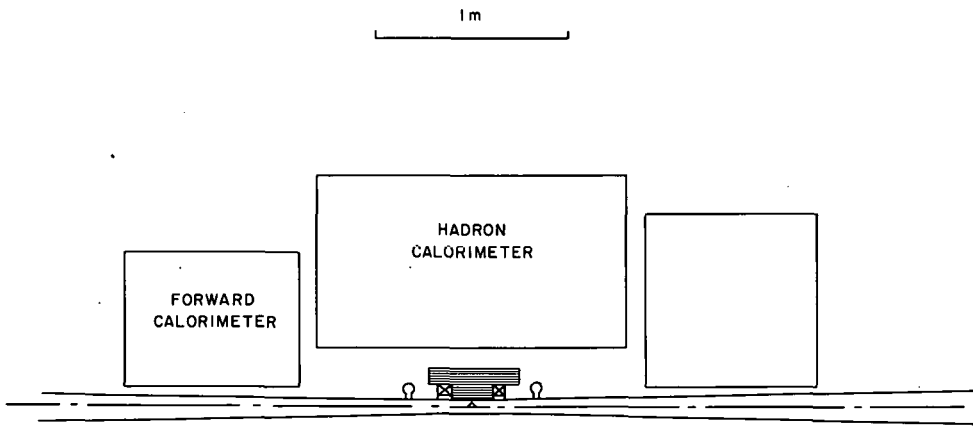


Fig. 3. Alternative overall detector assembly without Cerenkov counters.

It is followed by a hadron calorimeter, where the use of uranium keeps the total calorimeter depth to 1 m.

Forward calorimeters are used to capture the particles traversing the coil region of the central detector. Still more forward calorimeters may be placed further downstream to capture the particles with small transverse momentum.

Alternatively, Fig. 3 shows how a calorimeter may be introi as the second detector layer, resulting in a very compact setup, well suited for a study of jets with an unbiased trigger.

Thanks are due to Drs. H. Walenta, M. Month and R. Majka for helpful discussions.

# SMALL ANGLE SINGLE ARM SPECTROMETER

C.Y. Chien

The Johns Hopkins University

We review in this report the experiment described in the 1975 Summer Study.[1] The purpose of this study is to take the general design and to review the adequacy of the apparatus for its physics goals, equipment needs, logistic needs, vacuum chambers, compatibility wit other experiments and to summarize its impacts on ISABELLE.

## 1. Physics Goals and General Design

The general design of the spectrometer is shown in Fig. 1. It is designed to study single particle inclusive spectra near x = 1 with particle identification and good momentum resolution. The general characteristics of the spectrometer are shown in Table I. The solid angle is very small ($\sim$ 1 $\mu$sr) due to the high momentum resolution desired, difficult constraints in the layout, and the desired compatibility with other experiments. The counting rate and acceptance are shown in Fig. 2.

Table I. Spectrometer Characteristics

| | | |
|---|---|---|
| Space angle range | $1 \leq \theta \leq 8$ mrad | positives |
| | $2 \leq \theta \leq 8$ mrad | negatives |
| Momentum range for particle identification | $20 \leq p \leq 200$ GeV/c | |
| Spatial solid angle | $10^{-6}$ sr | |
| Momentum acceptance | 10% | |
| Momentum resolution | $\Delta p/\Delta \sim 0.15\%$ | |

It is adequate to do the experiment it is designed for. No new technology in detection technique can appreciably improve the design. I should be noted that although the physics intended is interesting, ti scope is quite limited due to the small solid angle. On the other hand, the spectrometer will be an important addition to other experiments to

1. C.Y. Chang, E. Engels, M. Kramer, R. Lanou, L. Pondrom, Proc. 1975 ISABELLE Summer Study, Brookhaven, BNL 20550, p. 244.

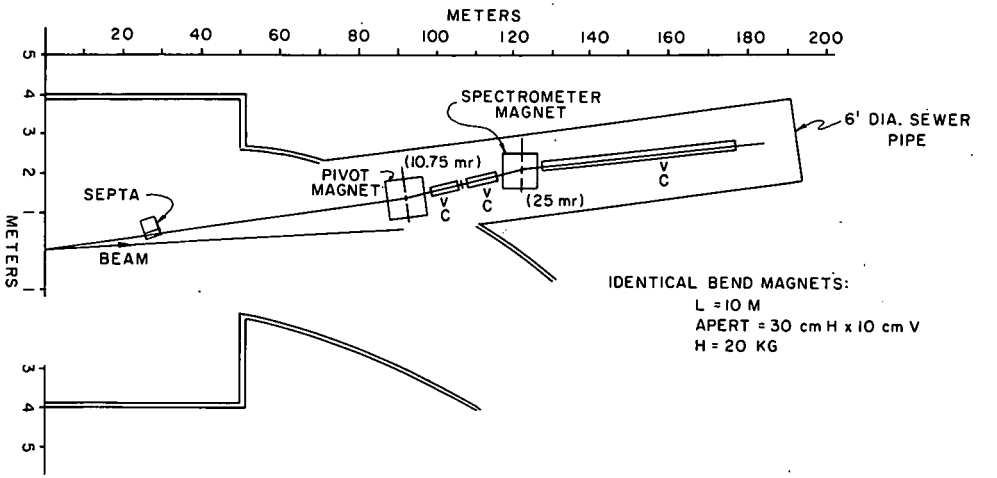


Fig. 1. Small angle spectrometer arrangement relative to ring tunnel and experimental hall.

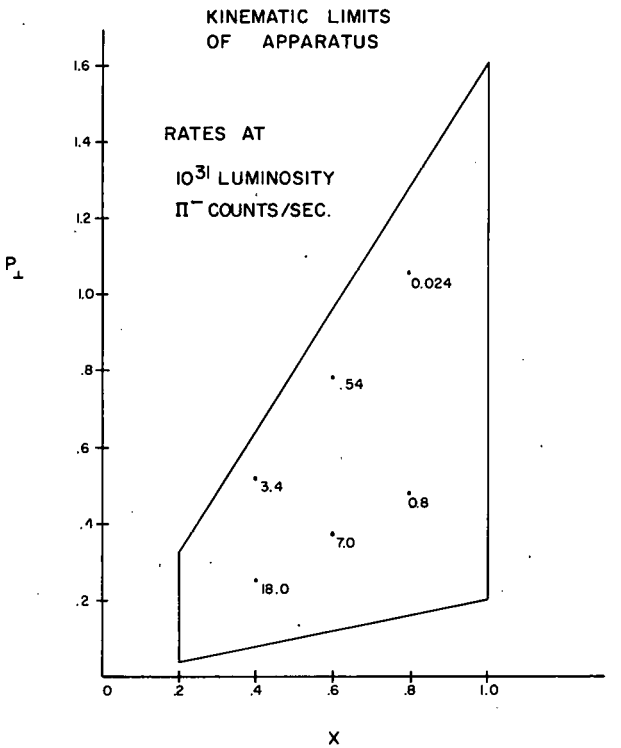


Fig. 2. Acceptance of spectrometer in X, $P_\perp$, space and typical pion counting rates.

cover a wider range of physics. Therefore, it is important to have several experiments in the same experimental hall with this experiment (see section 9).

## 2. Insertion

The experiment is compatible with a standard insertion (Q1, Q2 at 20 m). The only special requirement is to modify Q1 and Q2 by separating their windings to create a slot for secondary particles to go through (Fig. 3). These particles will then be sent by three septum magnets (with B = 4, 8, 10 kG, and $\int B d\ell$ = 80 kG m) into the spectrometer. Figure 4 shows an expanded view of these magnets and approximate particle trajectories.

## 3. Detectors

The spectrometer uses two 10 m and one 50 m gas Cerenkov Counters, and $\sim$ 2500 channels of proportional wire chambers. The cost of these counters is estimated at $\sim$ \$150 K. Other costs of the experiment are mainly magnets and cryogenics.

## 4. Magnets and Cryogenics

In addition to the modified Q1 and Q2 and three septum magnets, the spectrometer requires two modest analyzing dipole magnets (with apertures 5 cm high and 25 cm wide) which could be superconducting to avoid powerbus and cooling problems in the tunnel. The cryogenics for Q1 and Q2 will be standard. Cryogenics for analyzing magnets are quite modest.

## 5. Vacuum Chamber

The vacuum chamber needed has a single flare on the outside of the ring on one side of the interaction region. Figure 5a shows the plan view of the vacuum chamber. The elevation view with clearing electrodes and pumps is shown in Fig. 5b. A titanium wire will also be used in the flare to achieve high vacuum. Figure 5c shows the end view of the flare which is 2 mm thick with a 0.5 mm thick stainless steel window

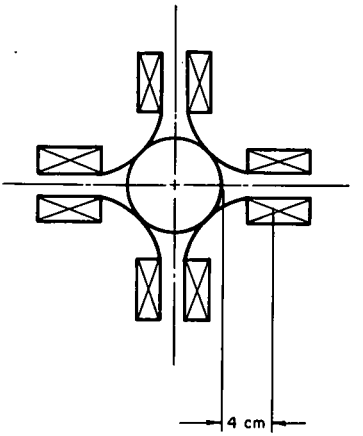


Fig. 3. Schematic of quadrupole magnet with slot for secondary particles.

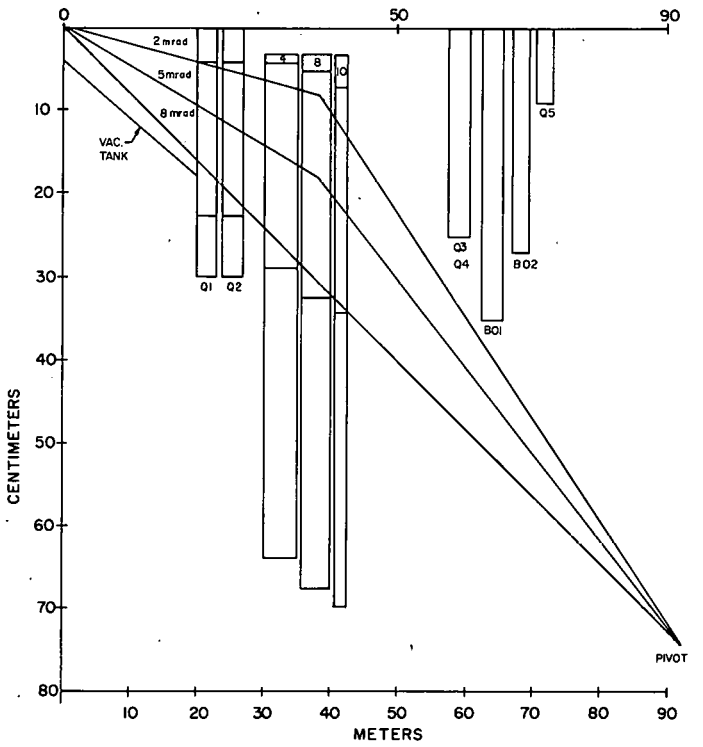


Fig. 4. Expanded view of intersection region showing location of septum magnets for spectrometer.

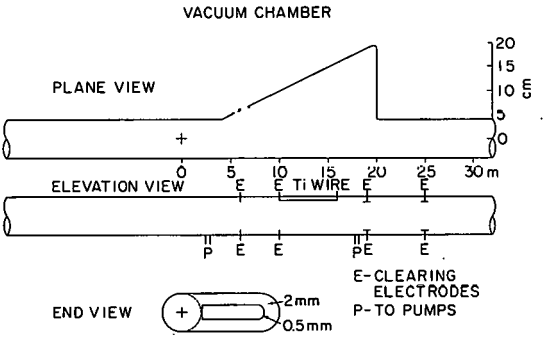


Fig. 5. Schematic of vacuum chamber.

for secondary particles. The aperture of the window matches the slot in Q1 and Q2. The ISA vacuum group feels that this schematic design is realistic. The exact shape, of course, will depend on detailed designs.

## 6. Arrangement for Electronics and Controls

The spectrometer is relatively simple: three septum magnets, two small analyzing magnets, three threshold Cerenkov counters, $\sim$ 2500 channels of proportional wire chambers. The amounts of electronics and controls are thus minimized. Besides, the small solid angle and long tunnel length also reduces the radiation and background problems. Therefore, it can fit into most of the experimental halls. The important point is to place it in a hall with other experiments to broaden the scope of the experiment later on.

## 7. Parts List

The parts needed for this experiment are:

| Item | Quantity |
|---|---|
| Modified Q1 and Q2 | 1 each |
| Septum magnets (4, 8, 10 kG, $\int Bd\ell$ = 80 kG m) | 3 |
| Threshold gas C 10 m length | 2 |
| Threshold gas C 50 m length | 1 |
| Dipole magnets and cryogenics (aperture 5 cm h x 25 cm w, preferably superconducting) | 2 |
| Proportional wire chambers | 8 triplets |
| Electronics for proportional wires | 2500 channels |
| Tunnel | 1 |
| Miscellaneous Scintillation counters | |

## 8. Time Table

The construction of the tunnel and the special slots on Q1 and Q2 should be arranged as part of the main ring tunnel and magnets schedule. Due to the modest size and scope of the apparatus, the

construction, setup, and testing time of the spectrometer is quite modest. The construction is about 1-2 years; the setup time is about 2-6 months; and the testing time is about 2 months with beam on. The running time depends on the number of data points in $\sqrt{s}$, $P_{\parallel}$, and $P_{\perp}$ and particle mass to be taken and, of course, the luminosity available. Assuming $L = 10^{31} cm^{-2} sec^{-1}$, it takes 1000 h of running time to measure $\pi$, K, P spectra with 10 different settings in x and 5 settings in $P_{\perp}$ at five different energies with about 3% accuracy. If the large x points are done with higher luminosity, the running time will be certainly shorter.

## 9. Compatibility with Other Experiments and Possible Growth

As we discussed in paragraph 1, the present design is adequate to yield interesting single particle inclusive spectra for $\pi$, K and P with momentum $20 < P < 200$ GeV/c and $60 < \sqrt{s} < 400$ GeV. To measure particles with very low yield (e.g. $\bar{d}$) threshold Cerenkov counter will be needed.

We want to emphasize the following points:

a. The spectrometer is compatible with most of the hadron experiments.

b. The scope of physics is specialized and limited.

c. The spectrometer will be a very important improvement to other experiments.

Therefore, it is advantageous and also very important that this spectrometer be placed in an experimental hall with other experiments. This can be done easily and it is very important to yield more interesting results after the first round experiment. For example, the small angle single arm spectrometer can be placed in the wide angle hall. It should have provisions for the addition of a symmetrical second tunnel. At turn-on, this small angle single particle inclusive experiment, the high $P_{\perp}$ experiment at $90^{\circ}$ (Ref. 2) and possibly the $4\pi$ detector experiment[3] can run separately and simultaneously in the

---

2. C.Y. Chien, H. Gordon, A. Kanofsky, M.A. Kramer, J. Russ, Proc. 1975 ISABELLE Summer Study, Brookhaven, BNL 20550, p. 255.

3. Suh-Urk Chung, P. Grannis, D. Green, ibid p. 183.

wide angle hall. After the first round of experiments, a second small angle arm could be added together with other improvements and additions[4,5] as dictated by the physics results. Then these experiments can run with joint trigger which will allow other studies, e.g., double Regge exchange, double diffractive processes, multiparticle correlations, etc. This kind of scenario gives great flexibility and provides optimum use of equipment.

4. J. Kirz, Proc. 1975 ISABELLE Summer Study, Brookhaven, BNL 20550, p. 269.

5. P. Grannis and D. Green, ibid, p. 277.

# ELASTIC SCATTERING AND DIFFRACTION DISSOCIATION IN THE ANGULAR RANGE 0 - 50 mrad

P. Limon
Fermi National Accelerator Laboratory
and
R. Majka
Yale University

## I. Introduction

After reviewing the work of R. Edelstein and M. Zeller[1] we have decided to emphasize elastic scattering. The diffraction dissociation experiment requires moving the straight section quadrupoles and is not likely to be done in the first years of ISA operation. The diffraction dissociation also places stringent requirements on the rate capabilities of the detectors and may be better done in a different setup such as the large hadron detector designed at this year's workshop.

We also feel that the experiment should begin with the magnets in place (Fig. 1) rather than starting with the magnetless Phase I proposed by Edelstein and Zeller.

## II. Physics Goals

We see three natural regions to study which we list below. These regions may even be considered two or three different phases of the experiment since the luminosity requirements and to some extent the detector requirements vary from region to region.

A. Forward Slope and Structure: $0.1 < - t < 1.0$ GeV$^2$

The ISR data indicate a break or change of slope in the forward p-p elastic cross section at about $t = - 0.14$ GeV$^2$. The s-dependenc

1. R.M. Edelstein and M. Zeller, Proc. 1975 ISABELLE Summer Study Brookhaven, BNL 20550, p. 234.

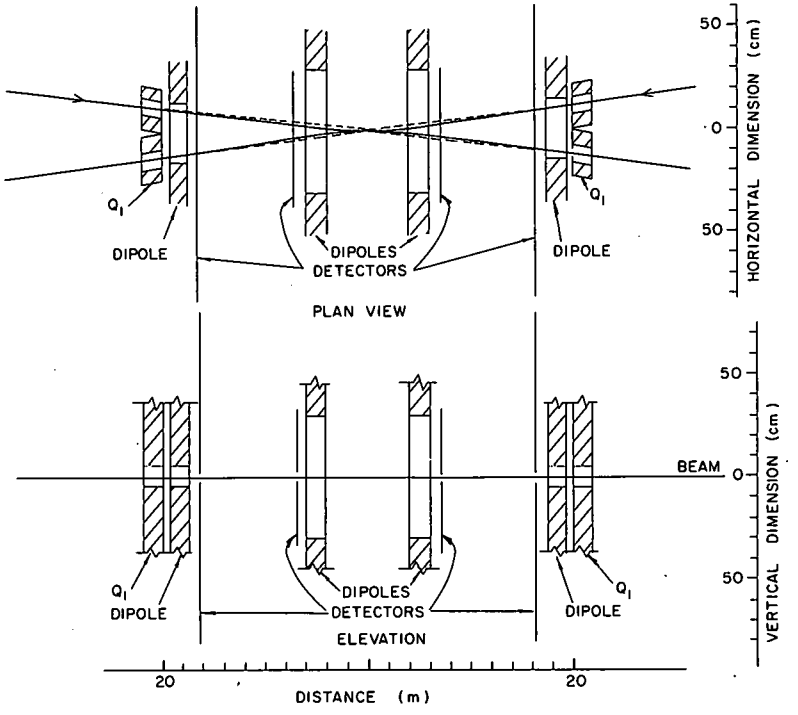


Fig. 1. Magnets and detectors for elastic scattering.

of this phenomenon should be studied at the ISA. One will need 1 to $2 \times 10^6$ events at several s values.

B. Dip Region: $0.5 < - t < 2.0$ GeV$^2$

The s-dependence of the position and depth of the dip and the height of the secondary maximum should be studied. For a high precision study of this phenomena one will need $10^4$ events/0.1 GeV$^2$ through the range of the dip.

C. Very High t Elastic Scattering: $- t > 5$ GeV$^2$

Little data exists on elastic scattering for $- t > 5$ GeV$^2$. The ISA presents a unique opportunity to study this region. A sample of $10^3$ events/GeV$^2$ for $- t > 5$ GeV$^2$ at several values of s will be very useful. The design of Edelstein and Zeller can measure events out to $t = - 100$ GeV$^2$.

We feel that elastic scattering should be studied early in the ISA program. The apparatus described below is sufficiently simple to lend itself to a first round experiment.

## III. Magnets, Counters, Wire Chambers

The magnets needed for elastic scattering are $0.8 \times 0.8$ m$^2$ aperture with 20 kG m field integral. Large superconducting dipoles are probably required. One could accomplish all but the very high t measurements with conventional 48D48 magnets by shimming the gap for the highest s and running at different fields for each s. The compensating dipoles are outside of the apparatus and may be any convenient size.

About 40 m$^2$ of scintillation counter is required for vetoes around the interaction region. The chambers can be used in the trigger so very few other counters are needed.

The chambers in the experiment described by Edelstein and Zeller are proportional wire chambers with 0.5 mm wire spacing. The small

wire spacing is needed to tolerate the very high counting rates at small angles so that one can study double diffraction dissociation using the highest luminosity. This requires a system of about 40 000 wires. If one designs a system only for elastic scattering, however, drift chambers with 1 cm wire spacing are adequate. In the forward direction where the rates are high, the cross section is also high so that one may run with reduced luminosity. For higher [illegible] one can deaden the central region of the chambers and run with [illegible]ier luminosity.

One gains further with drift chambers. The rate is limited by the first chamber (the one closest to the interaction region). Since the resolution of a drift chamber varies closely with drift distance, one may use a larger wire spacing in the rear chambers which are almost twice as far from the interaction region as the front chambers.

A drift chamber system with 1 cm wire spacing in the front chambers and 2 cm spacing in the rear chambers would require 1400 wires.

## IV. Cabling, Electronics, etc.

The magnets will require the usual control and monitor cabling and electronics available in the counting house outside the experimental hall.

There will be about 50 scintillation counters requiring high voltage and fast signal cables to the counting house. The counters will require fast discriminators and coincidence logic.

Readout for 1400 wires of drift chamber will be required. A fast processor or matrix logic will be used to incorporate the chamber information in the trigger. This is most easily accomplished by rapidly digitizing the chamber data and transferring the coordinates to the [illegible]unting house. This implies that in addition to preamplifiers mounted on the chambers there will be encoding logic inside the experimental hall.

About 120 fast cables will be required for fast parallel transfer of the chamber coordinates to the counting house (Fig. 2).

A data acquisition system and small computer will be required. Any standard system such as CAMAC with a PDP-11 and branch driver should be adequate.

The various elements required are summarized in Table I along with cost estimates.

## V. Vacuum Chamber

The vacuum chamber is shown in Fig. 3. The central portion is a simple cylindrical tank about 70 cm in diameter. Since no detect except vetoes are at $90^{\circ}$, the thickness, bake out, and pumping do not pose problems for the experiment. Thin end windows are required for the central section for particles exiting at up to 50 mrad from the interaction region. The section through the detectors is tapered in the vertical from 3 cm near the interaction region to 6 cm at the last detector so that it essentially follows the dump profile. In the horizontal, this section may be as wide as necessary to facilitate pumping. We have shown a 12 cm wide section which should require a pump every 2-3 m. The chambers are all split in the horizontal to accommodate the vacuum pipe and to allow vertical movement of the detectors away from the vacuum pipe for bake out. Clearing electrodes may be thin, and should not prove to be a problem for this experiment.

## VI. Luminosity and Background

Inelastic background has been discussed thoroughly in the work of Edelstein and Zeller. The improved resolution of drift chambers (vs PWC) should help reduce the inelastic background even further.

The drift chambers cannot tolerate the maximum luminosity at the smallest angles (1 mrad). At $10^{32}$ $cm^{-2}sec^{-1}$ the wires closest to the beams will have rates as high as 1 MHz. As mentioned above, the small angle scattering should be done with reduced luminosity. A luminosity of $10^{31}$ $cm^{-2}sec^{-1}$ can be tolerated, but $10^{29}$ $cm^{-2}sec^{-1}$ is sufficient for the low t phase. For large t, the central region of the chambers will be deadened and the luminosity $10^{32}$ $cm^{-2}sec^{-1}$ will be required.

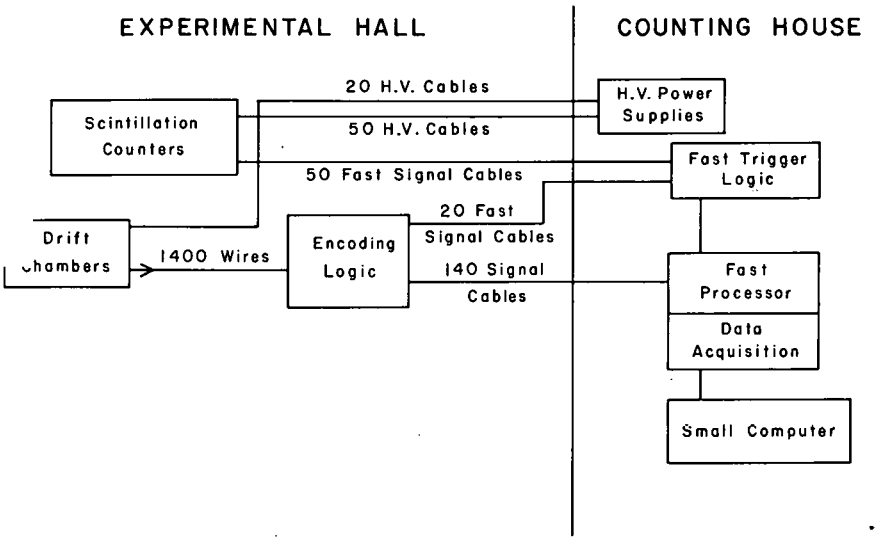


Fig. 2. Block diagram showing deployment of apparatus, logic, and cables.

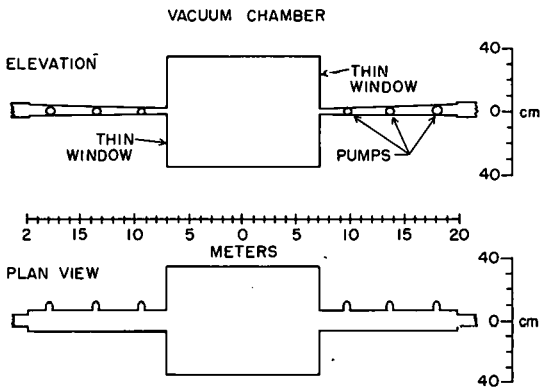


Fig. 3. Vacuum chamber for elastic scattering.

VII. Relevant Times

A. Installation

The major rigging will be for the installation of the magnets and vacuum chamber. This could be done either before the machine turns on or during a scheduled shutdown. Two months should be adequate. The detectors are relatively simple and should require a minimum of time for installation.

We presume all the detectors will be pretested so that a minimu amount of debugging will be required.

B. Data Collection

For the low t region one would like 1 to 2 $\times$ $10^6$ events in the range $0.1 < -t < 1.0$ GeV$^2$. For a cross section:

$$d\sigma/dt = 80\ e^{12t}$$

one has 2 mb in this t range. A luminosity of $10^{29}$ cm$^{-2}$sec$^{-1}$ gives 200 events per second so that about 2 hours per s is required. The time required for this phase is certain to be dominated by the time required to schedule running at several different values of s.

Through the dip region, the elastic cross section at the ISR is about $10^{-4}$ mb/GeV$^2$. For a luminosity of $10^{31}$ cm$^{-2}$sec$^{-1}$ one will get about 8500 events/0.1 GeV$^2$ in one day. Thus, one day per s value should be adequate. A scintillation counter may be used to tag and prescale very small angle events so that data on low and medium t may be taken simultaneously.

For $-t > 5$ GeV$^2$, elastic cross sections are typically $10^{-6}$ to $10^{-7}$ mb/GeV$^2$. We assume that for this phase of the experiment, the central region of the chambers will be deadened so that a luminosity of $10^{32}$ cm$^{-2}$sec$^{-1}$ can be used. This implies about one event per minute per GeV$^2$, or 1400 events/GeV$^2$ in one day. One to a few days per s value should be adequate. Some time (perhaps a two month shutdown) will be required to deaden the center of the chambers.

With some loss of acceptance for medium t events, one could use higher luminosity by simply moving the chambers away from the beams. Since this can be done rapidly (and perhaps even remotely), and is provided for anyway to allow bake out of the vacuum pipe, this may be a preferable alternative to deadening the centers of the chambers.

## VIII. Parts List

Table I summarizes the elements required for this experiment.

TABLE I

| Element | Size or Number | Cost (k) |
|---|---|---|
| Magnets | Two with 0.8 x 0.8 $m^2$ aperture and 20 kG m field integral. Two compensating dipoles | |
| Scintillation Counters | 50 counters with photo-tubes and bases. (40 $m^2$ scintillator for vetoes.) | $ 60 |
| Drift Chambers | 24 chambers up to 0.3 x 0.7 $m^2$ with 1 and 2 cm sense wire spacing. | 50-100 |
| Chamber readout. | Readout for 1400 wires | 140 |
| Encoding logic and interface | | 50 |
| Cables | 210 coax, 70 high voltage | 5 |
| Fast Electronics | 50 channels of discriminator. Veto coincidence and misc. gating. | 30 |
| Fast Processor | | 10 |
| Small Computer | | 100 |

# LARGE APERTURE TWO ARM MAGNETIC SPECTROMETER AT ISABELLE

B. Knapp and W. Lee
Columbia University

We consider the use of a large aperture double arm spectrometer similar to experiments described in the 1975 ISABELLE Summer Study for high resolution measurements of massive lepton pairs ($\mu^+\mu^-$, $e^+e^-$, $\mu^\pm e^\mp$) and high $p_\perp$ single leptons.[1,2] The primary objectives of the experiment are to detect the $Z^o$ (weak intermediate neutral boson) a the $W^\pm$ (weak intermediate charged boson). In addition, one might find very massive stable vector mesons and massive stable hadrons with leptonic or semileptonic decays.

The spectrometer, for which a single arm is shown in Fig. 1, is designed for measurements at collision rates of several million per second, but with a sufficiently large aperture to allow preliminary experiments at lower rates. Each arm contains two analyzing magnets. At interaction rates below a megacycle, an inner detector could be placed between the inner magnet M1 and the interaction region. We do not discuss this detector in this report.

The inner magnet M1 has a field integral of 400 MeV/c, and accepts only particles produced at more than $45^o$ out of the beam pipe. Low momentum particles produced at more than $45^o$, with at least 400 MeV/c momentum, can reach the second magnet M2, which has twice the field integral and opposite polarity from M1. Thus, only particles with horizontal component of $p_\perp$ greater than 400-MeV/c emerge from M2.

The spectrometer measurement planes $p_1p_2p_3p_4p_5$ each consist of three drift chamber planes: one vertical and two rotated away from

---

1. C.Y. Chien, H. Gordon, A. Kanofsky, M.A. Kramer, J. Russ, Proc. 1975 ISABELLE Summer Study, Brookhaven, BNL 20550, p. 255.
2. D. Cheng, K. Goulianos, B. Knapp, J. Rosen, P. Schlein, Proc. 1975 ISABELLE Summer Study, Brookhaven, BNL 20550, p. 319.

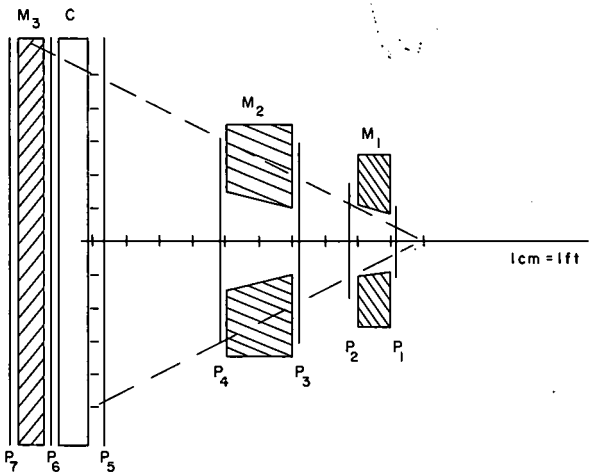


$M_3$ ; MAGNETIZED IRON (S', $P_\perp \simeq$ (GeV/c)

C ; ELECTRON IDENTIFIER

$P_1$ ; SPECIAL DETECTOR

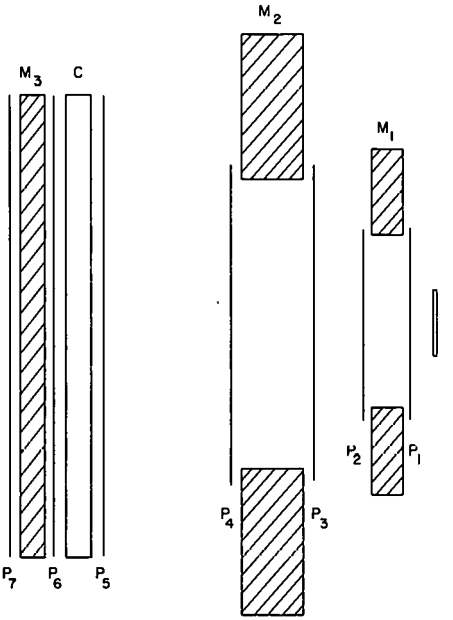


Fig. 1. One arm of double arm spectrometer.

vertical by about 20 mrad. This permits immediate unambiguous measurement of the horizontal (bending plane) coordinate to better than 0.1 mm, the vertical coordinate to better than 5 mm, and also provides nanosecond time resolution. The detector is quite amenable to rapid hardware track processing. We foresee no difficulty in handling on the order of 100 out-of-time tracks within the roughly half-microsecond resolving time of the detector. The drift chamber resolution should permit measurement of the bend angle in the field of M2 to within 0.1 mrad. The mass resolution of a 100 GeV dimuon shou be a few hundred MeV.

The spectrometer is followed by a particle identification system. A magnetized iron filter, M3, rejects hadrons and checks the muon momentum. The best detector for electron identification, C, is not yet obvious. There is insufficient path length for a Cerenkov counter immediately after M2. A fine resolution shower detector, perhaps detecting transition radiation, seems mandatory, but must tolerate a large total rate of low-energy photons from $\pi^o$ decays.

Rates for various processes are given in Ref. 1 and Ref. 2. We give here the rate for detection of $W^{\pm}$ which decays into e or $\mu$.

$$R = (10^{-34}\text{cm}^2) \times (2.5 \times 10^{32}/\text{cm}^2\text{sec})(10^5\text{sec/day}) \times (1/3\ \text{B.R.}) \times (1/10\ \text{Acceptance})$$
$$= 100/\text{day}.$$

We foresee that this detector system can easily be improved and expanded for other physics after the initial lepton measurements. We have ignored some obviously important features of the magnet system which must be considered carefully before construction, particularly the location of the flux return yokes. In view of the demand for large quantities of iron for muon filters, calorimeters, etc., one might consider maximizing the utility of the iron in the magnet yoke by using a lamina-construction with imbedded detectors.

# STUDY OF HADRONS AT LARGE TRANSVERSE MOMENTUM

J. Peoples
Fermi National Accelerator Laboratory

## I. INTRODUCTION

The production of particles with large $P_\perp$ has been reviewed in the past for ISABELLE, most recently by Chien et al[1] for the 1975 Summer Study. The original objective of this note was to determine what requirements such an experiment placed on the insertion region and what equipment would be needed to do the experiment. The discovery of charmed particles and the growth of the evidence in favor of the existence of jets in hadron-hadron collisions were obtained from experimental data which did not exist a year ago. For these reasons the physics which could be studied with the detector of Ref. 1 was reexamined.

It is a large aperture spectrometer, the axis of which was perpendicular to the colliding beams. The multiparticle acceptance for a jet of particles emitted near $90^\circ$ with respect to the colliding beams is good. It stressed particle identification by Cerenkov counters. It had no neutral particle detection. Its physics would be the study of the leading charged particles in a jet. The discovery of charmed particles, in particular the charmed baryon, is a reminder that $\Lambda^\circ$'s and $K^\circ$'s are very important particles to detect. Furthermore these particles can be identified in clusters of charged particles. In the same situation the conventional threshold counter is not very effective. On this basis, the distance between the beam and the magnet was increased to provide one meter of observable decay path.

The hard scattering of a parton (quark) in one hadron off a parton (quark) in another hadron is expected to give rise to a pair of

---

1. C.Y. Chien, H. Gordon, A. Kanofsky, M.A. Kramer, and J. Russ, Proc. 1975 ISABELLE Summer Study, Brookhaven, BNL 20550, p. 255.

jets. By adding a second spectrometer arm on the opposite side of the beam, correlations between jets can be studied. If one assumes that the rapidity distribution along the jet axis is 1.5 particles per unit of rapidity and if the CCR data[2] is taken to represent the leading particle in a jet, then each spectrometer as designed in Ref. 1, will observe jets which contain a leading 10 GeV particle at a rate of 1/min. Furthermore, the spectrometer will usually detect two or three more particles in the jet with momenta greater than 1 GeV. Such a jet would have between 15 and 20 GeV of visible energ This could represent between 75% and 100% of the energy in the jet. Under these circumstances it seems feasible to be able to study parton-parton scattering by detecting correlated jets with $P_\perp > 10$ GeV/c.

In addition to jets which are produced by parton-parton scattering, there will be jet pairs due to the decay of massive objects such as the $W^+$, Higgs' bosons, and $Z^o$'s. For example, the $W^+$ will decay into charmed quark and antistrange quark as often as anything else. With the currently popular theory, the quarks don't get out, and one sees two jets of hadrons carrying integral charge, charm or strangeness. These jets can most easily be detected by using two back-to-back spectrometers which detect both charged and neutral particles. Clearly one can look to see if there is a peak in the transverse energy distribution. A $W^+$ of 65 GeV, a popular number, would give two jets, each containing 32 GeV.

Since the hadron decay modes of $W^+$'s are expected to be as large as 90%, a limited acceptance but good resolution spectrometer is matched to studying the copious decay modes. If there are more flavors of quarks there may be more wondrous phenomena. If the quarks can get out, the charmed quark will be a very penetrating particle since its nuclear cross section is only 1 millibarn on nuclei, compar

---

2. F.W. Büsser, L. Camilleri, L. DiLella, B.G. Pope, A.M. Smith, B.J. Blumenfeld, S.N. White, A.F. Rothenberg, S.L. Segler, M.J. Tannenbaum, M. Banner, J.B. Chèze, H. Kasha, J.P. Pansart, G. Smadja, J. Teiger, H. Zaccone, and A. Zylberstejn, Nucl. Phys. B106, 1 (1967).

to 10 millibarns for the more abundant up and down quarks, and 30 millibarns for standard hadrons. The authors of Ref. 1 recognized most of these possibilities and included them as options. It seems appropriate to consider them as the starting point now.

## II. APPARATUS

The apparatus consists of two magnetic spectrometers oriented endicular to the colliding beams as shown in Fig. 1. Charged icle trajectories are determined by proportional chambers $P_o^i$ and drift chambers $D_1^i$, $D_2^i$, $D_3^i$, and $D_4^i$. Photon momenta are measured by liquid argon-lead plate calorimeters placed at the end of each spectrometer.[3] Following the argon-lead plate calorimeter there is a steel-argon calorimeter which, together with the lead, measures the hadronic energy in the jet. The Cerenkov counters $C_1$ and $C_2$ are used to provide a particle identification for some of the hadrons. The cleanest particle identification is obtained by reconstructing V's due to $K_s^o \to \pi^+\pi^-$ and $\Lambda^o \to p\pi^-$ decays. Finally a one meter thick steel wall followed by scintillation counters provides for muon identification and a crude measure of hadron energy which escapes the calorimeter.

The proportional chambers $P_o^i$ consist of two sets of vertical wires which have a horizontal spacing of 2/3 mm. Each set of wires is displaced relative to the other by 1/3 mm. This technique has been used before to provide accurate position information in a high rate environment.[4] Each drift chamber consists of three pairs of planes which provide the Y coordinate (vertical), U ($20^o$ from the horizontal), V ($-20^o$ from the vertical). Each pair of drift planes consist of parallel sets of sense wires in which the wires of one

---

D. Hitlin, J.F. Martin, C.C. Morehouse, G.S. Abrams, D. Briggs, W. Carithers, S. Cooper, R. DeVoe, C. Friedberg, D. Marsh, S. Shannon, E. Bella, and J.S. Whitaker, SLAC Pub. 1761, LBL-4890 (May 1976).

4. J. Lach, Fermilab CONF-76/15-EXP (January 1976).

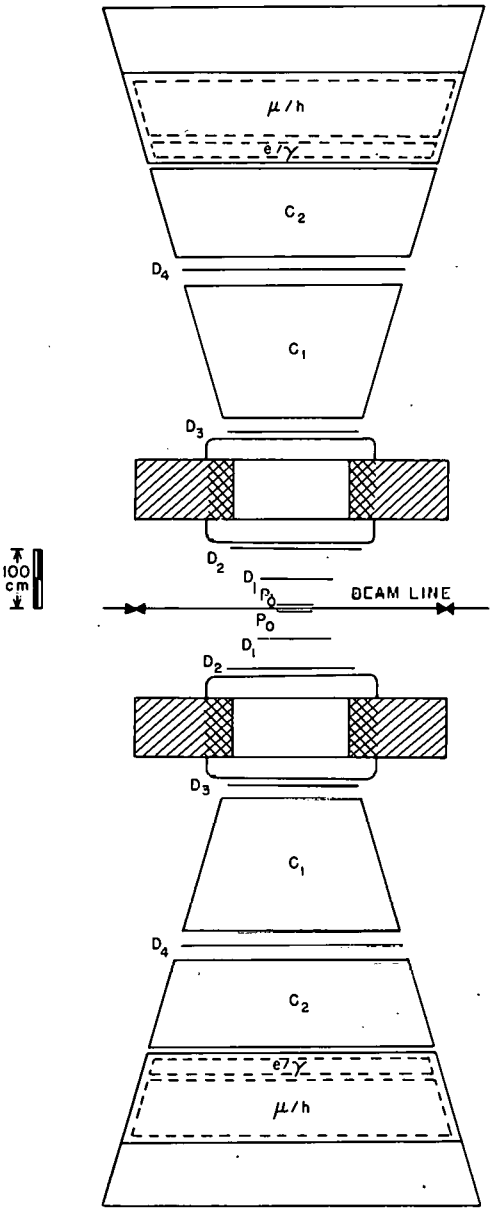


Fig. 1. Large aperture spectrometer with two arms at 90° for study of large $P_\perp$ hadrons.

plane are displaced by half a cell width from the other plane in the pair.

The drift chamber dimensions and cell sizes are given in Table I. The spacing of sense wires is 2 cm in all cases.

TABLE I. Track Chamber Properties

| Chamber | Dimensions (cm) | Type | Sense wires/arm |
|---|---|---|---|
| $P_o^i$ | 50 x 10 | MWPC | --- |
| $D_1^i$ | 150 x 75 | Drift | 210 |
| $D_2^i$ | 230 x 115 | Drift | 330 |
| $D_3^i$ | 230 x 115 | Drift | 330 |
| $D_4^i$ | 400 x 200 | Drift | 570 |

The separation of 1.5 meters between $D_2$ and the beam axis is a compromise between the length of the decay path for $\Lambda^o$ and $K_s^o$ and the solid angle acceptance. The probability that a 10 GeV $\Lambda^o$ will decay before $D_1^i$ is 66%. Moreover, the decay path between the colliding beams and $D_2^i$ is long enough to detect $\Xi^o$ decays and $\Omega^-$ decays. At 10 GeV the momentum resolution for tracks which are measured at $D_1$, $D_2$, $D_3$, and $D_4$ is 1%, for a spatial resolution of 200 $\mu$.

The liquid argon lead plate calorimeter consists of 80 alternating layers of 2 mm thick Pb and 2 mm of liquid argon. The charge is collected on 2 cm wide strips, thereby providing spatial resolution 15 cm for the conversion point of $\gamma$-rays. The $\gamma$-ray angles are determined to a precision of 1.5 mrad and the energy resolution is $0.1/\sqrt{E}$ rms for this type of construction.[3] This accuracy is sufficient to reconstruct $\pi^o$, $\eta^o$, and $W^o$ masses from the $\gamma$-rays for particle momenta between 2 and 240 GeV. Following the lead there are 160 alternating layers of 7 mm thick steel sheets and 2 mm of liquid argon. The overall thickness of the steel is 100 cm. The resolution for hadrons is of the order of $0.2/\sqrt{E}$ rms. The readout strips for

the steel can be as large as 15 cm. Behind the calorimeter there is a meter of steel and a set of liquid scintillation counters which identify muons.

If the detection of the jets proved to be interesting, the detector could evolve in several ways. First, calorimeters and track chambers could be placed upstream and downstream of the interaction region in order to determine if the properties of the forward going hadrons, presumably from noninteracting partons, depended on the $P_\perp$ of the jets. Second, track chambers and calorimeters could be placed around the beam pipe. Finally each spectrometer could be moved by $\pm 45^\circ$ in order to map out jet-jet correlations.

## III. RATES, TRIGGERS, AND BACKGROUND

Each spectrometer subtends relative to the colliding beams $\pm$ 1.4 units of pseudorapidity. At least for good old ("1975") hadron interactions each interaction will produce about 4 particles in this rapidity interval. Since $\Delta\varphi^i/\pi$ is only 0.125, the mean number of particles detected per beam interaction is only 0.5. If there were a 30 GeV jet pointing into one of the spectrometers, one would expect 3 to 5 particles to go through the magnet if the spacing of particles in rapidity along the jet axis were 1.5 particles/unit of rapidity. The number of particles in $P_o^i$ and $D_1^i$ per interaction will be higher but only by a factor of two. Certainly no element such as an MWPC wire or drift cell will count above 200 kc because of beam-beam interactions due to good old hadron interactions. These numbers are, of course, consistent with Ref. 1.

Monitor counters would be placed next to the beam pipe downstream and upstream of the interaction. Each counter would consist of a pair of counters which would surround the beam pipe. Each pair would be designed to subtend a maximum of one to two units of pseudorapidity ($\ell n \tan \theta$). Their size would be picked to coincide with reasonable counting rates.

The photon-hadron calorimeter can be used to provide a simple trigger for $P_\perp$. It would be a simple threshold on the sum of the charge collected in each calorimeter. This technique has been used successfully at Fermilab. The rate of events with a single particle of $P_\perp$ more than 5 GeV/c has been calculated in Ref. 1. This is a lower bound to the trigger rate if a 5 GeV/c threshold for $P_\perp$ is chosen. It is probably reasonable to assume that the data acquisition rate will ıe equivalent of one standard magnetic tape per half hour, if the ɜntional procedure of writing all of the raw data on the tape is followed. The threshold for acceptable $P_\perp$ events will be set low enough to match the two tape per hour rate. This possibility will raise a number of serious computing problems.

## IV. DATA ACQUISITION AND DATA REDUCTION

The detector will require a minicomputer and peripherals for data acquisition. The power of the minicomputer or the higher level computer for fast turn around analysis should be enough to carry out the fundamental track reconstruction. This is based on the observation that the group which does an experiment will need an extended residency at BNL. With detectors of such complexity an extensive data analysis must be done almost simultaneously with data acquisition. When an experiment is complete so that the experimenters can return to their home institutions, the track reconstruction will be complete. Even in the event that major reanalysis needs to be done it is unlikely that track reconstruction will be done at the users home institution. First, the typical university computing center does not have the necessary power, nor does it make sense to reproduce the standard reconstruction at each collaborator's institution. The standardization of the analysis at the reconstruction level is essential. This pattern has already ırred at Fermilab, CERN and SLAC. It is reasonable to assume that reconstructed events which have been filtered can be analyzed at the home institutions. Thus one must prepare for one of the following: a small data acquisition computer which ties into a large computer center as in the SLAC triplex; minicomputers which, together with hardware microprocessors, do all of the track reconstruction and pattern

recognition in real time; or relatively large general purpose computers which are dedicated to each intersection region. This is probably the main area where the traditional way of doing business will have to change.

## V. DETECTOR HALL REQUIREMENTS AND INSERTION REQUIREMENTS

The length of the two spectrometers is nearly 20 meters from the muon identifier in one spectrometer to the muon identifier in the other spectrometer. If the Cerenkov counter $C_1$ were eliminated, some reduction could be achieved. Nevertheless, a detector which must measure particle momenta of 10 GeV to 1% and make e, h, $\mu$ particle identification will have a length of 7.5 meters if the measurements are made with conventional equipment such as magnets, track chambers, calorimeters, and steel absorbers. It a double arm spectrometer is a reasonable way of studying parton-parton collisions through the jet-jet correlations, then the hall should be at least 25 meters across with 10 meters on each side of the beam detectors. The active area of the detector does not exceed a vertical height of 2 meters above or below the beam line. The wide angle hall appears to satisfy these requirements.

The vacuum pipe requirements require nothing extraordinary. The first detector $P_o^i$ should be located 5 cm from the beam. The beam pipe could be an aluminum pipe with a wall thickness of 0.75 mm and a diameter of 50 mm for the 50 cm length of the interaction region. Outside of this region there are no unusual requirements.

## VI. EQUIPMENT TO BE PROVIDED BY BNL

I have assumed that drift chamber electronics will have reached a sufficient state of standardization that HEEP will provide them, as well as the conventional fast electronics. I have assumed that the amplifiers and pulse height analyzers for liquid argon calorimeters will also be sufficiently standard that they will be provided by BNL. There are two good reasons for having BNL provide the equipment. Since nearly every detector will incorporate this type of electronics, there is much to be gained by a single purchaser engaging the several manufacturers in competitive bidding. This has been done extensively at Fermilab with good success. Second, by standardizing, the size of the

spares pool maintained by HEEP will be smaller than if many different types of units must be held in reserve.

If one considers that each experiment done in a given intersection region during the lifetime of the ISA will be located in the same place, and that the electronics trailers do not have to move, it suggests that the flow of information between the detector and the electronics trailer should have a standard solution. Elements of the solution will ude a normally unoccupied trailer - the fast electronics trailer - in the experimental enclosure, which contains all of the fast electronics and the first level of standard electronics. Typically, this electronics is connected to the detector by the order of 5000 channels of cables with a 1000 mc bandwidth. A second trailer - the data acquisition trailer - is normally occupied and is outside of the intersection region. The connections between the fast electronics trailer and the data acquisition trailer do not have to require a large number of cables, nor does the bandwidth of the cables have to be as large as in the first case. Because the detector, the fast electronics trailer, and the data acquisition trailer are in fixed locations, the cables should be strung early with sufficient spares to allow reasonable growth.

Each magnet has a field volume of 200 x 100 x 100 cm. If the magnet were a conventional design the power consumption per magnet would be between 500 kW and 750 kW. With this power consumption there is no clear choice between superconducting magnets and conventional magnets.

Each magnet has a mass of 110 tons of steel. The cost estimates for this equipment given in Table II, while very crude, do set the scale for the modest experiments at nearly $2 000K.

TABLE II. BNL Provided Equipment

| | | |
|---|---|---|
| 2 | 200 x 100 cm magnets & stands | $600 K |
| | Power Supplies & Refrigeration | 60 |
| 3000 | Channels of drift chamber electronics | 150 |
| 1000 | Channels of Pulse Height Analyzers for the Argon Calorimeters | 200 |
| 1000 | Channels of Proportional Chamber Electronics | 20 |
| | Conventional Fast Electronics | 150 |
| | Minicomputer Data Acquisition System | 200 |
| | Muon Identifier Steel (500 tons) | 100 |
| | Liquid Argon Calorimeters | 500 |
| | Cables | 400 |
| | | $1980 K |

## VII. EQUIPMENT TO BE PROVIDED BY THE EXPERIMENTERS

The experimenters would build the Cerenkov counters, scintillation counters, and track chambers. The experimenters would also build all of the special purpose trigger electronics, electronics which filters the data or even processes it before it is recorded on tape. Some consideration must be given to the steps of pattern recognition and track reconstruction. The use of simple geometries and detectors with better pattern recognition can reduce the amount of analysis which has to be done on large general purpose computers. The use of hardware processors for the job of pattern recognition and track reconstruction can potentially reduce the computing significantly. These processors are probably unique to each detector geometry. In spite of the large task that such a development project appears to impose, the cost pales compared to the dollar value which must be assigned to general purpose computing for track reconstruction. For example, several large counter experiments at Fermilab are using computing resources which Fermilab places a value of $150 000/year, for two or more consecutive years. Since the ISA has a nearly 100% duty cycle, the cost could easily increase by an order of magnitude, unless steps were taken to change the methods of reconstruction.

TABLE III. Equipment Provided by the Experimenters

| | |
|---|---|
| Drift Chambers | $100 K |
| Proportional Chambers | 10 |
| Scintillation Counters | 50 |
| Trigger Processors | 150 |
| Track Reconstruction Processor | 100 |
| Cerenkov Counters | 100 |
| | $410 K |

VIII. RUNNING TIME REQUIREMENTS

The detector would use the low $\beta$ insertion which would provide a maximum luminosity of $4 \times 10^{32}$ cm$^{-2}$ sec$^{-1}$. In general the running would be done at equal beam energies and lower luminosities. At the highest energy, the objectives would be to:

1. Establish the existence of large transverse momentum jets.
2. Determine the properties of the leading particle in the jet (charm, strangeness, baryon, lepton...).
3. Determine the nature of jet-jet correlations.
4. Search for any object which can decay into a pair of jets (for example, $W^+$, $Z^o$, Higgs' bosons...).

At lower energies the objective would be to establish the energy dependence of the preceeding properties. For example, 120 on 120; 60 on 60; and 30 on 30. Unequal energies could be useful if the spectrometer arms can be readily rearranged. If the arms remain at 90$^o$, unequal energies only allow one to explore a limited range of x. Although the experiment is not terribly sensitive to unequal energies, useful data still can be obtained. The initial running for all energies would be 1000 hours.

IX. SET-UP REQUIREMENTS

At turn-on, both magnets would be required. An area equivalent to one trailer (10' x 30') will be required for the fast electronics at the rear of the inside arm. The electronics should be shielded and should have a shielded access tunnel to allow limited access during

beam-on operation if possible. The data acquisition trailer or counting room will require an area of 1000 $ft^2$.

# SOME NOTES CONCERNING ISABELLE ELECTRONIC INSTRUMENTATION

M. Schwartz
Stanford Linear Accelerator Center

The main purpose of this note is to stimulate early thought relative to the electronic instrumentation which will be required at ISABELLE at the inception of its experimental program. This represents ique opportunity to approach the instrumentation problem rationally, ng provisions for most of the needs in the various intersection regions at minimal cost. In particular, as will be seen, it may be possible to develop a number of specialized integrated circuits which will go a long way toward facilitating the rapid acquisition and examination of data.

## I. Nature of the Primary Instrumentation

At the present time there are basically three types of instrumentation which one might expect to find in any of the proposed ISABELLE experiments.

1. Scintillation counters. Here the primary data is a pulse, typically 20 nsec in length and with a pulse height of the order of 1 volt. The time of this pulse can be usefully digitized to $\sim \pm \frac{1}{4}$ nsec and its height to ± 1%. A typical experimental setup may have of the order of 100 such counters.

2. Proportional and drift chambers. Here we deal with pulse heights of the order of tens of millivolts and pulse lengths of the order of 50 nsec. It is generally desirable to determine the pulse time (determined by its leading edge) to about ± 1 nsec and its height to ± 1%.

3. Calorimetry devices. Here the time resolution is typically better than 10 nsec but a pulse height resolution of ± 0.1% would be desirable.

The large bulk of the instrumentation, from the point of view of expenses, is clearly in the second category, namely the proportional

and/or drift chambers. A typical experimental setup, as currently planned, would have of the order of 10 000 wires, of which perhaps 100 may participate in any given event. If the overall event rate is $10^7$/sec then one might expect a typical wire to have a pulse rate of $10^5$ pulses/sec. Some wires may have substantially higher rates, perhaps up to $2 \times 10^6$ pulses/sec.

The problem we will address ourselves to is that of sorting through such a large bulk of data in a reasonable time so as to enable the experimenter to log meaningful results on magnetic tape for further analysis.

## II. A Proposed System for Analog Storage and Decision Making

One of the more interesting technologies which may help considerably in solving the decision making problem is that of charge coupled devices (CCD's). These devices, which have come on the market during the last year or so, are basically analog shift registers. A small amount of charge can be moved from one bucket to its neighbor by means of an external clock. Typically, a chain consists of $\sim 100$ of such buckets and the typical time between clock pulses can be $\sim 100$ nsec.

Consider then a typical proportional chamber pulse. We first generate a 100 nsec discriminator pulse whose leading edge coincides with that of the proportional chamber pulse, as shown in Fig. 1.

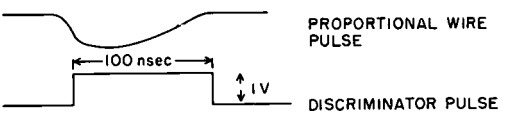


Fig. 1. Typical proportional chamber pulse.

The discriminator pulse is then fed to the front end of a dual channel CCD. (For example, the Fairchild CCD 311.)

The sampling and shifting of the pulse illustrated in Fig. 2 goes as follows.

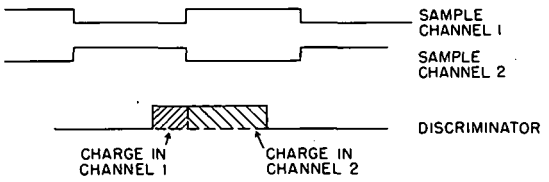


Fig. 2. Pulse division and storage in CDD.

After the number of clock cycles necessary to move the charges to the end of the chain, one can determine the timing of the discriminator pulse by measuring the ratio of the two charges. This technique will permit the measurement of time to $\sim \pm$ 1 nsec with a dead time no longer than 100 nsec per pulse. Furthermore, it will store all such information for a period of 10 $\mu$sec or more, during which time decision-making apparatus will decide if the data is of further interest. If so, the clock can be stopped and the data can be digitized and read into a computer.

The essence of this technique is then:

1. All pulse height and time information on all wires is kept intact for a period of $\sim$ 10 $\mu$sec.

2. Dead time occurs only when interesting data is to be transred into the computer.

3. The cost per wire of such a system should be no more than about $5 to $10.

# OVERVIEW OF MACHINE STUDY GROUP*

M. Month

Brookhaven National Laboratory

The machine group was charged with looking into the following questions:

- What is the range of flexibility of the ISABELLE collision region parameters? What constraints are imposed by the ISABELLE "operational philosophy"?

- What are the implications with respect to machine performance of six insertions rather than eight?

1. First, let us consider what conclusions were arrived at with regard to collision region parameters.

- The crossing angle could be reduced substantially from the 11.4 mrad standard value. This is accomplished at the expense of straight section length. Also, of course, the collision diamond increases proportionately with $(1/\alpha)$. Essentially angles very close to zero are possible with about $\pm$ 4 m still available.

- The horizontal $\beta$ value could be decreased from its nominal value of 20 m to about 5 m in the low-$\beta$ configuration. This would require increasing the gradient in the special focusing doublet near the collision point to about 3.8 kG/cm rather than the design 3.1 kG/cm.

- The small diamond configuration was studied. Increased bending allows a crossing angle of 50 mrad with a free space length for experimental apparatus of $\pm$ 2.5 m. The geometric configuration is given in Fig. 1. The potential collision characteristics are: ($\alpha$ = 50 mrad).

Standard focusing, p = 200 GeV/c ($\beta_v^* = 4$ m, $\beta_{h}^* = 20$ m)

$\ell_{int} = \pm 5.5$ cm

$L = 4.8 \times 10^{31}$ cm$^{-2}$sec$^{-1}$

*R. Chasman, D. Edwards, A. Garren, D. Johnson, J. Herrera, G. Parzen, E. Raka, H. Wiedemann.

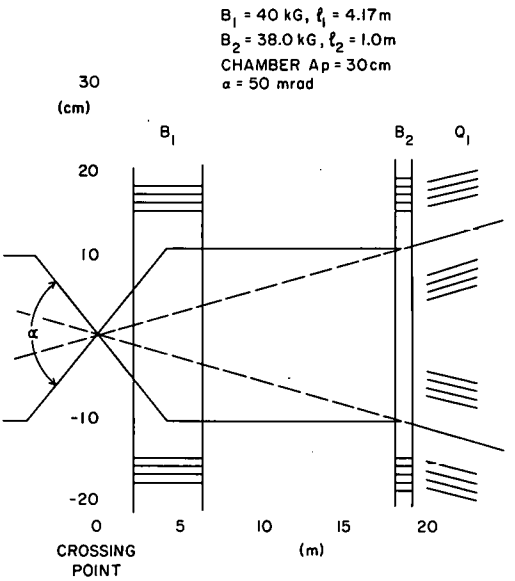


Fig. 1. Small diamond beam geometry.

Low $\beta$, $\beta_v^* = 1$ m, $\beta_h^* = 20$ m $\quad \begin{cases} \ell_{int} = \pm 5.5 \text{ cm} \\ L = 1.0 \times 10^{32} \text{ cm}^{-2}\text{sec}^{-1} \end{cases}$

Low $\beta$, $\beta_v^* = 1$ m, $\beta_h^* = 5$ m $\quad \begin{cases} \ell_{int} = \pm 2.8 \text{ cm} \\ L = 1.0 \times 10^{32} \text{ cm}^{-2}\text{sec}^{-1} \end{cases}$

- The ISABELLE design philosophy allows the preserving of high symmetry and mild focusing in the identical insertions, meaning a large momentum aperture, during injection, stacking and acceleration. The collision diamond character can be changed at collision time. The momentum aperture is reduced because of the change in focusing in the insertions, but this is consistent with the reduced momentum aperture required for a simple coasting stack.

- The high-$\beta$ insertion was studied as well as an operating state having 2 symmetrically placed low-$\beta$ insertions. The conclusions are that: 1) the momentum aperture is slightly worse in the 2 low-$\beta$ case, but not significantly, 2) further study on the effect of the sextupoles on the betatron motion should be done, 3) the use of more than 2 sextupole families should be pursued to see if the momentum aperture could be opened up if one or more than one low-$\beta$ is used, and 4) the high-$\beta$ insertion is not a significant perturbation on lattice stability.

- The free space for experimental gear is <u>not</u> fixed forever. There is the possibility of increasing it, although this is not planned in the first stages of ISABELLE operation and it is not encouraged. The impact, of course, is that it essentially means that stacking and acceleration would have to be done with reduced symmetry. Remember that the <u>total</u> straight length of the insertion is fixed at about 116 m. Much of this must be used for the matching and focusing quadrupole system.

- The effect of the vacuum chamber design in the insertions were considered. The required high-vacuum conditions seemed achievable. For rapid changes in vacuum chamber cross section, it was concluded that clearing electrodes would be required because regions

of radius change represent potential wells where electrons tend to get trapped and neutralize the proton beam. In fact, it appears that changes of chamber radius larger than about 1 cm require special clearing precautions.

2. In considering the 6 vs 8 insertion ISABELLE, it was assumed that 2 insertions were simply removed with no other changes.

This is a reasonable comparison. Attempting to complicate the ›arison by keeping the circumference the same and increasing the bending length in the 6 insertion case is not meaningful. Increasing the bending and thereby the energy would either substantially increase ISABELLE's susceptibility to longitudinal instability and/or increase the spatial aperture required for the beam (meaning, of course, a larger magnet aperture!). We therefore ignore this possibility.

It should be kept in mind that the possibility of increasing the energy in ISABELLE by increasing the bending length, i.e. the circumference, with either 6 or 8 insertions is feasible. However, to accomplish this would require the inclusion in the ISABELLE complex of a 3rd, conventional stacking ring. It would have the size roughly of the AGS ($\sim$ 800 m circumference). Although certainly an interesting and beneficial addition to the ISABELLE complex, the 3rd ring is not in the immediate ISABELLE plans.

The <u>main effects</u> of going to 6 insertions:

- Circumference reduced ($3\text{-}2/3\ C_{AGS} \rightarrow 3\text{-}1/3\ C_{AGS}$) by about 270 m.

- Insertion quadrupoles removed for 2 insertions (reduction is 8/insertion $\times$ 2 insertions $\times$ 2 rings = 32 quadrupoles).

Conclusion: It is primarily a cost consideration. There is no 1st order effect on ring stability.

The Secondary Effects on Ring and Beam

- Insertions add to ring chromaticity so, 6 fold symmetry → increased momentum aperture.

However, the dominant impact on the momentum aperture is the low-$\beta$ insertion (s) and this effect is independent of whether we have 6 or 8 insertions.

- The beam is quite dense in the insertions since there is zero momentum dispersion. The removal of 2 insertions, therefore, implies a slight decrease in the beam self-field tune shift as well as the resistive wall instability threshold and further implies a slight decrease in overall electron clearing requirements. The order of magnitude resulting corresponds to 15 - 20% effects.

- The optimization for ring tune (21.6 rather than 25.6) in the 6 insertion case yields longer cells and correspondingly longer bending magnets,

$$\ell_B = 4.25 \text{ m (8 insertion case)}$$
$$\rightarrow \ell_B = 4.50 \text{ m (6 insertion case)}$$

The implications of this are: Slightly reduced transition energy, meaning $(Z/n)_{limit}$ for longitudinal stability increased by about 60%, and slight increase in dispersion, which means increased spatial aperture required at injection.

Conclusions on 6 vs 8 insertions

There is some advantage to 6 insertions from the machine view point.

But, both are feasible.

There is no compelling argument for one or the other.

Other considerations, such as capital cost, or the cost of support requirements to operate as many as 8 facilities, should be used to come to a final decision on this point.

# COMPARISON OF INSERTION CONFIGURATIONS

A. Garren
Lawrence Berkeley Laboratory

and

D. Johnson
Fermi National Accelerator Laboratory

A study was made during the 1975 Summer Study of the effects of uding one low-beta insertion with seven normal ones in ISABELLE.[1] ..ng the 1976 Workshop, we have extended these studies to two other cases: one high-beta insertion and two low-beta insertions.

The beta values at the crossing points for the three cases are tabulated below:

TABLE I

| | Normal Insertions | Low-beta | High-beta | $\hat{\beta}_v$ Maximum |
|---|---|---|---|---|
| $\beta_h$ | 20. | 20. | 61.67 | |
| $\beta_v$ | 4. | 1. | 69.19 | |
| Case 1 | 7 | 0 | 1 | 104 m |
| Case 2 | 7 | 1 | 0 | 396 |
| Case 3 | 6 | 2 | 0 | 394 |

As in the 1975 Study, two sets of sextupole corrections were assumed, SF and SD, located respectively in the centers of the F and D quadrupoles of the normal cells. These are set to correct the horizontal and vertical chromaticities to zero values.

The procedure was as follows. First, a fitting run was made with the SYNCH program to match the normal and high or low-beta insertions to the cells and obtain the desired tunes (25.65 was chosen). Second, sextupole strengths were calculated to make the omaticities be zero. Third, a run was made with the FXPT ..struction of SYNCH, that calculates closed orbits, betatron functions, etc. for off-momentum particles in the presence of

1. A. Garren, Proc. 1975 ISABELLE Summer Study, Brookhaven, BNL Report 20550, p.372.

sextupoles. The FXPT runs covered the range $-0.01 \leq \Delta p/p \leq 0.01$ in steps of 0.0025.

The results are shown in Figs. 1-5. In each graph the numbers refer to the three cases of Table I. Figs. 1-2 show the tunes, Fig. 3 the relative variation of $\beta_v$ at the crossing point in the low or high-beta insertion, Fig. 4 the relative $\beta_v$ variation at the normal insertion crossing that is most strongly affected by the special insertion, while Fig. 5 shows the variation of the maximum $\beta_v$ values in the entire ring. The $\beta_H$ variations are less than those of $\beta_v$.

Roughly speaking, there are no striking differences between the three cases, except for the larger variation of $\nu_v$ in the case of two low-beta insertions. This arises from the extra chromaticity correction that must be provided.

Before concluding that one low-beta insertion is preferable to two, the effects of nonlinear resonances should be studied, for example with tracking runs. The two low-beta case has the advantage of suppressing odd order structure resonances, especially the third order one at $\nu = 25\text{-}2/3$.

Better compensation can, of course, be obtained by adding new independent sextupole sets. For example, if the sextupoles in one or two octants are different from the others, it should be possible to cancel the third order resonances at 25-2/3, or possibly to lessen the tune variations.

We wish to thank Dr. M. Month for stimulating discussions and advice.

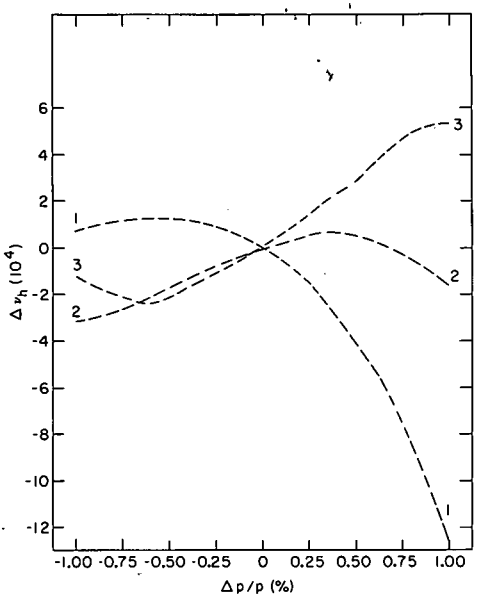


Fig. 1. Horizontal tune change vs percent momentum offset.

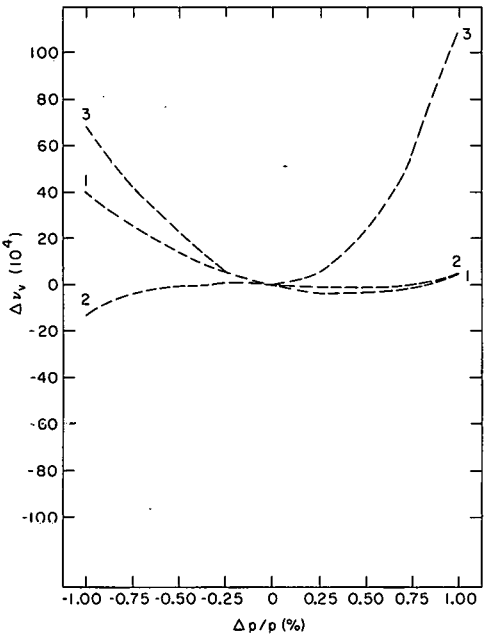


Fig. 2. Vertical tune change vs percent momentum offset.

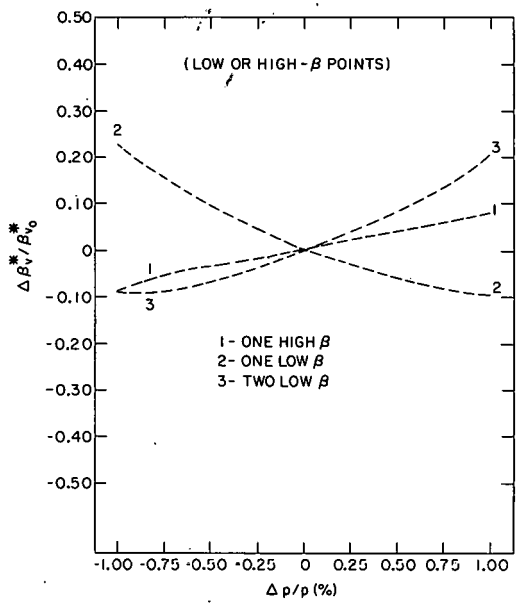


Fig. 3. $\Delta\beta_v^*/\beta_{v_o}^*$ vs percent momentum offset.

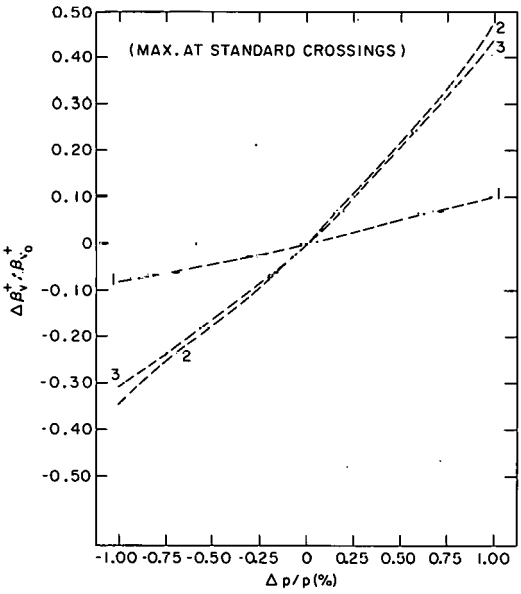


Fig. 4. $\Delta\beta_v^+/\beta_{v_o}^+$ vs percent momentum offset.

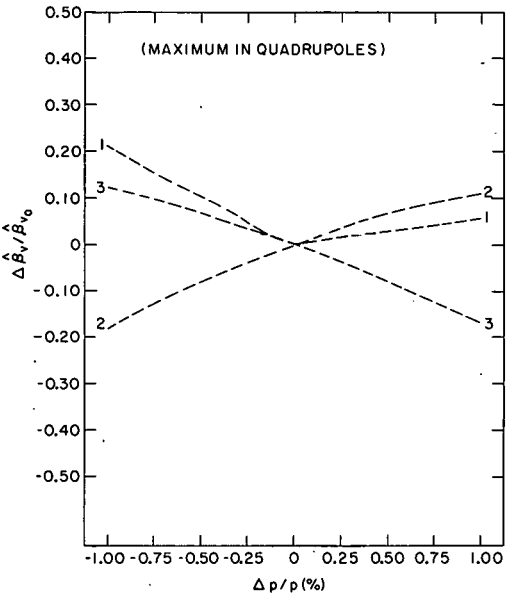


Fig. 5. $\Delta\hat{\beta}_v/\hat{\beta}_{v_o}$ vs percent momentum offset.

# POSSIBLE EFFECTS OF LOWERING THE PERIODICITY IN ISABELLE

G. Parzen
Brookhaven National Laboratory

The replacement of one or more of the standard insertions by either a low-$\beta$ or high-$\beta$ insertion will reduce the periodicity of ISABELLE, with resulting effects on the particle dynamics. Some of the possible dynamics effects are listed and discussed below.

Beam-Beam Interaction

A measure of the beam-beam interaction is the $\Delta\nu$ per insertion caused by the beam-beam interaction. This has been computed[1] to be $\Delta\nu = 1.4 \times 10^{-3}$, $\Delta\nu = 0.7 \times 10^{-3}$ and $\Delta\nu = 2.3 \times 10^{-3}$ for the standard, low-$\beta$, and high-$\beta$ insertions respectively. This measure of the beam-beam interaction does not appear to be appreciably larger for the non-standard insertions.

The nonlinear resonances driven by the beam-beam interaction depend on the differences between the beam interaction in the eight interaction regions. At first sight, the driving term would appear to be larger for the lower periodicity ISABELLE. The beam-beam interaction is different in the low or high-$\beta$ insertions than for the standard insertion, because of differences in the beam size, crossing angle and interaction length. This effect deserves further study. The ISR does not appear to notice any difficulties with the beam-beam excited nonlinear resonances when running with a periodicity of one.[2]

$\beta(p)$ Effect

It has been computed by A. Garren[3] that the ISABELLE lattice with just one low-$\beta$ insertion results in an appreciable variation of $\beta$ with momentum. A variation of $\Delta\beta/\beta = 100\%$ is found for $\Delta p/p = \pm 1.8\%$. However, at 200 GeV, the beam $\Delta p$ is $\Delta p = \pm 0.22\%$, with $\Delta\beta/\beta = 10\%$.

1. M. Month, BNL Formal Report ISA 75-10 (1975).
2. B. Zotter, private communication.
3. A. Garren, Proc. 1975 ISABELLE Summer Study, Brookhaven, BNL 20550, p. 372.

The 10% variation in $\beta$ would decrease the luminosity somewhat, by about 5%. There is a slight loss in the aperture since the beam is everywhere larger by about 5%, which does not seem important as the beam is quite small, $\Delta x = \pm 0.35$ cm, compared with the vacuum tank dimensions of $\pm 4$ cm.

The variation of $\beta$ with momentum also affects the ability to ect nonlinear resonances if this proves desirable. The ing term for these resonances depends on $\beta$ and thus one can correct the resonance with a given set of correction coils at only one value of the momentum. At present, there are no plans to correct the nonlinear resonances, and it is not believed to be necessary to do so. A 10% variation in $\beta$ still allows the driving term of the resonance to be reduced by 90%. Further, the variation of $\beta$ with momentum can be reduced by introducing more families of sextupoles, which can be separately excited, than the present 2 families of sextupoles which are used to control the chromaticity. This is being studied at this workshop by Garren and Wiedemann.

$\nu(p)$ Effect

The variation of $\nu$ with momentum computed by Garren for the case of one low-$\beta$ insertion is different but not worse than was found for the standard case. The working line correction coils in ISABELLE, which can correct the $\nu$ variation up to terms which go like $p^4$, can provide the required working line shape.

Machine Nonlinear Resonance

In the case of the ISABELLE lattice with reduced periodicity, one might expect that the machine nonlinear resonances which are driven by nonlinearities in the magnetic field would be considerably onger. In particular, the structure resonances, driven by the ential periodicity of the machine, would be much more dense for the reduced periodicity ISABELLE.

The main source of nonlinearities is the sextupoles in the ring. It is found[3] that these resonances have a width of about $\nu \leq 1 \times 10^{-3}$. Because of the small size of the working line at 200 GeV, $\Delta\nu \simeq 0.013$, it does not appear difficult to avoid the resonances introduced by the sextupoles.

These sextupole resonances are relatively strong, and further computer study is merited to back up the result found by the simple calculation of the resonance width. Another feature of these resonances that may be troubling, is that they are accompanied by a relatively strong variation of $\beta$ across the aperture, which makes it difficult to correct these resonances over more than a small portion of the aperture.

Conclusions

There appears to be no overwhelming difficulty to operating ISABELLE with reduced periodicities. However, the following three topics are suggested for further study:

1) The nonlinear resonances excited by the beam-beam interaction. The lower periodicity appears to make these resonances stronger by a large factor.

2) A system of several families of sextupoles all separately excited, so that the sextupoles can control both the chromaticity and the variation of $\beta$ across the aperture. Without this, the available aperture at 200 GeV may be severely limited.

3) A computer study of the resonances introduced by the sextupole system.

# CHROMATICITY CORRECTION IN ISABELLE WITH LOW-β INSERTIONS

H. Wiedemann

Stanford Linear Accelerator Center

## 1. INTRODUCTION

To maximize luminosity in a storage ring, the natural chromaticities, e ~ the linear changes in the betatron frequencies with momentum, are p to very large values. These chromaticities have to be compensated by means of sextupole magnets. To compensate for the vertical as well as the horizontal chromaticities, two families of sextupoles are needed. Large chromaticities as they appear in storage rings like ISABELLE, PEP, and PETRA, however, are accompanied by other perturbations that should not exceed certain values. In this note we will discuss some of these perturbations and possible compensatory methods.

## 2. LOW-BETA INSERTIONS IN ISABELLE

The standard beam dynamics configuration in ISABELLE assumes beta function values of $\beta_x^* = 20$ m and $\beta_y^* = 4.0$ m at the interaction point. For certain experiments, however, a low-β configuration with $\beta_x^* = 20$ m and $\beta_y^* = 1.0$ m has been worked out.[1] The problem with this configuration is how to have the low-β in only some of the eight interaction points. In this note we will not discuss the effects of nonsymmetry if standard superperiods are replaced by low-β superperiods in an unsymmetric manner. We will, however, discuss the matching conditions between two superperiods of different types.

## 3. BETA VARIATION WITH MOMENTUM

For the following discussion we define a superperiod in ISABELLE as ighth of the ring starting in the middle of one arc (called symmetry

---

1. "A Proposal for Construction of a Proton-Proton Storage Accelerator Facility", BNL 50519 (May 1976).

point) and going to the middle of the next arc. The interaction point is then in the center of a superperiod. It is clear that if a standard superperiod is followed by a low-β superperiod, the following matching conditions have to be met:

$$\beta_{x,y,ST} = \beta_{x,y,LB} \tag{1a}$$

$$\alpha_{x,y,ST} = \alpha_{x,y,LB} = 0 \tag{1b}$$

Here "ST" and "LB" stand for standard and low-β superperiods, respec
Usually these matching conditions are met for on-momentum particles l
proper setting of the quadrupoles. For off-momentum particles, Eq. (1a), in general, is no longer true. The variation of the beta-function with momentum is given by[2]:

$$\frac{\Delta\beta}{\beta}(\varphi) = -\frac{\Delta p}{p} \sum_{n>0} \frac{2a_n}{4\nu_o^2 - n^2} \cos n\varphi \tag{2}$$

where the coefficients $a_n$ are the Fourier components of $\nu_o^2\beta^2(k - m\eta_o)$; $\nu_o$ is the tune of the superperiod; $\varphi$ is the betatron phase which runs from 0 to $2\pi$ in one superperiod; k and m are the quadrupole and the sextupole strengths defined by $k = (1/B\rho)(\partial B_y/\partial x)$ and $m = (1/B\rho)(\partial^2 B_y/\partial x^2)$; and $\eta_o$ is the dispersion function obtained from linear beam dynamic. At the symmetry point, $\varphi = 0$, it is obvious that the beta variation with momentum depends on the Fourier components $a_n$ only and in turn on the beta-function as well as the distribution of the sextupoles. A lower value of the beta-function in the interaction point creates a larger value in the interaction region quadrupoles and therefore enhances the contribution $\beta^2 k$ for the Fourier components. We also see that the on-momentum beta-function is matched at the symmetry point while the off-momentum beta function is not. From Eq. (2), however, we conclude that it might be possible by proper arrangement of the sextupoles to make the beta variation with momentum vanish. Because of the limited numb

2. E.D. Courant and H.S. Snyder, Ann. Phys. 3, 1 (1958).

of sextupoles, it may not be possible to make $\Delta\beta/\beta = 0$ everywhere, but it can be made zero at the symmetry point which is the main goal of this study.

## 4. VARIATION OF THE SEXTUPOLE STRUCTURE

In the ISABELLE lattice we assume a focusing sextupole SF in each QF and a defocusing sextupole in each QD, except in the QD at symmetry point. The last sextupole at the symmetry point is not for computational convenience only. In this sextupole arrangement we have 10 SF and 8 SD per superperiod. If we power all SF and all SD in series to compensate the chromaticities only (we call this the configuration A), we end up with a beta variation at the symmetry point as shown in Fig. 1. The linear beta variation in the vertical plane along half a superperiod is shown in Fig. 2. The following is a compilation of some of the characteristic parameters:

| Sextupole | Number/ Superperiod | Strength ($m \cdot \ell$) |
|---|---|---|
| SF | 10 | $-0.149\ m^{-2}$ |
| SD | 8 | $0.511\ m^{-2}$ |

| Beta variation at | Symmetry point | Interaction point |
|---|---|---|
| $(\Delta\beta_x/\beta_x)/(\Delta p/p)$ | 2.0 | 9.5 |
| $(\Delta\beta_y/\beta_y)/(\Delta p/p)$ | 53.5 | 35.0 |

In an attempt to reduce the beta variations at the symmetry point by varying the strengths of some of the sextupoles, we have to keep in mind that not only the beta variation but also the nonlinear variation of the tune with momentum and the variation of the tune with the betatron amplitude are changed. All these effects and methods to reduce them are discussed in detail in Ref. 3.

---

3. H. Wiedemann, PEP Note 220 (1976).

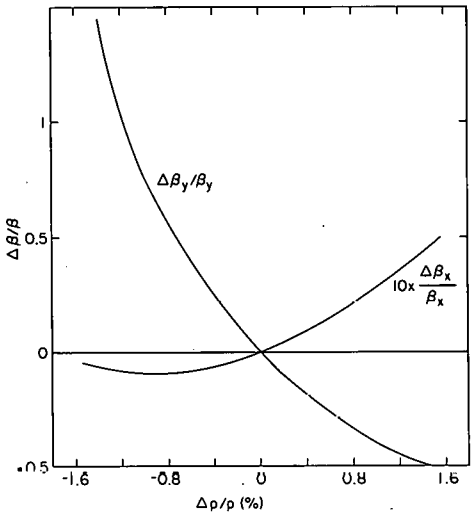


Fig. 1. Beta variation with momentum at the symmetry point. Configuration A.

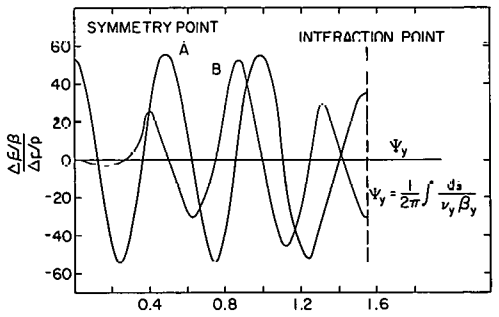


Fig. 2. Vertical beta variation with momentum.

Keeping these effects in mind and with the help of the computer code PATRICIA,[3] the optimum sextupole configuration has been found as follows (we call this configuration B):

| Sextupole | Location $\psi_y = \frac{1}{2\pi}\int \frac{ds}{\nu_y \beta_y}$ | Strength $m \cdot \ell [m^{-2}]$ |
|---|---|---|
| ? | 0.124 | - 0.161 |
| SY1 | 0.249 | 0.778 |
| SF | 0.373 | - 0.161 |
| SY3 | 0.497 | - 0.050 |
| SF | 0.622 | - 0.161 |
| SY2 | 0.746 | 0.790 |
| SX1 | 0.870 | - 0.113 |
| SD | 0.995 | 0.538 |
| SF | 1.118 | - 0.161 |

The chromaticities are zero for this sextupole structure. In Figs. 2 and 3 the beta variation with momentum for configuration B is shown. We see that apart from small quadratic terms, the beta variation is zero at the symmetry point.

The tune variation with momentum is shown for both configurations A and B in Fig. 4. We see that the tune variation in the horizontal plane is a little worse in configuration B than in A and about the same but of opposite sign in the vertical plane.

Although the beta variation is made zero at the symmetry point, it is not zero at other points. The variation of the beta function at the interaction point is of special interest and it is shown in . 5. Extensive attempts have been made to further reduce the tune ation, Fig. 4, and the beta variation at the interaction point, Fig. 5, while keeping $(\Delta\beta/\beta)_{sym} = 0$. No improvement beyond the results shown could be reached because not enough sextupoles were available.

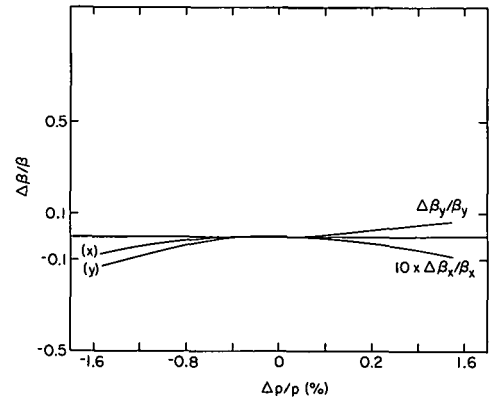


Fig. 3. Beta variation with momentum at the symmetry point. Configuration B.

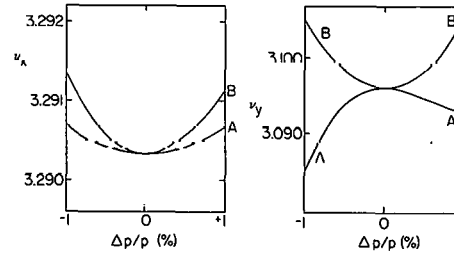


Fig. 4. Tune variation with momentum, (ν, tune of one superperiod).

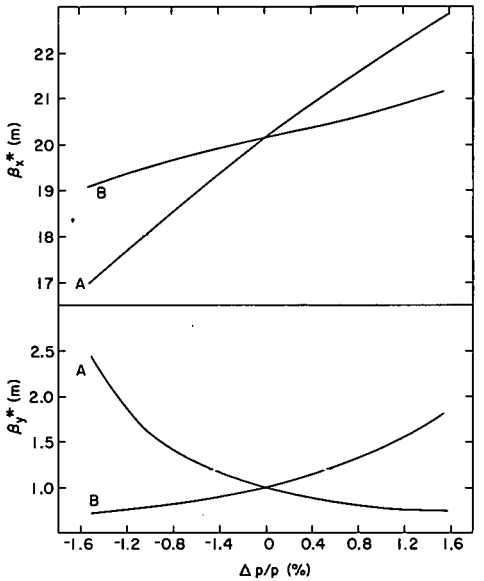


Fig. 5. Beta variation with momentum at the interaction point.

## 5. PARTICLE TRACKING IN CONFIGURATION B

Using the computer program PATRICIA,[3] particles with different betatron amplitudes were tracked in the presence of all sextupoles over 750 full turns around the storage ring. On-momentum particles have been found to be stable for amplitudes at least as large as those shown in the table below.

| $x_o$(mm) | $x_o'$(mrad) | $y_o$(mm) | $y_o'$(mrad) |
|---|---|---|---|
| 40.0 | -- | -- | -- |
| -- | -- | 56.0 | -- |
| 20.0 | -- | 33.0 | -- |

Here $x_o$, $x_o'$, $y_o$ and $y_o'$ are the initial particle parameters at the symmetry point.

For off-momentum particles the stable region is found to be as follows:

$\Delta p/p = + 1.5\%$

| $x_o$(mm) | $x_o'$(mrad) | $y_o$(mm) | $y_o'$(mrad) |
|---|---|---|---|
| 39.0 | -- | -- | -- |
| -- | -- | 57.0 | -- |
| 18.0 | -- | 31.0 | -- |

$\Delta p/p = - 1.5\%$

| | | | |
|---|---|---|---|
| 36.0 | -- | -- | -- |
| -- | -- | 57.0 | -- |
| 18.0 | -- | 31.0 | -- |

## 6. CONCLUSION

For the low-$\beta$ configuration in ISABELLE, it has been shown that the values of the beta functions can be made independent of the part momentum. To achieve this independence more than two families of se poles are needed. Since the beta variation at the symmetry point can be made zero for the low-$\beta$ configuration, it seems obvious that the

same can be achieved for the standard configuration. If this is done, it is possible to have low-$\beta$ and standard superperiods in any order and switching from one configuration to another in one superperiod will not affect the other superperiods. As mentioned earlier in this note, however, other effects may occur due to nonsymmetry of the whole storage ring when different configurations are used in an arbitrary sequence.

# ELECTRON CLEARING AND DIMENSIONAL TOLERANCE FOR THE ISA CHAMBER

J. C. Herrera

Brookhaven National Laboratory

## I. Introduction

In the straight sections of the ISA ring the clearing of the low energy electrons produced by the beam-gas collisions will take place by longitudinal motion. Thus, an electron of low energy, which is prevented from escaping transversely by the attractive field of the beam, will receive successive kicks by the circulating protons and thereby acquire sufficient energy to travel longitudinally toward the clearing electrodes. However, a discontinuity or step in the chamber diameter, which occurs within an axial distance equal to a few diameters, gives rise to a potential difference along the chamber axis. In the case of a section of chambers which has a larger diameter, that is, a small cavity, the two steps result in a longitudinal potential well, or attractive region. It is then necessary that the electrons be given additional energy in order to overcome this longitudinal trapping potential. Though the ISA design[1] envisions the placement of clearing electrodes at the location of significant chamber discontinuities, particularly in the experimental insertions, it is desirable to have some estimate of the magnitude of the diameter discontinuity that can be tolerated without a clearing electrode.

## II. Longitudinal Potential

We assume a cylindrical geometry with a circular beam of diameter (2a) centrally located in a circular chamber of diameter D. The transverse potential V between the beam of current I and the wall is then

$$V = \frac{I}{2\pi\epsilon_0 c} \ell n \left( \frac{D}{2a} \right) . \qquad (1)$$

Corresponding to a small increment in diameter $\Delta D$ of the chamber, there is a change in the beam to wall potential $\Delta V$ given by

$$\frac{\Delta V}{V} = \frac{1}{\ell n\ (D/2a)} \frac{\Delta D}{D} . \qquad (2)$$

---

1. J.C. Herrera, Proc. 1975 ISABELLE Summer Study, Brookhaven, BNL 20550 p. 658.

Since, under the stationary electrical conditions that exist, the difference of potential between two locations on the chamber wall must be zero, it follows that $\Delta V$ in Eq. (2) is also equal to the longitudinal potential due to the diameter discontinuity. The ISA has a chamber diameter of 8 cm and a typical value of beam diameter (2a) is 0.28 cm. Equation (2) now takes on the form:

$$\frac{\Delta V}{V} = 0.3\,\frac{\Delta D}{D} \quad . \tag{3}$$

One can then see that a 10% change in diameter (8 mm) is associated with a longitudinal potential equal to 3% of the potential to the chamber wall. For a current of 10 A the latter voltage is, per Eq. (1), 2000 V and the longitudinal potential is therefore 60 V.

## III. Clearing Rate Due to Beam Heating

In a previous report,[2] the various mechanisms that contribute to the clearing of the proton beam have been discussed. It is there shown that in order to achieve the desired neutralization ($N_e/N_p$) of $10^{-4}$ in the ISA, a clearing rate, $R_c$, equal to 100/sec is necessary. Thus, in the presence of a chamber discontinuity, it is required that the clearing rate due to beam heating, $R_c^{BH}$, be at least equal to 100/sec. In this way the electrons will be pushed along by the protons and given the requisite energy, $\Delta V$, at a rate sufficient to yield a net neutralization of $10^{-4}$. Referring to Ref. 2, we see that $R_c^{BH}$ is given by the expression

$$R_c^{BH} = \frac{1}{\Delta V}\frac{d\bar{E}}{dt} = \frac{2I}{ea^2}\frac{mc^2}{\Delta V}\,\ell n\left[\frac{(\Delta V)}{2mc^2}\left(\frac{b}{r_e}\right)^2\right] \quad , \tag{4}$$

where:

$e$ = electronic charge (Coulomb)

$mc^2$ = rest mass energy of electron ($0.511 \times 10^6$ eV)

$r_e$ = classical electron radius ($2.818 \times 10^{-13}$ cm)

$b$ = maximum impact parameter (cm) .

---

2. J. C. Herrera, BNL Formal Report ISA 76-12 (1976).

Assuming a longitudinal potential equivalent to $\Delta V = 100$ eV, and using the typical values: $I = 10$ A, $a = 0.14$ cm, and $b = 0.28$ cm, we find that $R_c^{BH} = 119/\text{sec}$, a value greater than 100/sec.

## IV. Dimensional Tolerance

The discontinuity associated with a longitudinal potential of 100 V is now readily derived from Eq. (3). For $V = 2000$ V and $D = 8$ cm, we calculate a value of $\Delta D = 1.33$ cm. We may therefore conclude: If longitudinal beam heating alone is to provide adequate electron clearing in the ISA straight section chambers, radial discontinuities should be less than about 7 mm in a chamber of 8 cm diameter.

## Acknowledgment

I would like to thank Dr. Jack Sandweiss for enlightening discussions.

# VACUUM GUIDELINES FOR ISA INSERTIONS

D. Edwards, Jr.
Brookhaven National Laboratory

## I. INTRODUCTION

Vacuum requirements place design restrictions on the ISA insertions. The vacuum tube diameter, given a distance L between pumps, is determined by the desorption of molecules from the wall under the impact of ions created by the beam, whereas the thickness of the tube must be sufficient to prevent collapse. In addition, the entire vacuum chamber must be able to be baked out at $\sim 200^{\circ}C$.

## II. MINIMUM TUBE THICKNESS

For an Al tube with $L/d > 10$ where L is the tube length, d the tube diameter, t must be larger than 0.01d to prevent collapse under vacuum, t being the wall thickness.

## III. MINIMUM TUBE DIAMETER

The tube diameter is restricted by the wall desorption processes. For $\eta \simeq 2.5$, $I_{crit} \simeq 20$ A the relation between the diameter and length of a circular tube is given by:

$$d_{min} = 3.1\ L^{2/3}\ (cm)\ ,$$

where $d_{min}$ is the minimum allowable tube diameter in cm and L is the distance between large pumps in meters.

Using the tube thickness and $\eta$ restrictions one finds:

| L (m) | $d_{min}$ (cm) | t (mm) |
|---|---|---|
| 1 | 3.1 | 0.3 |
| 4 | 7.8 | 0.8 |
| 10 | 14.4 | 1.4 |
| 40 | 36.2 | 3.6 |

It is clear that fixing any 2 of the parameters determines the third.

In order to be able to easily evaluate tube diameters for arbitrary $\eta I_{crit}$ Fig. 1 has been drawn. Seen is the very slight dependence of the tube diameter on $\eta$ for a given length, critical current.

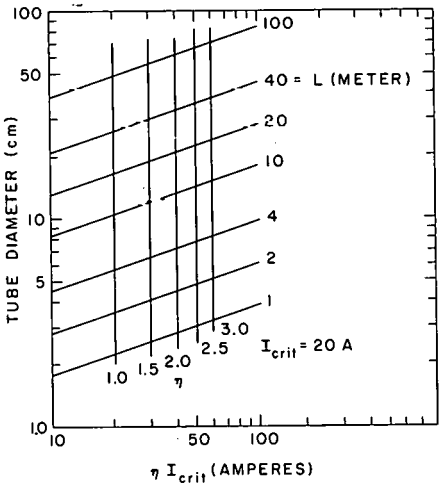


Fig. 1. The minimum tube diameter is plotted vs $\eta I_{crit}$ for various lengths between the large pumps.

# Workshop on Phase Space Cooling*

E.D. Courant
Brookhaven National Laboratory

A two-day workshop was held on August 5 and 6, 1976 to discuss phase space damping ("cooling") of particle beams. Interest in this topic derives chiefly from the possibility that antiproton beams pro-
d by collision of an intense proton beam with a target can be
ressed in phase space. This could make it possible to accumulate antiproton beams in a storage ring repeatedly, thus leading to a relatively high stacked $\bar{p}$ beam suitable for $\bar{p}p$ collisions with interesting luminosities.

Two cooling techniques have been developed: In stochastic cooling (invented by Van der Meer at CERN) the spread of amplitudes in a beam is reduced by a feedback signal derived from the statistical fluctuations in the beam. In electron cooling (first proposed by Budker in Novosibirsk) an electron beam having the same mean velocity as the heavy particle (proton or antiproton) beam coincides with the heavy beam in part of the orbit. Viewed in the center-of-mass system, the electrons are "cold" and the protons "hot", and in the approach to thermal equilibrium the protons are cooled down; in the lab system this means their fluctuations from the mean are reduced.

In the workshop, both these cooling techniques were discussed, especially with a view to their application to the production of intense high-quality antiproton beams suitable for colliding beam physics.

M.Q. Barton described the work on electron cooling at Novisibirsk, where he had visited earlier in the year. In a small experimental

---

). Barton, R. Chasman, Y. Cho, D. Cline, J.G. Cottingham, E.D. Courant, _. Crosbie, R.L. Gluckstern, H. Hahn, H. Hereward, D. Johnson, T. Khoe, L.J. Laslett, P.M. McIntyre, E. Messerschmid, M. Month, R.B. Palmer, E.C. Raka, C. Rubbia, L. Smith, B. Zotter.

storage ring there, proton beams of about 65 MeV have been cooled by 35 keV electrons. Damping times as short as 50 milliseconds have been observed with the beam dimensions shrinking by factors as large as 100.

Theory indicates that the damping time should scale approximately as

$$\tau_p \sim \beta^4 \gamma^5 \langle\theta\rangle^3 / J$$

where $\langle\theta\rangle$ is the larger of the angular spreads of the electron and ion beam, and J the electron current density. Extrapolating from the 65 MeV experiment at Novosibirsk to, say, 2 GeV, one may envisage cooling times of the order of 5 seconds for a narrow beam. However, it should be noted that, because of the $\theta^J$ dependence, the cooling works best for beams that are already narrow, and works more poorly for wider ones.

Stochastic Cooling

In this method the mean deviation from nominal of the transverse or longitudinal momentum is measured for a sample of the beam, and then a correction is applied. The process is continued for other samples constituting the whole beam, and repeated indefinitely. Damping depends on maintaining the randomness of the sample, specifically the statistical randomness relation

$$\langle\bar{x}^2\rangle = 1/N \langle x^2\rangle \qquad (1)$$

where the bar denotes sample averages, and the bracket ensemble averages. Here x stands for the variable to be "cooled", and N is the number of particles in the sample.

On one pass of the cooling system, x for each particle is reduced by a factor g times the mean value $\bar{x}$ measured for the sample. This duces the variance $\langle x^2\rangle$ by $(2g - g^2)\bar{x}_p^2$. If the randomness relation continued to hold, this could be repeated indefinitely, and exponential

damping could be obtained. The theory of this process predicts a cooling rate

$$\frac{d}{dt}\langle x^2\rangle = \langle x^2\rangle \, F \frac{W}{N_p}\left[ g - \frac{g^2}{2}\left(1 + \frac{n^*}{s^*}\right)\right] \qquad (2)$$

where $W$ = bandwidth of feedback system

$N_p$ = total number of particles in beam

$g$ = fraction of $\bar{x}$ corrected per pass

$n^*/s^*$ = ratio of pickup noise to signal

$F$ = 1 for transverse, $F$ = 2 for longitudinal cooling.

This expression is valid if the randomness relation (1) remains satisfied. However, randomness tends to be destroyed by the feedback process, but as Van der Meer already showed in his first paper on the subject,[1] it is restored if the particles have a spread of angular velocities so that the identity of the particles making up the pickup sample changes with time. A relevant "mixing parameter" is

$$M = \frac{4\pi}{F(g - g^2/2)} \frac{W\langle\Delta\omega\rangle_{rms}}{\omega^2} \qquad (3)$$

which is the rms spread in azimuth of the beam in $[F(g - g^2/2)]^{-1}$ revolutions, divided by the effective angular pickup sample length $\omega/2W$. E. Courant showed computer calculations which indicate that the effective damping rate is close to that given by (2) when $M \geq 3$, and reduced by a factor of approximately $0.7\, M^{\frac{1}{2}}$ for $M \leq 1$.

Some important features of the theory[2] are: With noise large compared to the signal, one can still obtain damping if one makes the gain parameter $g$ smaller than $2s^*/n^*$.

For longitudinal (energy) damping and $n^* \gg s^*$, the amplifier power goes mostly into amplifying noise. If the available amplifier power

---

S. Van der Meer, CERN Report CERN/ISR-PO/72-31 (1972).

2. See, for example: L. Thorndahl, CERN Report CERN/ISR-RF/75-55 (1975).

and bandwidth are given, g must be restricted and the damping rate becomes

$$\frac{1}{\tau} = \frac{2}{\pi} \frac{\omega W e^2 Z}{(\Delta pc)_{rms}} \sqrt{\frac{P}{P_n}} \qquad (4)$$

where Z is the geometric mean of input and output impedances, P is the amplifier power, $P_n$ the pickup noise power, $(\Delta p)_{rms}$ the absolute rms momentum spread of the beam; then the damping rate becomes independent of the beam current. With parameters such as: P = 10 kW, $P_n = 10^{-12}$ W = 100 MHz, $\omega/2\pi = 10^5$ Hz, Z = 100 Ω, $(\Delta p)_{rms} = 3 \times 10^8$ eV/c ($\Delta p/p = 0.01$ at 30 GeV) we obtain a damping time of the order of one hour, independent of current.

B. Zotter (CERN) reported on some recent tests of stochastic cooling in the CERN ISR. Earlier experiments[3] showed that cooling rates in accordance with theory were obtained with a vertical feedback system; however, the rate was very slow (2% per hour). More recent experiments, however, are more ambiguous: observed cooling rates are slower than theory by a factor of 3 or more. Further investigations are planned.

Use of Cooling Techniques for Antiproton Beams

To produce an antiproton beam containing N particles in a time T one may produce a fraction N/k of that beam k times and cool each burst in a time T/k.

According to the 1974 ISABELLE design study, an antiproton beam of the order of $5 \times 10^{10}$ particles (1 milliampere) is obtainable without cooling techniques. This requires 10 ISA cycles or approximately one hour. To enhance this by cooling, one would have to cool the $\bar{p}$ beam's phase space by a factor of around 10 (three exponential times) before injecting the next batch of antiprotons; thus, the overall stacking rate may be around $2 \times 10^{10}$ $\bar{p}$ per hour. In 24 hours one might obtain as much as 5 to 10 milliamperes, or a luminosity around $5\text{-}10 \times 10^{29}$ $cm^{-2} sec^{-1}$.

---

3. P. Branham, G. Carron, H. Hereward, K. Hübner, W. Schnell and L. Thorndahl, Nucl. Instrum. & Methods 125, 201 (1975).

It is assumed here that the antiprotons are produced at 30 GeV by the 200 GeV protons of one ISA ring, and cooled in the other ring. Cooling times could be reduced by producing the antiprotons at lower energy, but there the production efficiency is lower.

C. Rubbia (Harvard) proposed an alternate scheme: Produce $\bar{p}$ at $\sim$ 4 GeV/c directly from the AGS 30 GeV protons. Build a special large acceptance ring for 4 GeV/c, which has a total momentum acceptance 25%, he estimates that 4 x $10^8$ antiprotons can be injected in this 3 per AGS pulse ($10^{13}$ protons). If these antiprotons can then be cooled very fast, one could stack $10^{12}$ $\bar{p}$ per hour. However, this implies a cooling system that can reduce the energy spread by a factor of 10 in the order of a second. This might be accomplished by "peeling" off a small part of the beam at a time, decelerating it and cooling it with electrons. It would seem difficult to do this for the whole beam in 1 second; more likely the cooling time is the bottleneck, and the effective stacking rate would be smaller than $10^{12}$ per hour by one or two orders of magnitude.

R. Palmer (BNL) pointed out that the 1974 ISA scheme is based on the ISA beam that is optimized for pp collisions, not for $\bar{p}$ production. By operating the ISA ring in a different mode, one could optimize it for $\bar{p}$ production. With vertical multiturn stacking and a small momentum spread in the ISA ring, one could conceivably bunch the beam much more than in the 1974 scheme and longitudinally stack the antiprotons from 100 ISA cycles instead of 10 as envisaged in 1974, thus increasing the luminosity to well above $10^{30}$ even without cooling.

Conclusions

It is not clear whether cooling techniques can help appreciably in :aining high intensity antiproton beams suitable for colliding beam ›eriments. Electron cooling suffers from the drawback that the damping time increases very rapidly with energy; therefore, antiprotons would have to be produced at very low energies — or else decelerated — in order to be cooled by this method.

Stochastic cooling is inherently slow, especially with high intensity beams, and requires a large product of bandwidth and amplifier power, together with a very low noise pickup system. With optimal performance of the cooling systems, one may at best hope for an increase of an order of magnitude in the antiproton beam intensity obtainable as compared to schemes without cooling. (This rather pessimistic conclusion represents the present reporter's opinion, which may not be shared by all participants in the workshop.)

# ELECTRON COOLING FOR PEDESTRIANS*

L. Pondrom
University of Wisconsin

Electron cooling was suggested by Budker in 1966 as a method of decreasing the transverse kinetic energy of protons in a storage ring by Coulomb collisions with electrons moving with the same longitudinal city. Recent interest in the phenomenon has developed because of success of Budker's Novosibirsk group in demonstrating that the cooling process works in accord with simple theoretical expectations, and because its application to antiprotons might lead to the storage and acceleration of useful fluxes of $\bar{p}$'s in existing proton accelerators.

The Landau collision integral, which gives the drag force on a proton in a frame moving with the e's and p's can be derived from the Bohr formula for dE/dx energy loss in condensed matter. The damping constant is proportional to the derivative of the drag force with respect to velocity. Transformation to the laboratory gives damping time $\tau = \gamma^2 T_e'^{3/2}/n_e$, where $n_e$ is the electron density, and $T_e'$ is the transverse electron temperature. Properties of the electron gun preserve the electron angular spread rather than the transverse momentum, giving $\tau \sim \gamma^5$. The Novosibirsk setup consists of a very idealized weak focusing low current 65 MeV proton storage ring, and a 1 meter long straight cooling region with 35 keV electrons moving parallel to the protons. Great care has been taken in the design of the electron gun, and in the methods for measuring proton beam size and damping times. The most recent results have given cooling times following induced betatron oscillation of the order of 100 millisec, in substantial agreement with the simple formula.

*Summary of a talk presented on August 1976.

AUTHOR INDEX